An Investigation Into A Magnetic Compaction Technique for Composite Manufacturing

Submitted in fulfilment of the requirements for the degree of Master of Engineering: Mechanical Engineering in the Faculty of Engineering and the Built Environment at the Durban University of Technology

Yazid Salot

2022

Supervisor: Dr. M. Gilpin

Declaration

I, Yazid Salot declare that:

1. This dissertation has not been submitted for any examination at any other university.
2. The research work presented in this dissertation besides where otherwise indicated, is my original work.
3. This dissertation does not contain graphics, text, or tables that are copied from the internet, unless specifically acknowledged and the source being indicated in the dissertation and in the bibliography.

Student: Yazid Salot

Signature:.. .... Date:30/11/2021

Supervisor: Dr. M. Gilpin

Signature:…….. Date:30/11/2021….

Abstract

Fiber reinforced polymer composites are an aerospace and defense material. These materials are widely used in the production of components and parts which require high weight to strength ratios or corrosion resistance. The automotive, aero, marine as well as sporting industries are increasingly requiring components with such characteristics. This has led to an increase in demand in the composite industry. A composite is a material made from a combination of fiber reinforcement and resin. The reinforcement is generally made of Glass, Carbon or Aramid fiber which is woven in a fabric. While resins are typically thermoplastic such as polyester, vinyl ester, phenolic and epoxy. The fiber and resin are combined and compacted together in order to manufacture an item.

There are various manufacturing techniques which are utilized to produce fiber reinforced composite components. Many items are manufactured using closed moulding techniques. The process involves the combining of fabric preform with a liquid resin within the mould cavity. After a certain period the component is removed from the mould. The strength, stiffness (mechanical properties) and strength to weight ratio of a composite material are affected by voids (air pockets) and the component's thickness. Both the air voids and thickness are influenced by compaction during the manufacturing process. Increasing compaction during moulding improves the material properties and ultimately the final product, component or part.

This research is aimed at investigating the possibility of utilizing magnetic compaction in fiber reinforced composite manufacturing. The desired technique will be intended to offer improved compaction without requiring any tooling modifications. The proposed technique would fall into the category of the light closed mould compression techniques which utilizes Glass Reinforced Plastic (GRP) tooling. This technique will also attempt to address certain issues experienced in light closed mould techniques. The magnetic compaction technique would be investigated in an effort to offer a scalable technique which has an improved fiber volume fraction and mechanical properties.

Currently no closed mould techniques implement magnetic compaction. The research will review the combination of light closed moulding techniques and the working principles of magnetism.

Acknowledgements

I would like to thank the following individuals and company who played a role in assisting this research project.

My family and friends for their help and support.

Dr Mark Gilpin for his time, assistance, input, guidance and supervision.

The Technology Station for their guidance and assistance in multiple avenues.

Freedom Stationary (Pty) Ltd for their financial support.

Contents

List of Figures

List of Tables

Nomenclature

P_{comp}	-	Compaction Pressure	(Pa)
P_{atm}	-	Atmospheric Pressure	(Pa)
P	-	Fluid / Resin Pressure	(Pa)
V_f	-	Fibre Volume Fraction	(-)
n	-	Number of Layers	(-)
S_d	-	Fabric Density per Meter Squared	(kg/m_2)
ρ	-	Density	(kg/m_3)
h	-	Cavity Height	(m)
E_m	-	Matrix Elastic Modulus	(Gpa)
E_f	-	Fiber Elastic Modulus	(Gpa)
B	-	Magnetic Flux	(Wb/m^2)
H	-	Magnetic Field Strength	(A/m)
BH	-	Magnetic Energy Density	(KJ / m^3)
μ	-	Magnetic Permeability	(H/m)
N	-	Number of Turns	(-)
I	-	Electric Current	(A)
L	-	Length	(m)
F	-	Force	(N)
A	-	Area	(m^2)
q	-	Electron Charge	(C)
h	-	Planck's Constant	(js)
M_e	-	Electron Mass	(g)
μ_B	-	Bohr Magneton	(A/m^2)
ρ_{Ni}	-	Atomic Density	(g/cm^3)
N_A	-	Avogardo's Number	(g)
A_{Ni}	-	Molar / atomic Mass	(g/mol)

List of Acronyms:

VARTM	-	Vacuum Assisted Resin Transfer Method
RTM	-	Resin Transfer Moulding
VI	-	Vacuum Infusion
GRP	-	Glass Reinforced Plastics
HLU	-	Hand Layup
CSM	-	Chopped Strand Mat
MDF	-	Medium Density Fiberboard
SRIMP	-	Seemann's Composite Resin Infusion Molding Process

1. Introduction

The aim of this research is to investigate the use of magnetic forces to increase the compaction pressure in a fiber reinforced polymer composite lay-up during manufacturing. In fiber reinforced polymer composite manufacturing, there are many factors which are required to produce an item. However, a highlighted factor which is closely related to this research is that of compaction pressure. Pressure is required as it consolidates the fibers and assists the fabric in taking the form of the tool design. The pressure compacts the fibers allowing the manufactured part to become thinner. This will then lead to an item which has a more desirable volume fraction and potentially improved mechanical properties.

The pressures can differ according to a particular manufacturing technique. The general techniques which utilize wet fiber, require large equipment to generate high positive compaction pressure. While other techniques which utilize dry fiber [Vacuum Assisted Resin Transfer Method (VARTM), Vacuum Infusion (VI) or Hand Lay-up (HLU)] use negative compaction pressure. The high-pressure techniques have elevated economic requirements when compared to that of the lower negative pressure techniques which are more economically viable.

However, a major drawback of utilizing negative compaction pressure is that these techniques are limited to negative 1 atmospheric pressure. Furthermore, the added complexities related to these techniques contribute to items which are produced inconsistently. These items have a variation in thickness which is due to the pressure gradient that is experienced during the manufacturing process. The inconsistent thickness variation leads to an item which possesses inconsistent mechanical properties. At times this is undesirable as the item may not achieve the desired design specification.

In order to investigate the laminate thickness based on pressure alone; experiments which require all parameters to be limited would be conducted. A comparison would be conducted between three panels produced using the same fiber reinforced composite technique. For experimental purposes the VARTM technique is ideal as it will limit variations with regards to laminate thickness inconsistencies when compared to other vacuum forming techniques such as VI and HLU. Hence the VARTM technique was selected for the comparative experimentation for this research.

The VARTM technique is a vacuum assisted resin transfer method. This technique utilizes the difference in air pressure, to draw resin through the mould cavity and infuse the fiber reinforcement as well as compact the fibers. Further details related to the VARTM tooling, process and advancements are described in section 2.1.5.3.

The novel contribution of this research is to illustrate the direct effects of magnetic assisted compaction in composite manufacturing. The aim is to devise a scalable solution which would be implemented onto the VARTM technique without significantly increasing tooling cost or requiring major tooling modifications. A comparison between 3 identical VARTM panels, one of which being a regular VARTM panel and the remaining two panels utilizing magnetic assistance would be analyzed. The material (fiber reinforcement) used for the comparative experiment would be seven layers of 390g, twill glass fiber. The comparison would require all the parameters to be identical and fixed, allowing the magnetic forces to be the only differentiating factor. By limiting all the variables, the comparison between the two processes (magnetic assisted VARTM vs VARTM) would isolate the thickness variation. If any variation is identified, it would be due to the direct effects of the additional positive magnetic compaction pressure.

A comprehensive experimental investigation was undertaken in order to fully understand the force-distance nature of permanent magnets at incremental distances. The experimentation would comprise of two sections, the first of which would be related to various magnetic materials, dimensions as well as layouts and the second would be related to, two comparative VARTM experimentation sets. The raw data provided by the magnetic experimentation would be interpreted and processed providing a clear indication on the type of magnet as well as the layout that would be utilized and integrated into a comparative VARTM experiment. The VARTM technique would be used in order to conduct a comparative experiment to investigate the use of magnets in composite manufacturing. The experiment would be conducted in such a manner that all parameters and conditions are fixed. The constraining of parameters would emphasize the only additional variable which is the additional magnetic units. The intended result would be aimed at obtaining a panel which is more consolidated than that of a regular VARTM technique. This would provide a positive outcome to the investigative research. Further tests would be conducted to verify the panels once manufactured. These tests would highlight the composite panels volume fraction, mass fraction and mechanical performance. The volume fraction tests would be both, destructive and non-destructive in the forms of an ignition loss test and physical measurement analyses. The

mass fraction results would be derived from the volume fraction tests and further mechanical (tensile) tests would analyze the panels tensile properties.

This research would be presented in the following manner.

Chapter 2 describes the background of composite manufacturing and briefly touches upon what is required and how various techniques meet these requirements. More detail is placed on the GRP tooling techniques and the limitations pertaining to these techniques. The field of magnetism is described in detail. Both the permanent magnetic and electromagnetic fields were researched. However, due to certain factors, permanent magnets were selected as the desired type for this research. The force-distance relation between magnets were the focal point of the investigation, as it is this force that would govern whether or not magnetic compaction is a viable addition to an existing process.

The force-distance investigation was conducted in order to understand magnetic behavior and how the magnetic forces could be utilized to generate positive compaction pressure. The desired distance takes into consideration two 5mm thick GRP tools and fiber preform up to 5mm. Hence the distance (related to the force-distance) would be targeted between 10mm-15mm. In order to achieve better compaction, the positive magnetic pressure generated, would be utilized independently (externally), yet in parallel (during the manufacturing process) with the negative vacuum pressure in the VARTM process. With the intention of having a more consolidated panel without increasing the GRP tooling design and costs.

The experimentation is divided into two main parts. The first part is associated to the magnets while second part is related to both comparative VARTM experiments. In Chapter 3 the magnetic experimental equipment as well as setup was described. The detailed procedures related to the experimentation of the permanent magnetic materials, dimension, combinations and possible application methods.

The results related to the magnetic experimentation are discussed in Chapter 4. The results will be discussed according to the experimental pattern. The initial experimentation is related to magnetic materials. Once the desired material is selected, further experiments would continue in order to understand the force-distance relationship. The magnetic dimensions and particularly the magnetic combinations were investigated and obtained through these experimentations. A summary of the results as well as the possible implementations into a comparative experiment are discussed.

Following on from the magnetic experimentation, the details related to the two comparative VARTM experimental sets will be discussed in Chapter 5. Details related to the experimental equipment and procedures are mentioned; as well as the maintaining of uniformity between the panels and ensuring the magnets are the only differentiating factor. The 3 panel VARTM comparison was run twice to ensure the magnetic compaction is consistent and a repeatable process.

The results from the VARTM experimental sets 1 and 2 are presented in Chapter 6. Details pertaining to the panel thicknesses as well as the improved fiber volume fraction will be compared and a summary of the findings are discussed.

The final aspects of the research are discussed and concluded in Chapter 7 with regards to the design of the magnetic units which were obtained through the comprehensive experimentation. Details pertaining to the implementation of these magnetic units on current GRP tooling were discussed. Lastly, the aim of this research is to investigate the possibility of utilizing magnetic compaction for composite manufacturing was confirmed. This research was conducted in order to introduce a manufacturing process which has design flexibility, scalability and practicality, in order to produce a product that potentially has improved mechanical properties.

2. Literature Review

The following chapter is divided into two main sections. The first being fiber reinforced polymer composites and the second being magnetism; both of which comprise of multiple sub-sections. These sections are unique, yet they are related to one another in the context of this research.

An in-depth investigation would be conducted within both fields in order to gain an understanding of the working principles of each field. A broader description related to both the fiber reinforced composites as well as magnetism would be funneled down to the point of focus of this paper, which is how the two sectors would be integrated with one another.

The aim of this research is to investigate the use of magnetic forces to compress a fiber reinforced composite lay-up during manufacturing in order to achieve a more desirable volume fraction. This will potentially lead to an item which has improved mechanical properties.

2.1 Fiber Reinforced Composites Overview

Fiber reinforced polymer composites are a material made from a combination of fiber reinforcement and resin. This combination is generally referred to as a laminate. In order to manufacture a laminate, the resin and fiber combination would be placed under pressure in order to compact the fibers. This will in turn lead to a more compact laminate which would then result in an item which has improved mechanical properties as shown by Prof. Jagadale Vishal S [7, 8].

The variety of materials used to make the fiber reinforcements are Carbon, Glass and Aramids. These fibers can be combined with one another or used independently. The fibers are manufactured in a desired way to enhance the mechanical properties of the materials [9, 10]

2.1.1 Fiber Manufacturing

The fiber reinforcement can be either synthetic or natural and can vary in length. The fiber can be short (discontinuous) or long (continuous). The long continuous fibers can be assembled to produce rovings or yarns. The roving's can then be woven into weave patterns to produce fabrics. These weave patterns can be either twill, plain or unidirectional. The short fibers are scattered and they are misaligned with regards to orientation. These fabrics are held together using a binder also known as resins. However, the laminates compaction is closely related to the fabric's weave patterns and weight. The finer details relating to each materials manufacturing process is complex

and is unique to the manufacturer. These processes may differ depending on the manufacturer as well as the core ingredient material utilized in the manufacturing process. More details relating to glass fiber, carbon fiber and aramids can be found in [11-13], [14-17] and [18] respectively.

2.1.2 Resins

Once the desired fabric is selected an accompanying resin will be chosen. There are a variety of resins available. The resins keep the fibers together which in turn forms the laminate and distributes the loading. Certain types of resins can protect the fibers from environmental and chemical damage. The resins mechanical properties [19, 20], is not always a governing point with regards to their selection. Particular points which are related to resin selection are at times based upon certain aspects, such as cost, permeability (Specific viscosity requirements for infusions or hand lay-up), flame resistance and curing time. P.K.Mallick [21] as well as S. K. Mazumdar [[22] chapter 2.1.3] have gone into further details regarding the types of resins and their respective properties. Valuable knowledge regarding the desired design needs to be known on whether the part being produced is either a structural or non-structural. Once this is known the selected combination of fiber and resin must meet the required design specifications.

2.1.3 Background to Fiber Reinforced Composites

In order to achieve the desired design properties, the most ideal composite material is used and it is referred to as prepreg [23]. The fiber has resin that is pre-impregnated. The impregnation process can range from solvent impregnation, hot melt coating and a dry powder deposition [22]. However, due to these impregnation processes the prepreg fabric has certain advantages and disadvantages. Some of the advantages are, exceptional resin consistency and an optimum fiber volume fraction (*Vf*) [22, 24]. Disadvantages are the material costs, cold storage, shelf life and a minimum purchase quantity.

In order to manufacture an item from prepreg material certain manufacturing equipment is required. The equipment depends on the items being produced. An autoclave, hydraulic press and filament winding are generally the preferred methods of manufacturing with prepreg material [22]. These methods of production have desirable benefits, one of which being exceptionally high compaction pressures. However, these methods require high capital investment as well as tooling and equipment costs that are necessary to consolidate and cure the material [7]. The process also requires annual maintenance, skilled labour as well as having geometric limitations.

Attempts have been made to lower the cost of both the prepreg material cost; as well as manufacturing techniques which use lower pressures and temperatures. These prepregs are generally referred to as out of autoclave prepregs [25].

Composite manufactured parts using prepreg is an option for the manufacturer who has the ability to do so. Due to the negative aspects related to prepreg material and its respective manufacturing methods; a composite manufacture may explore other avenues. These avenues [26] (Hand Lay-Up, RTM, VI and VARTM) generated more financially attainable items and the possibility to produce much larger items geometrically with a trade-off of being limited to lower compaction pressures.

The diagram below encapsulates a general overview of the current composite manufacturing techniques that are available. With reference to the opening paragraph in the introduction, compaction pressure is required in composite manufacturing. The Figure 2.1 highlights the different types of composite manufacturing processes. There are two distinct sectors, both of which are primarily governed by compaction pressure. The left-hand side which is circled in red is the high-pressure processes and the lower pressure processes are circled in green. Several techniques within the red region make use of close moulds and processes within the green region use either open or closed moulds.

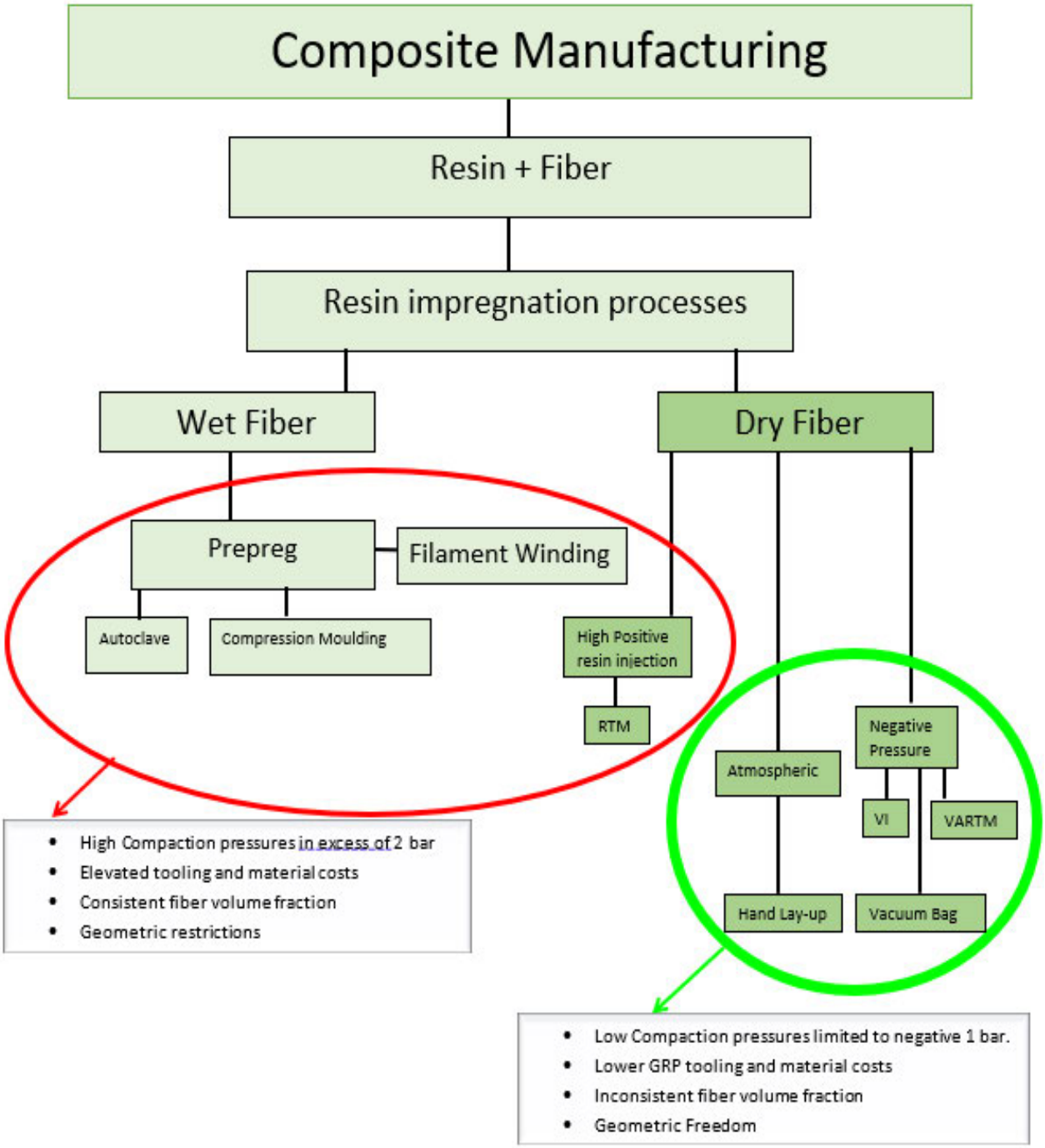

Figure 2. 1 General overview of the current composite manufacturing techniques.

Due to each item being unique; there are various branches related to one or more of the above-mentioned manufacturing methods. Under the umbrella of a particular manufacturing method, a composite part has its very own bespoke process which has been tailored in order for the desired performance requirements to be obtained.

This research is focusing on the closed mould techniques (VARTM) and more so, within the lower pressure region.

2.1.4 Closed Mould

As mentioned in the closing paragraph of section 2.1.3 above, the closed mould techniques are divided into the two sections of high and low pressure. The high-pressure processes make use of alloy (steel, aluminium or copper) tooling [21, 27]. The advantages of using these rigid tools are the ability to apply excessively high pressure (in composite manufacturing terms) to the fiber which will then in turn lead to a laminate which is more consolidated and have consistent fiber volume fraction (further details in section 2.1.7). The downside to these tools are, the elevated manufacturing costs and size limitations.

However, the low-pressure processes make use of semi-rigid tools in the form of glass reinforced plastics (GRP). This type of tooling has various advantages such as requiring lower financial investment [28] as well as being able to manufacture much larger items such as boat hulls [22, 29]. The capital expenditure ranking is based on a comparison between composite manufacturing techniques and no other manufacturing industries. The set-back to the GRP tooling is that it is limited to negative one bar pressure irrespective of the manufacturing process or if it is either an open or closed mould technique. The other negative aspect related to these types of tooling processes is that they produce items that have inconsistent fiber volume fraction.

2.1.5 Low Pressure Techniques

The following manufacturing processes (HLU, VI, RTM light and VARTM) [30] share a common factor; which is the use of GRP tooling in either one or two parts (one part being an open mould and two parts being a closed mould) as well as a using vacuum pressure. However, they do differ on other aspects, such as resin impregnation techniques and the process of generating the tool cavity.

The resin impregnation process is due to a pressure difference which is generated by the vacuum line and the resin pot [31]. The vacuum line is at negative one bar and the resin pot is at atmospheric pressure. There are multiple factors [32] which are taken into consideration during the impregnation process. One of the most important aspects is the permeability [33]. Certain setbacks related to the vacuum infusion processes are the potentially unpredictable flow pattern

as mentioned by J. Li and M. Gilpin [34, 35] as well as thickness and fiber volume fraction variations and inconsistencies [36].

There is a common issue with all parts which are manufactured using the vacuum infusion process. The issue being referred to is an inherent flaw associated with these techniques. It is more noticeable within the VI process which utilize flexible tooling and less noticeable with the VARTM process which uses two the semi-rigid GRP tooling.

The flaw being referred to is the thickness variation. For descriptive purposes only, the flaw being described is a "wedge-shape" side profile. Figure 2.2 illustrates the side profile of a flat composite fiber plate which has a "wedge shape" profile. As mentioned by D. Modi, M. Johnson, A. Long, and C. Rudd [37] the wedge profile is also known as the pressure profile in a rectilinear and radial flow vacuum infusion When a vacuum is drawn through a mould cavity, the pressure differential across the semi-rigid tool is supported by both the resin and the fabric as mentioned by M. Gilpin and C. Polowick [31, 38].

Once a part has been produced it has a wedged shape side profile which is due to the pressure gradient that is present in the mould cavity during the infusion process [31]. Further studies have been conducted by Li. Jing [34], Chen, Dingding, Arakawa, Kazuo Uchino and Masakazu [39] as well as Woods, Jack A Modin, Andrew E Hawkins, Robert D Hanks and Dennis J [40] in order to better understand, reduce and control the rectilinear and radial flow.

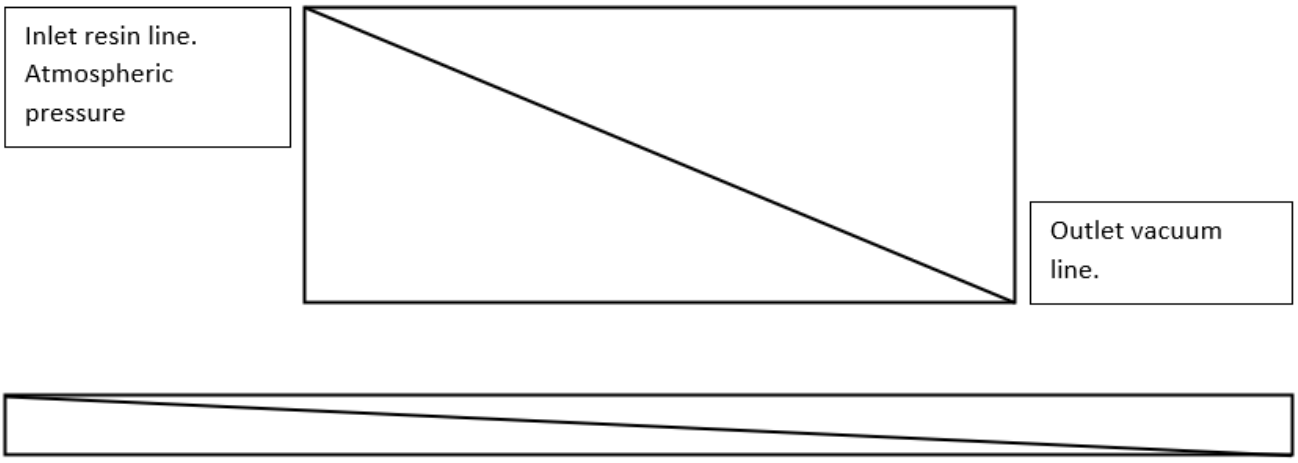

Figure 2. 2 Wedge shape profile.

2.1.5.1 Hand Layup (HLU)

The Hand Lay-Up process is one of the more accessible manufacturing techniques upon which a composite part can be produced. It only requires one GRP tool and can be produced with or without a vacuum bag [41]. This procedure is more laborious and requires the resin impregnation to be applied by hand (as the name mentions). This potentially leads to a part that is prone to voids, which then lowers the mechanical performance [22].

2.1.5.2 Vacuum infusion (VI)

The Vacuum infusion techniques requires only one GRP tool and the other side is a flexible vacuum bag. This technique utilizes atmospheric pressure to consolidate the fibers. The resin is stored in a resin pot next to the tool. The resin is then drawn into the tool cavity and impregnates the fibers.

2.1.5.3 Resin Transfer Method (RTM) Light

The RTM light technique utilizes a two-piece mould, one of which is a GRP tool and in certain cases the other the tool can be aluminium [42]. This technique is approximately a third of the RTM costs. Certain RTM light processes, the resin pot is subjected to an additional positive pressure. By having a pressurized resin pot and a tool cavity that is under vacuum pressure; a larger pressure difference is generated, which in turn causes the resin to flow more effectively through the cavity. Due to the tools being rigid and semi-rigid there would be less thickness variations than the VI and VARTM processes. Further research has been conducted by O. Maclaren, J.M. Gan, C.M.D. Hickey, S. Bickerton and P.A. Kelly in the field of RTM-light manufacturing [43].

2.1.5.4 Vacuum Assisted Resin Transfer Method (VARTM)

The VARTM technique is classified as a closed mould method as this technique utilizes two GRP tools. The fiber is laid by hand in the desired directions as well as required number of layers. The tools are then closed and sealed. A vacuum removes all the air from within then mould cavity. The resin is drawn through the mould cavity due to the pressure difference (very similar to the VI process). Due to the two GRP tools; the thickness variation (wedge shape) is subtle as well as consistent when compared to the VI process. The resin inlet pressure is atmospheric and the clamping pressure is limited to 1 bar. The resin flow through the fiber layup can be expressed as

flow through a porous media [44], further details can be found in by Suresh G. Advani and Kuang-Ting Hsiao .

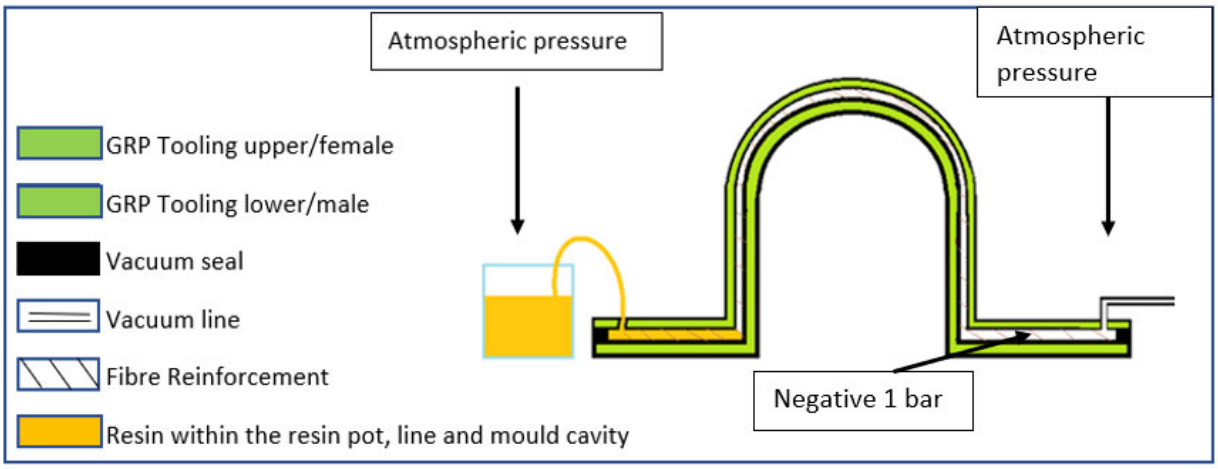

Figure 2. 3 A vacuum assisted resin transfer method (VARTM) infusion illustration.

The VARTM technique is the more attainable technique which provides a consistent fiber volume fraction within the GRP tooling techniques and geometric benefits.

Advances have been pursued in the VARTM field; research done by Yalcinkaya, M Akif, Sozer, E Murat and Altan, M Cengiz [45]. Have shown that, by increasing the external pressure in a VARTM technique, improves the fiber volume fraction and the mechanical properties.

GRP tooling has major advantages with regards to fiber reinforces composite manufacturing tooling. These tools are cost effective to produce; possess larger geometric freedom when compared to the aluminium tooling and are easier to manufacture.

The fiber reinforced composite manufacturing processes; utilize GRP Tooling in either one or two parts. The manufacturing aspects in which these techniques differ on were touched upon as well as the common problem of inconsistent fiber volume fraction were revealed. However, the GRP tooling has major advantages with regards to fiber reinforces composite manufacturing tooling. These tools are cost effective to produce; possess larger geometric freedom when compared to the aluminium tooling and are easier to manufacture.

2.1.6 Semi-Rigid GRP Tooling

As mentioned above the tooling related to this research would be Semi-Rigid tooling that is constructed from Glass Reinforced Plastics. The details pertaining to this tooling are as follows.

Tooling manufacturing

There are several steps which are required to manufacture a GRP tool. The steps below are the manufacturing procedure of a GRP tool at the Advanced Composite Lab based in the Durban University of Technology.

1. Manufacture a plug.

   A plug is the desired composite design which is initially made from certain materials. The desired design is either machined with a CNC or manufactured via other unconventional methods such as hand crafting. As Figure 2.4 shows, a desired design was machined from MDF (Medium Density Fiberboard) board. Other materials can be used such as foam or polystyrene. It is then filled and sand papered with various grits ranging from 200-600 by hand or machine in-order to obtain a Class A finish [46]. Once the plug has been made it is then painted, sand papered and polished to a gloss finish.
2. The manufacturing of the GRP Tooling

   The GRP tooling comprises of several layers (Appendix A) of various types of glass fiber, a desired gel coat and lastly a desired resin. These materials are placed onto the actual plug, in order to get the GRP Tooling. The detailed description of the industrial grade GRP Tooling Layers, construction pattern as well as duration can be found in Appendix A. One of the various reasons to the particular lay-up structure of the GRP tooling is based on force distribution throughout the tooling [47].
3. Once the GRP tooling has been constructed, it is then demoulded from the plug and the required seal and release agents would be applied to the GRP tool.
4. If a second (male-female) GRP tool is required for a VARTM process then the very same procedure would be conducted once again to produce the opposite GRP tooling.
5. Once the tool has been prepared then an item can be produced.
6. A common and advisable practice is to manufacture a master item. This item would not be used as the end result, but rather as a long-lasting reusable plug. This Master Item can be reused to manufacture multiple GRP Tools.

7. Once the desired manufacturing technique, material and resin have been selected, the parts can be produced.

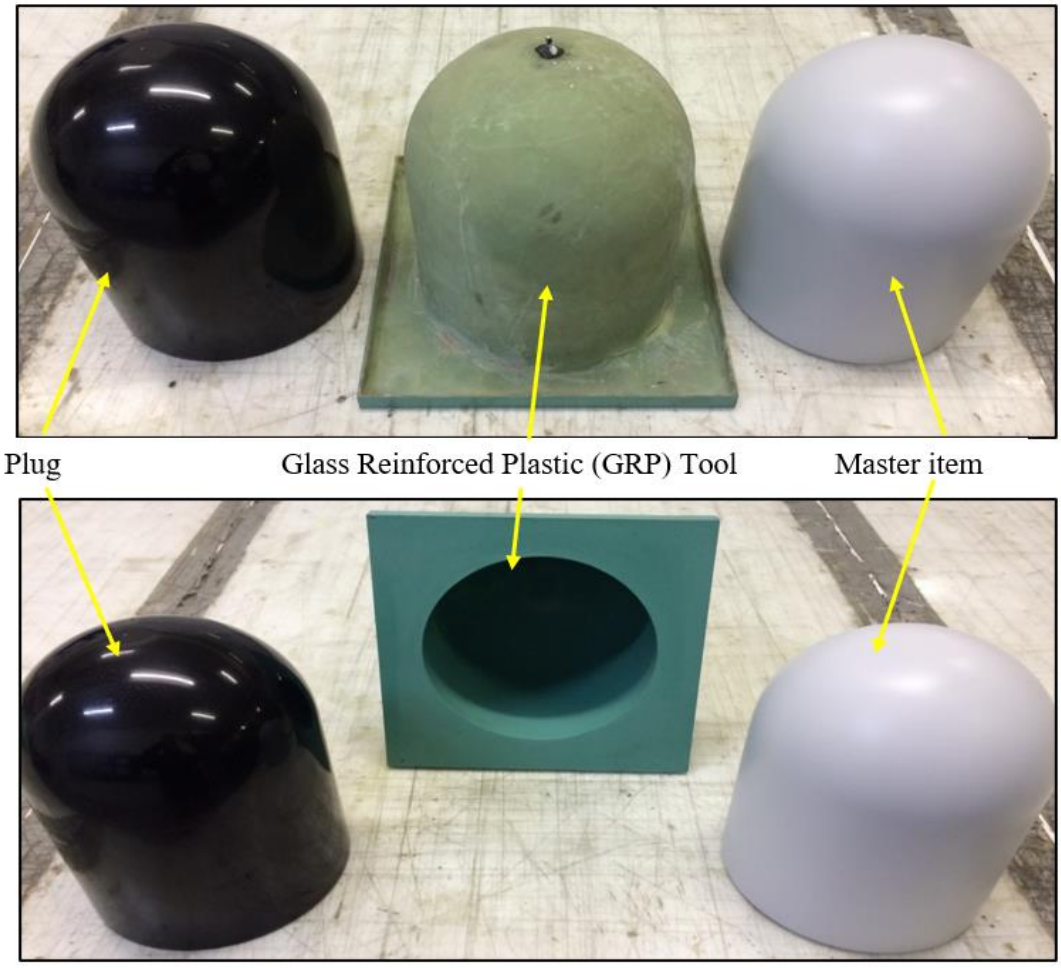

Figure 2. 4 The Plug, GRP Tool and Master Item.

The tooling related to the research experimentation will be Polymethyl Methacrylate plates (PMMA). More details pertaining to the tool rigidity and the effects it has on the laminates produced can be found in [39] by Chen, Dingding, Arakawa, Kazuo and Uchino, Masakazu. Their research investigated different tooling materials (stiffness) and the effects it has on the produced laminates However, these experiments were done under vacuum pressure alone and with no additional (external) forces. This research will be utilizing the additional magnetic forces to further consolidate the fiber preform. PMMA was used to view the resin flow front. If two GRP tools were used, then the flow front would not be visible. The other reason as to why PMMA was used

was based on material thickness consistency. A GRP tool is manufactured using the HLU method. As mentioned under section 2.1.5.1, there is a lack of consistency between manufactured parts. It is this inconsistency that would lead to an experiment that has inaccurate and results, as one GRP tool maybe different to the other. Hence PMMA sheets were used.

With the composite aspect of the research being described and expanded on, the second aspect pertaining to the research will now be focused on. The primary aim of this research is to investigate the use of magnets for composite manufacturing. Once the required field of magnetism is understood through research and the comprehensive experimentation, various implementation methods would be reviewed to investigate the usage of magnets in one of the above-mentioned techniques. If the experimentation is successful, the magnets would be aimed at increasing the compaction pressures of GRP tooling for the lower compaction pressure negative one bar techniques. This is due to the magnets using positive attractive forces, as well as producing items that obtains a consistent and improved fiber volume fraction.

2.1.7 Fiber Volume Fraction and Mechanical Properties Relation

When it comes to manufacturing an item from a composite material, one of the most critical aspects that require attention, is known as the fiber volume fraction. As mentioned in section 2.1.3 the most ideal and consistent fiber volume fraction is obtained with the use of prepreg materials. The amount of fiber in a composite directly relates to the mechanical properties. As mentioned by P.K Mallick [48] a 60% volume fraction is considered an industry standard for the aerospace industry. However, due to various reasons, other techniques have been used to manufacture composite parts with the risk of having inconsistent fiber volume fraction. Due to certain manufacturing parameters linked to other techniques, the fiber volume fraction is usually in the range of 50% to 65% [49].

The volume fraction is a combination of fiber, resin and voids [50-52]. If there is too much or too little resin, there can be a possible reduction in mechanical performance. Therefore, the optimum amount is always desired [7]. The volume fraction can be found in the following ways [53]:

- Destructive testing
    - Matrix digestion test.
    - Ignition loss test.
- Non-destructive testing
    - Physical measurement
    - Image analysis

With regards to the destructive testing, the matrix digestion test is a process in which the resin matrix is removed from the laminate leaving only the fabric behind. The ignition loss test is a process which is conducted in a furnace at approximately 600˚C. The laminates are weighed before and after the desired process and the values are then inserted into a formula (formula 2.1).

The volume fraction calculation for a destructive (ignition loss) method comprises of several factors which are all linked together. The volume fraction formula can be viewed below.

$$V_f = \frac{w_f / \rho_f}{(w_f / \rho_f) + (w_m / \rho_m)} \qquad (2.1)$$

Where:

- w_f = Fiber weight after ignition loss
- ρ_f = Fiber density
- w_m = Resin weight (laminate specimen weight before – fiber weight after (w_f)).
- ρ_m = Resin density

Another aspect related to the ignition loss test, is obtaining the laminates mass fraction. During the manufacturing process in which the resin is incorporated and infused into the fibers, air voids may get trapped within the material. The mass fraction assists in estimating the void content within the composite laminate. The mass fraction formula is a direct ratio between the mass of the laminate (w_c) before and the mass of the fiber (w_f) after the ignition loss test (w_f / w_c). The difference in weight (w_c - w_f) is the amount of resin that was burnt-off during the ignition loss test.

With regards to the volume fraction calculation for a non-destructive (physical measurement) method, the formula comprises of several factors which are all linked together. The volume fraction formula can be viewed below.

$$V_f = \frac{\eta S_d}{\rho h} \qquad (2.2)$$

Where:

- V_f = Volume fraction
- η = Number of layers
- S_d = Fabric density per meter squared
- ρ = Material density
- h = Cavity height

The reason as to why the fiber volume fraction is such an important aspect to the composite world, is because it has a close relation to the mechanical performance [54, 55]. When an item is required to be designed from a composite material, one of the key advantages is that it can be tailor made for the required task. Hence only the required amount of fiber will be used in certain areas of the design and less material used where there is less of a load required. The item can then be manufactured to be lighter, yet it can withstand the desired loads. However, void content (air pockets) is a manufacturing defect that is present within the laminates. These voids reduce the quality and potentially the mechanical performance of the laminate.

The relation between fiber volume fraction and mechanical properties are to follow. Equation 2.3 illustrates the relationship between the fiber volume fraction and the elastic modulus of a unidirectional composite laminate.

$$E = (1 - V_f)\, E_m + V_f\, E_f \qquad (2.3)$$

Where:

- V_f is the fiber volume ratio and
- E_m is the elastic modulus of the matrix.
- E_f is the elastic modulus of the fibers

As mentioned by W. D. Callister [56] equation 2.2 illustrates that the volume fraction and the Young's modulus [**E**] of both the fiber as well as the resin are related to one another. In short, Young's Modulus (also known as the modulus of elasticity) is equal to stress over strain. If there

is a change in volume fraction, there will be a direct change to the mechanical performance. This research is aimed at improving the compaction and fiber volume fraction of the VARTM technique.

Formulae related to; the relationship between the mechanical performance of various fiber (continues or discontinuous as well as the alignment and orientation.) composite panels and the fiber volume fraction. can be found in [56].

However, in relation to this research, the GRP tooling techniques mentioned in section 2.1.4 have a considerable number of inconsistencies with regards to fiber volume fraction. Inconsistent fiber volume fraction leads to an item which performs undesirably.

In the section above relating to the low pressure techniques, there are multiple factors which are taken into consideration during the impregnation process. One of the most important aspects; is the permeability.

2.1.8 The Permeability of Woven Fabrics

The major disadvantage of VARTM is slow filling due to the limited pressure differential between the inlet and exit which cannot exceed one atmospheric pressure. However, the SCRIMP (Seemann's composite resin infusion molding process) method overcomes this hurdle by adding a distribution medium which has a much higher porosity / higher permeability than the fiber preform. By placing it between the fiber preform and the vacuum bag the resin would travel through the distribution medium due to its high permeability in the in-plane directions. By doing so, the resin only needs to penetrate only across the thickness of the mould cavity (approximately 3 mm) rather than as compared to the in-plane directions which are usually in 10–100 m long.

The flow through a porous medium can be calculated using Darcy's formula.

$$v = -\frac{K \Delta P}{\mu L} \qquad (2.4)$$

Where:

v = Velocity

K = isotropic permeability of the porous sand column,

μ = viscosity of the water,

ΔP = is the pressure difference and

L = height

A few other factors which the permeability is related to are mentioned below [33]:

- Type of fiber (Glass, Carbon, Aramids),
- Density of the fiber (Glass, Carbon, Aramids)
- Fiber weave pattern (Twill weave, plain, unidirectional)
- Fiber mass per square meter
- Fiber structure
- Orientation of the plies,
- Number of fiber layers,
- Boundary conditions

The types of resin in terms pot life, viscosity and atmospheric conditions as well as one-dimensional linear or radial inject all play a role with regards to the preforms permeability. Suresh G. Advani and Kuang-Ting Hsiao [57] went into significant detail regarding the Experimental characterization of permeability as well as in-plane permeability of a porous preform. Further research was also conducted by Arbter, R., Beraud, J. M., Binetruy, C., [58] regarding the experimental determination of the permeability of textiles.

This research will be focusing on what effects the additional magnetic forces have on a VARTM manufactured composite part. These forces are related to the difference in pressure that is present within the mould cavity.

2.2 The Effects of Compaction Pressure on Volume Fraction and Resin flow

Unlike the VI process, the VARTM technique has two GRP tools. The semi rigid tools allow for a more consistent component thickness with less variations. However, the common characteristic between the VI and VARTM techniques is the use of vacuum pressure. The vacuum is performing two tasks. In reverse order, these tasks are:

- The pressure difference created by the vacuum draws the resin through the fabric preform. The result of which creates a thickness variation (wedge-shape profile) as discussed in section 2.1.5
- The atmospheric air that is removed from within the mould cavity generates a difference in pressure between the fabric preform and the outer atmosphere. The pressure difference generates the external compaction pressure, which compacts the fabric preform.

The compaction pressure can be calculated via the following equation:

$$P_{atm} = P_{Comp} + Presin \quad (2.5)$$

This formula can be rearranged to the following:

$$P_{comp} = P_{atm} - P_{resin} \quad (2.6)$$

Where P_{comp} is the compaction pressure; P_{atm} is the atmospheric pressure and P_{resin} is the resin pressure. The compaction pressure is further related to the components volume fraction. The relation is represented by the following formula [59]:

$$V_f = V_{fo} P_{comp}^{B} \quad (2.7)$$

Where V_f is the fiber volume fraction; V_{fo} is the fiber volume fraction with a compaction pressure of 1 Pa and P_{comp} is the compaction pressure. The exponent **B** is determined experimentally.

Researchers such as X. Song [60]; F. Robitaille and R. Gauvin in [61] and B. W. Grimsley [62]

have shown the relationship between the compaction pressure and the fiber volume fraction. Research conducted by E. J. Rigas, T. J. Mulkern, S. M. Walsh, and S. P. Nguyen [63] have shown that the fiber volume fraction can be increased by approximately 16% if the fiber preforms are mechanically loaded and unloaded prior to the infusion process. However, this research will load (magnetic compaction) the fiber preform during the infusion process.

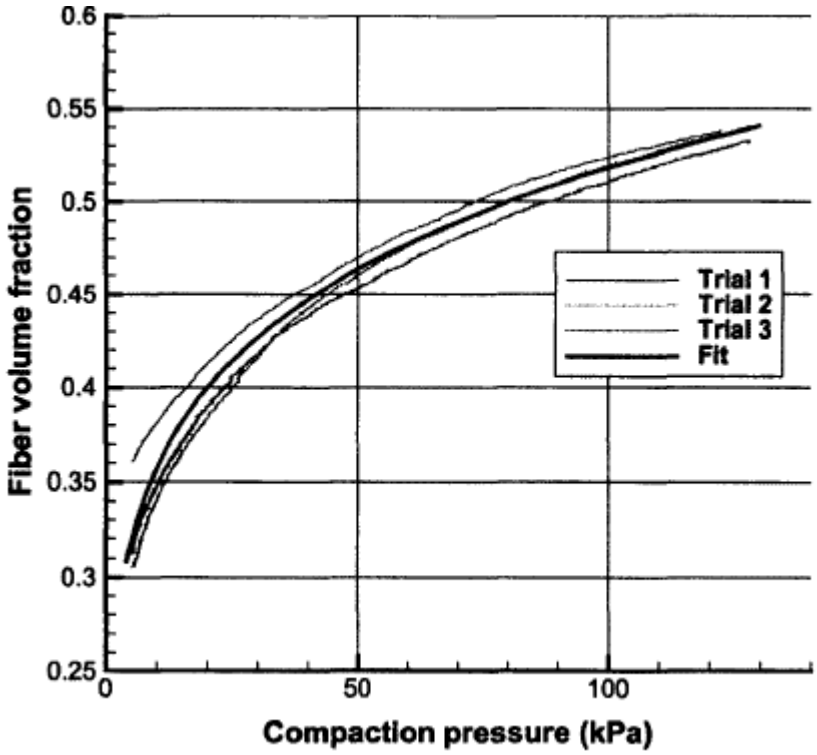

Figure 2. 5 Fiber volume fraction vs compaction pressure [5]

C.Polowick [5] has shown the relationship between compaction pressure and fiber volume fraction to be in the region on 50% - 55%. According to Yalcinkaya, M Akif; Sozer, E Murat and Altan, M Cengiz [45] an increase in fiber volume fraction from approximately 50% - 60% is obtained by applying ~ 130 kPa (external pressure) on laminates with various thicknesses. Their research had also shown that an improved fiber volume fraction improves the flexural properties by approximately 20%.

In conjunction with Darcy's formula, the relationship between the compaction pressure and the resin flow front are also related to formula 2.5. When the resin enters the mould cavity the resin pressure is equal to the atmospheric pressure, hence there is little to no compaction pressure. As

the resin travels through the cavity the resin pressure decreases and the compaction pressure increases. The vacuum line exit has the largest compaction pressure and very low resin pressure. As illustrated in Figure 2.7, the VI process has a higher compaction pressure when compared to the RTM method.

A direct experimental comparison was conducted by M. Gilpin [31] between the VI and RTM processes. The experiment directly compared the resin flow between the two processes. In line with this research the experimental conditions, fiber layup and other parameters were identical and fixed. The comparison isolated the effects of the preform thickness variation as the differentiating factor which influenced the resin flow.

The research had shown that the fill time for the VI process was slower than the RTM process as well as noting that the VI fill times were not only proportional to the square of the fill length, as in the RTM case, but also proportional to the square of the mass present.

The fill time is also controlled by the inlet conditions. The rate of resin flow determines the flow front progression and the resulting fill times. The inlet-controlled filling pattern was found within the comparative tests. The inlet velocity is determined by a combination of both the increase permeability and reduced pressure gradient at the inlet. This in turn results in a specific flow rate through the constant inlet area. The reduced flow rate in VI is responsible for the difference in fill times between the RTM and VI methods. The flow rate in VI however remains proportional to the filled length as in RTM.

The fill times in the VI process will always be longer when directly compared to the RTM process under identical flow conditions. As the distinguishing factor between the VI and RTM processes, is the pressure balance between the resin and compacted fiber preform.

The pressure gradient for the VI process is less than the RTM process at the inlet (see figure 2.7). This is due to the flexible tooling in the VI process, whereas the RTM tool has a rigid tool. The flexible cavity in the VI process effects the resin flow's behaviour from that of the RTM process. The pressure profiles were curved for the VI experiments and were linear for the RTM experiments. Due to the fiber stiffness and the resin viscosity being equal the only differentiating factor is the difference between the pressure.

In relation to this research, the comparison isolates the effects of the preform thickness variation and the differentiating factor between the laminates would be due to the additional magnets which potentially may influence the resin flow.

When the additional magnetic compaction is substituted into formula 2.5; it would be assumed to maintain a higher compaction pressure (in relation to the amount of magnets / magnetic force) during the infusion. It would then result in a larger delta pressure and thus a faster filling time.

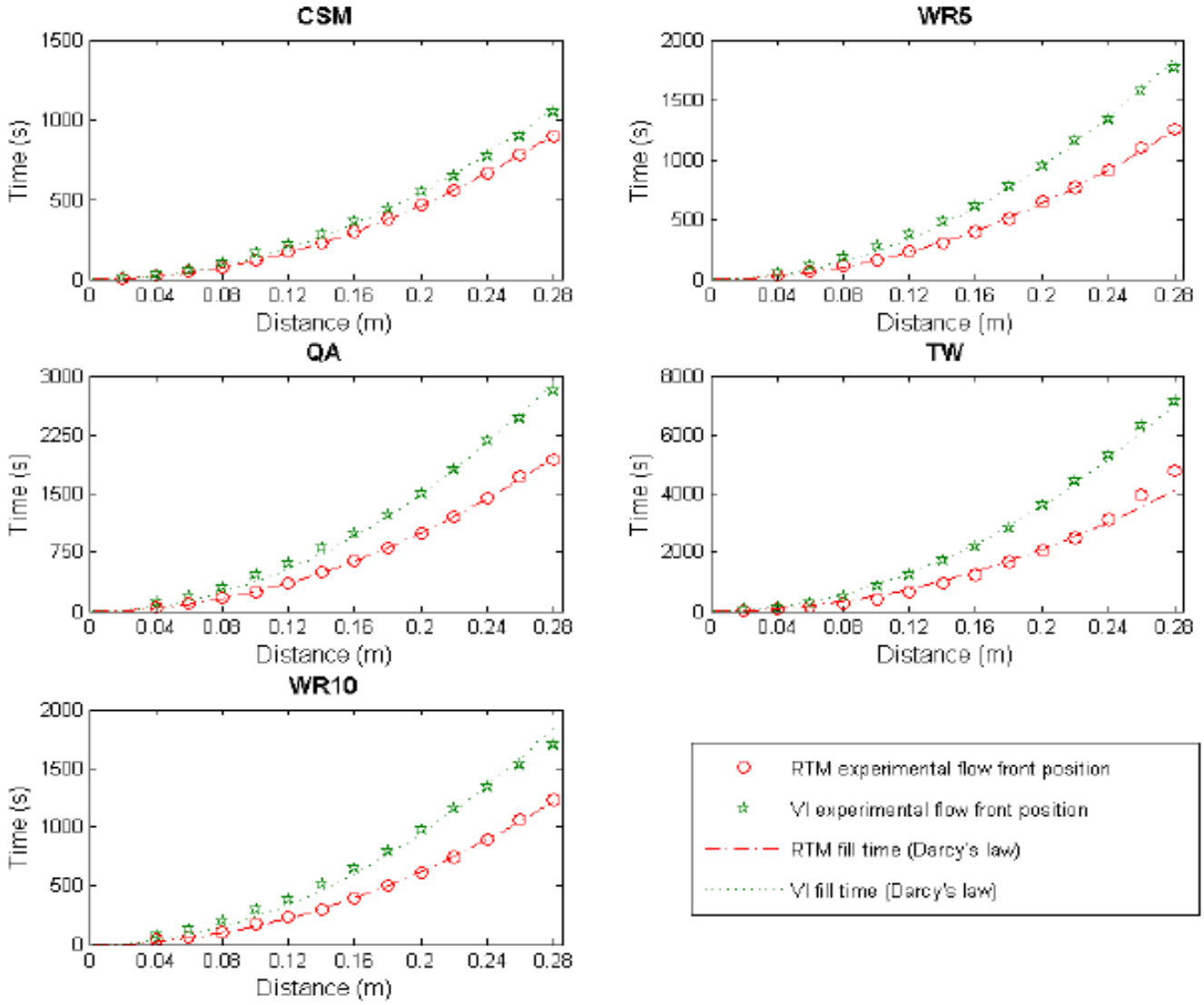

Figure 2. 6 Fill times related to various reinforced fabrics [31].

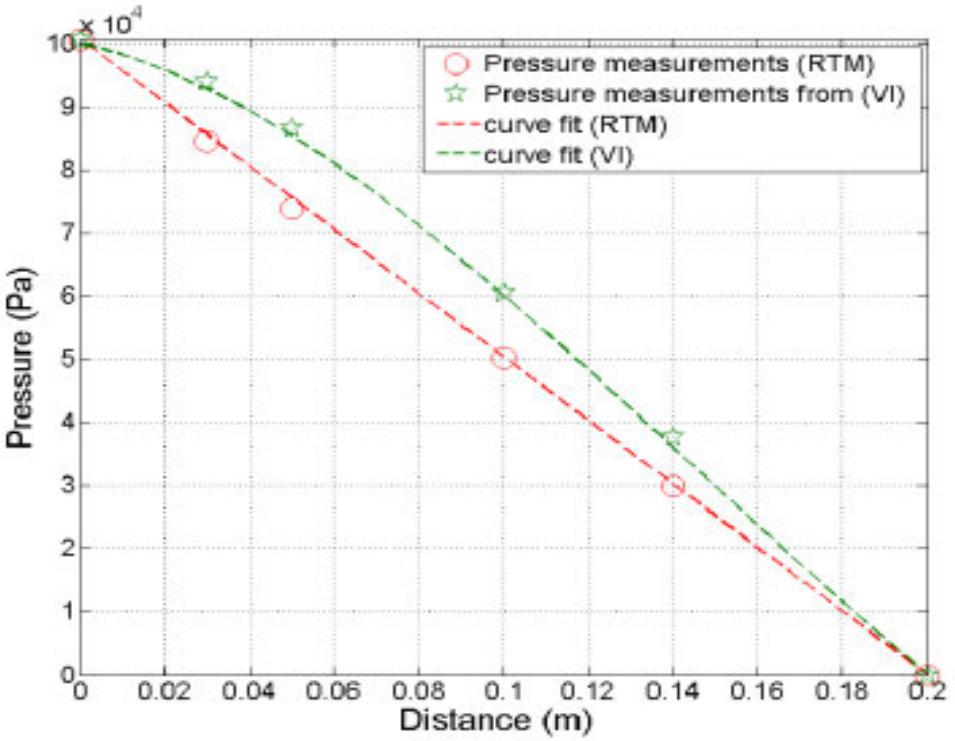

Figure 2.7 The linear RTM and the curved VI pressure profiles [31].

The RTM process had a linear pressure profile when compared to the curved VI process. The VI process had a completely flexible tool (membrane) and the RTM process had a rigid tool. Due to the VARTM process having a semi-rigid tool; an assumption is made that if a plot was to be made into Figure 2.7 the VARTM process would be in between the green VI line and the red RTM line. This research will focus on investigating the possibilities of using magnetic compaction in conjunction with the atmospheric pressure generated by the vacuum.

2.3 Magnetism

Due to the natural characteristics of magnetism, an investigation into the use of magnets in GRP tooling composite manufacturing techniques would be conducted in order to address the issue related to inconsistent fiber volume fraction. The intended strategy is aimed at investigating the use of magnetic forces to compress a fiber reinforced composite lay-up during manufacturing. Magnetic forces have been in use within industrial field such as the electromagnets used to lift scrap metal and cars within the material recycling industries. It is this magnetic clamping force that would be the point of focus for this research.

Once sufficient information has been obtained pertaining to the benefits and limitations of the different types of magnets, this information would then be compared and the most appropriate type of magnet would be selected. Further research would be conducted on the preferred magnet in order to determine their properties and to establish a full understanding of the underlying theory of magnetism.

Once the required magnetic details are understood, the experimentation related to the force of the selected magnets would commence. The initial steps of this research revolved around gaining in-depth knowledge in the field of magnetics. More so, how the flux in a magnetic field is obtained [64, 65] and how it is related to the force which is generated [66], depends on the type of magnets. This is required in order to make a precise decision on the type of magnet being selected.

2.3.1 Background

Magnetism primarily comprises of two sectors, the one being permanent [56, 67] magnets and the other being electromagnets [64, 68]. Each sector has its own variations and within each variation there are certain aspects (behavior and nature) which possess certain characteristics [69, 70] that are unique to that sector. The common factor that links the two sectors is known as magnetic flux density. The flux lines flow in a particular direction from north to south [71] [72]. The flux lines are either generated in electromagnets or they are permanent in a permanent magnet, hence the flux lines are either permanent or temporary which are dependent on various factors within both sectors.

2.3.2 Magnetic Theory

The field of magnetic theory is extensive, hence only the aspects related to this research will be discussed. The magnetic behavior experienced when dealing with magnets can be described in terms of field vectors. The externally applied field vector is at times referred to as the magnetic field strength, which is denoted as **H** is measured in amp/meters. The internal field strength within a substance that is subjected to an external field strength (H) is known as magnetic flux density, which is denoted as **B** and is measured in Tesla's or Wb/m^2. Both of which are related by the following formula.

$$\mathbf{B} = \mathbf{\mu H} \qquad (2.8)$$

This formula will calculate the magnetic flux density in a particular material, which is dependent on the following:

- B = Magnetic Flux Density
- H = Magnetic Field Strength
- μ = Permeability

The variable unit μ is referred to as permeability. This is a property of a particular medium in which the flux is measured in and the field strength passes through. More so, the permeability of free space is μ_0, which is equal to $4\pi \times 10^{-7}$.

Lastly relative permeability is μ_r, which is equal to $\mu_r = \mu / \mu_o$. This is specific to a material. It is the measurement to the degree to which a material can be a magnetized.

Another avenue in which the magnetic field strength and flux are related is known as the energy density or energy product of a magnet. It is equal to the **BH** which is measured in kJ/m^3 [73]. Further details pertaining to the energy density of magnets will be discussed in the permanent magnet section 2.4.

Details pertaining to the different fields of magnetism will be focused on in the sections to follow, as the magnetic flux calculation is unique to both the Electro-magnetic and permanent magnet fields.

2.4 Permanent Magnets

2.4.1 Background

The evolution of permanent magnets was perused in order to generate stronger magnetic flux lines, which in turn generates higher forces [56]. The details related to how a permanent magnet works, depends on the core materials from which the magnet is comprised of and how they are manufactured. There are specific manufacturing techniques [74, 75] which are used to manufacture the desired permanent magnets. During the manufacturing process the core ingredient materials have their respective atomic structure electronically charged and aligned in the same direction. It

is the atomic alignment as well as the electrically charged particles [76] that generates the external magnetic field.

2.4.2 Types of Permanent Magnets

There are approximately 5 major types of permanent magnets materials that come in different shapes [77] and sizes [78]. This research will compare the Ferrite and Neodymium magnets. These magnets obtain their magnetic properties through various manufacturing processes [78, 79]

The key performance characteristic related to permanent magnets. This characteristic is known as energy density. The energy density (section 2.4.5) of a permanent magnet is also a degree of measurement in which the performance of the permanent magnet may be categorized.

2.4.3 Primary Concepts

S. Laurent [80] has gone into detail describing how the magnetism of a the material is related to the electrons or the atomic nuclei and how the magnetic moment is aligned to the external magnetic field that is present during the manufacturing process. Whereas William D Callister [56] has gone into the details describing how the macroscopic magnetic properties are related to the magnetic moment which are associated with the individual electron spin. Each electron in an atom has its magnetic moment that originate from two avenues. The first being the orbital spin and the other being the electron spin. More precisely, this magnetic moment is known as the Bohr Magneton. It is the fundamental magnetic moment and it is equal to $\mu_B = 9.27 \times 10^{-24}$ A/m^2 [56]

$$\mu_B = \frac{q.h}{4\pi M_e} \qquad (2.9)$$

Where

- q = electron charge (c)
- h = Planck's constant (J·Hz^{-1})
- M_e = Electron Mass (g)

It is the manufacturing process which arranges the internal atomic microstructure [81] into a particular architecture [75, 82, 83]. There are a range of materials [67, 84] that are utilized in

manufacturing permanent magnets By aligning the desired atomic structure, it assists in securing the atoms permanently such that it will not be rearranged when exposed to other external magnetic fields. It is the internal microstructure that is formed which generates an external magnetic field.

Further research regarding the internal structure post manufacturing can be found in [85]. The classification of magnetic materials in which the magnetic fields are either fixed or altered are also referred to as soft magnetic materials, semi-hard materials and hard magnetic materials [86].

The evolution of permanent magnets was perused in order to generate stronger magnetic flux lines, which in turn generates higher forces. To summarize, there are various permanent magnets with different characteristics and properties which are ideally required to perform the same task. This task is to provide improved magnetic flux which provides the key characteristic associated with magnetism which are the attractive and repulsive forces.

2.4.4 Energy Density

As mentioned under section 2.3.2, the energy density of permanent magnets are closely related to the magnetic material properties (soft [87], semi-hard [88] and hard [86]) and the characteristic of being magnetized as well as de-magnetized. The energy density is the product between the magnetic flux **B** and the external field strength **H** of a magnet.

Energy Density = **BH** (KJ / m^3) (2.10)

The energy density is the amount of energy present per given volume within a magnet. It is also one of the few ways of measuring the performance of a permanent magnet. Figure 2.8 illustrates the difference between the different types of permanent magnets.

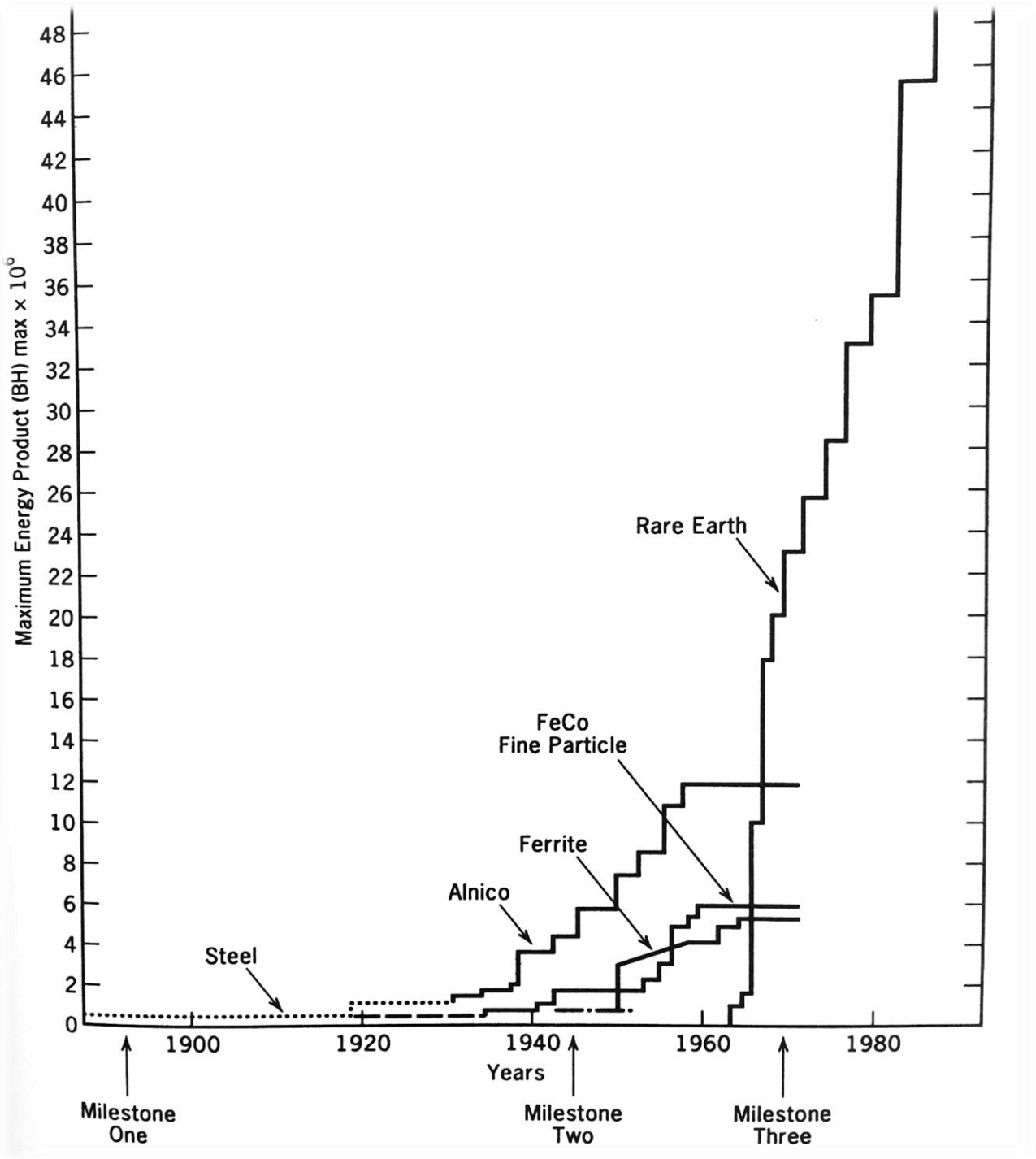

Figure 2.8 Energy density graph [1]

As Figure 2.8 illustrates, the energy density found in the Rare-Earth (Neodymium) magnets are significantly larger than the other permanent magnets. According to J.M.D. Coey [73] the ferrite magnets have one tenth the energy density than that of a rare-earth neodymium magnets, which is visible in the graph above. The energy density is the potential force available per given volume.

In a direct comparison between a ferrite and a neodymium magnet of identical volumetric dimensions, the neodymium magnet would obtain a force ten times that of the ferrite magnet.

A. **B.**

Figure 2.9 Ferrite magnet (A) lay side-by-side to a Neodymium-Iron-Boron magnet (B)

2.4.5 Permanent Magnet Force-Distance

The force formula of permanent magnets is directly related to the flux present within a magnet. The formula for calculating magnetic flux of a disk magnet at a fixed distance is presented in formula 2.10 [70].

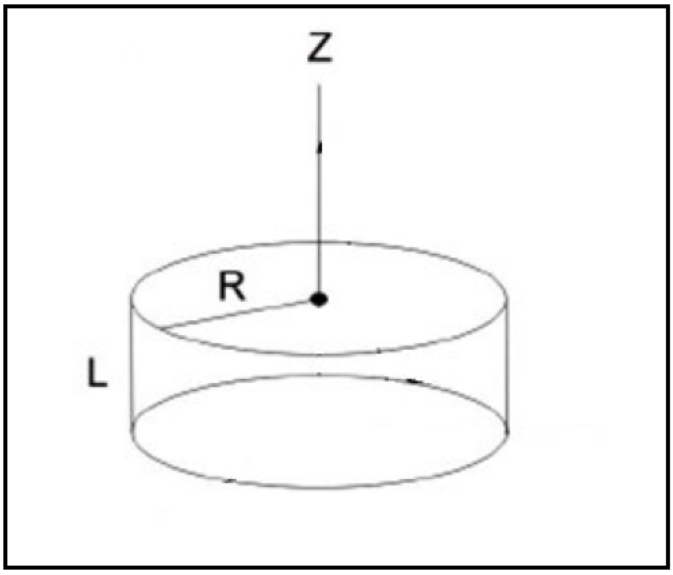

Figure 2.10 Diagram of cylindrical magnet.

$$B(z) = \frac{\mu_0 M}{2}\left(\frac{z}{\sqrt{z^2+R^2}} - \frac{z-L}{\sqrt{(z-L)^2+R^2}}\right) \qquad (2.11)$$

- B = flux (Wb/m^2)
- M = Magnetic saturation (T) (2.12)
- z = distance (m)
- R = Radius (m)
- L = Thickness (m)
- $\mu_0 = 4\pi \times 10^{-7}$ is the permeability of free space (N/A^2),

$$M = 0.60.\ \mu_B.\ N_{Ni} \qquad (2.12)$$

Where

- N_{Ni} = Number of unpaired electrons (2.12)
- μ_B = Bohr Magneton (A/m^2)

$$N_{Ni} = \frac{\rho_{Ni} \cdot N_A}{A_{Ni}} \qquad (2.13)$$

Where

- N_{Ni} = Number of unpaired electrons
- ρ_{Ni} = Atomic density (N)
- N_A = Avogardo's number
- A_{Ni} = Molar / atomic Mass (g)

According to V. S. Juan Manuel Camacho [70] M = Br = Remanence which is measured in Gauss or Tesla's. additional details related to the residual induction of permanent magnets can be found in R. J. Parker [75].

Once the required information has been substituted in the formulae above, the resulting flux gets substituted into the force formula. (2.14).

$$F = \frac{B^2 A}{2\mu_0} \qquad (2.14)$$

The current force formula (2.14) is only able to give the force at a fixed distance. Constant force analysis at incremental distances is to be explored in this research.

2.4.5.1 Permanent Magnet Force Enhancement

There are some particular avenues in which the magnetic flux lines from a permanent magnet can be manipulated as well as enhanced. Theses avenues are related to the magnet's placement as well as being incorporated with other external materials. The placements can range from stacking as well as being utilized in permanent magnet cores. Figure 2.11 is an illustration of the different types of core design in which a permanent magnet may be used.

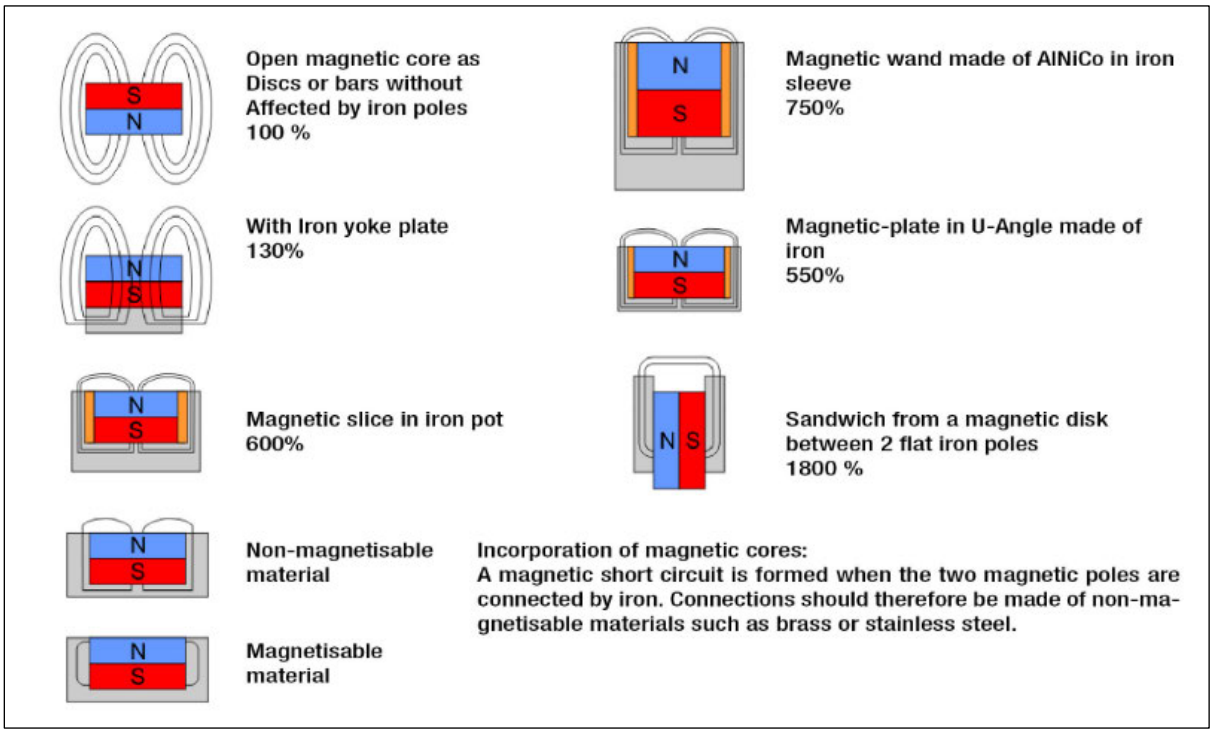

Figure 2.11 The nature and direction of the magnetic flux lines.[4].

All of the above-mentioned variations are utilized in unique methods to enhance the magnetic flux lines in order to improve the forces available.

2.5 Electromagnetism

2.5.1 Background

Electromagnetism was first discovered in 1820. An electromagnet is a combination of electricity and magnetism. The field of electromagnetics is vast and broad, ranging from electric motors, antenna's, transformers as well as PCB relays [66] [68] [89].

2.5.2 Primary Concept

When a current is passed through a conducting wire then a magnetic field (magnetic flux lines become present) is generated [67, 79]. If the current is turned off or stopped then the magnetic field is reduced to nothing and ceases to exist. This is a unique characteristic of electromagnetism in which the magnetic fields (magnetic flux lines) can be controlled via the flow of the electrical current.

The nature and behavior of the flux lines develop a range in shape, strength and direction [89, 90]. These are directly related to the amount and direction of the current flowing through the conductive wire as well as some additional elements. These elements range from the number of windings; type, shape [91] and material of the conducting wire [92]; the core materials[79] as well as the core designs dimension and shape [89]. The details related to the flux lines generated as well as the current-carrying conducting wire can be found in [93].

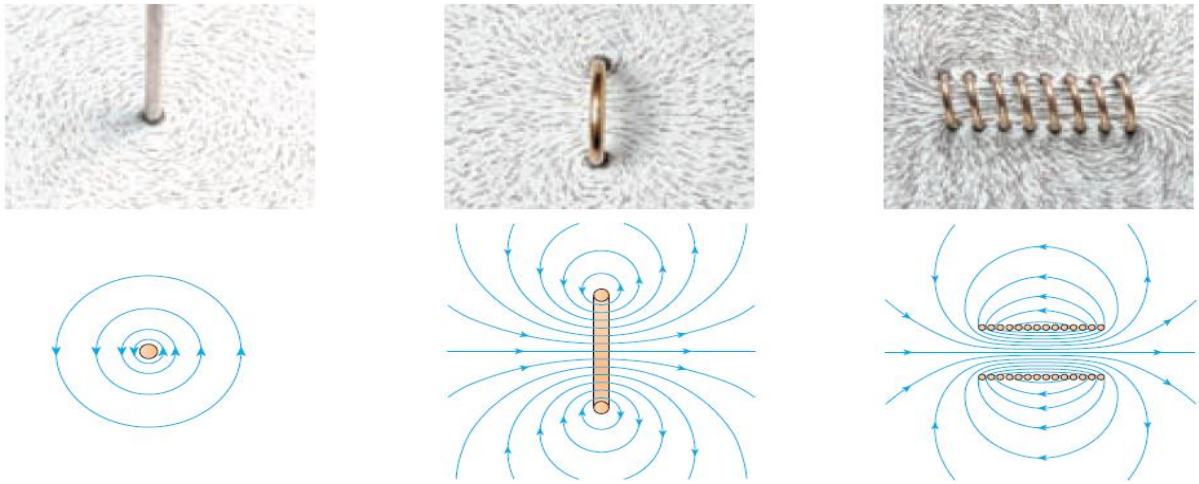

Figure 2.12 The nature and direction of the magnetic flux lines [6]

As mentioned above when the magnetic flux lines are generated, they vary according to certain aspects.

Figure 2.12 visually illustrates that nature and direction of the magnetic flux lines generated by a current passing through a conductive wire of various shapes and layouts. The first set off images on the left being a singular straight wire with the magnetic flux circulating around the wire. The second being a singular wire in a cylindrical loop in which the magnetic flux flows through the loop. Lastly the third set of images on the right illustrate a coil of conducting wire. This image clearly illustrates how there are more magnetic flux lines present due to there being more conductive material in the form of a coil. All off which contribute to the amplification of the magnetic flux present. Hence with this in mind, by adding more coils there would be a larger magnetic field present (See Formula 2.4 variable **"N"**).

The formula for calculating the flux of an electromagnet is shown here below.

$$B = \frac{N.I.\mu_0}{l} \quad (Wb) \qquad (2.15)$$

Where:

- B = is the magnetic field (Wb/m^2),
- $\mu_0 = 4\pi \times 10^{-7}$ is the permeability of free space (N/A^2),
- N = is the number of turns in the solenoid,
- I = is the electric current (A),
- l = is the length of the solenoid (m).

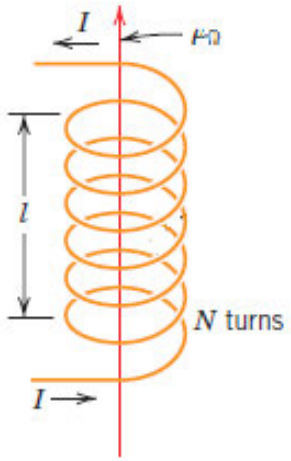

Figure 2.13 The working principle of an electromagnet. [3]

The conductive material from which the coils are manufactured, are affected by the material's internal resistance. The electrical conductivity of a material is the reciprocal quantity of its resistivity. The more conductive a material, the less resistive it is and vice versa. A material which has a high electrical conductivity is considered an electrical conductor [94].

A unique design has been utilized which is known as Bitter coils [92]. Instead of having a cylindrical cross-sectional area just like the conventional conductive wire, the Bitter coils are rectangular in profile. They are flat plates which are precisely stacked (with an electrical

insulator in-between) in a circular pattern to form a solenoid. There are two major benefits to this Bitter coil design. The first being the ability to obtain a higher number of turns **"*N*"** (stack more coils) in the same or a lower total coil height "***l***". The second benefit of the Bitter coil is a larger surface area in which more current **"*I*"** can be passed through the coil. Both of these major benefits lead to a larger magnetic field being generated.

The magnetic flux generated from the electromagnet contributes toward the force generated. See formula 2.15 [66, 68].

$$F = \frac{B^2 A}{2\mu_0} \qquad (2.16)$$

Where

- F = Force (N)
- B = flux (Wb/m^2)
- A = Cross sectional area (m^2)
- $\mu_0 = 4\pi \times 10^{-7}$ is the permeability of free space (N/A^2),

It is this force that this researched is focused on. As these forces will be analyzed on order to investigate the usability as well as practicality of being implemented into a composite manufacturing technique.

2.5.3 Electro-Magnetic Applications

The electromagnetic sector has two types of fields. One field is referred to as resistive electromagnets and closely followed by the other field being superconducting electromagnets [95]. Resistive magnets are made from normal material like copper or aluminium and it is used regularly in transformers etc. [96]. The superconducting magnets are used in MRI scanners in hospitals as well as other industrial applications such as the Maglev [97], which is a train that levitates and transverses with the aid of superconducting electromagnets. The difference between the two is that the superconducting magnets are cooled to approximately 4 Kelvin. The phenomenon linked to

lowering the temperatures of superconducting material are such that these materials can transfer an electric charge which does not experience any resistance [98] (one of which is lost in heat). Due to the zero-resistance characteristic the superconducting electromagnets, they can have larger currents flowing through which in turn produces exceptionally higher magnetic fields.

Both types of electromagnets possess unique qualities and purposes as well as generate large amounts of flux and therefore forces [92, 99]. These electromagnets require highly skilled personnel; substantial amount of electricity; large capital investments; additional safety; cooling and security.

In order to achieve these high flux and forces there are certain limitations that are present, and these are physical limitations; financial investments, magnetic saturation [56]; solenoid construction as well as heating issues. Most noticeably is the constant usage of electricity in order to remain working. In relation to this research, these types of magnets are not as diverse in terms of being easily scalable and flexible with regards to being implemented into a composite manufacturing technique. This research is focusing more on the techniques which are already linked to the more affordable route with lower financial requirements.

2.6 Electro-Permanent Magnets

2.6.1 Introduction

There has been a recent finding in the field of magnetism which utilize the positive aspects related to both the permanent and electro-magnets fields. It is known as the Electro-permanent magnet. It has the ability of being able to be controlled (on and off state) like an electro-magnet and the constant as well as consistent force of the permanent magnets [85]. The electro-permanent magnet illustrates the pole alternating of a semi-hard ferromagnetic material (Alnico magnet) with minor amount of electrical pulses. It is a device in which it remains in a particular (fixed) state and whose external magnetic field can be regulated by an electrical pulse. The major benefit of such a device is that it does not require constant electrical power to maintain the electromagnetic field as compared to the conventional electro-magnets which requires continuous power during use. The electrical power is only required to carry-out the mechanical work or to change the devices state (on / off).

2.6.2 Working Principle

The electro-permanent magnet consists of two magnetic materials wrapped in a copper coil with two iron (magnetically soft material) end caps. The two magnets are Neodymium-Iron-Boron (magnetically hard) and an Alnico magnet which is magnetically semi-hard.

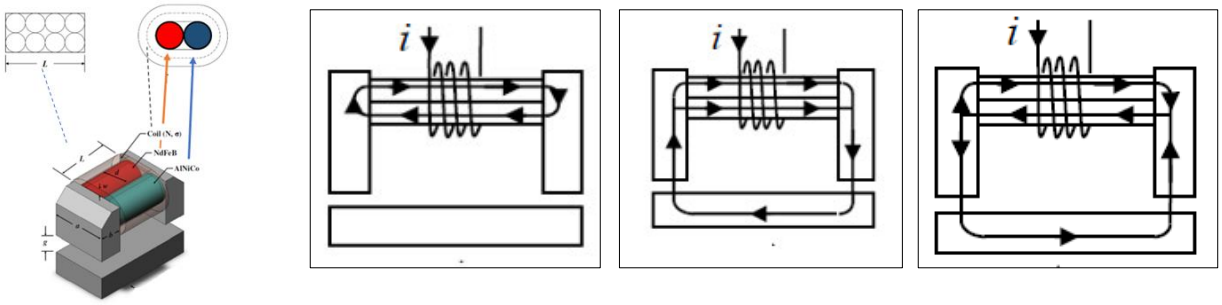

Figure 2. 14 An Electro-permanent magnet layout and flux flow [2]

When the electro-permanent magnet is in a "Neutral-state" the magnetic flux flows within the iron endcaps, traveling from the north pole of one magnet to the south pole of the other magnet.
There is no external flux generated to attract any magnetically susceptible objects. This is very similar to a conventional electro-magnet which is in its off state.

When a pulse of a desired strength, polarity and duration is passed through the coil windings, it magnetizes the semi-hard (Alnico) material such that an external magnetic field is generated by the flowing flux. The pulse alternates the poles of the semi-hard Alnico magnet. By this taking place, the magnets poles are now in the same direction.

This will cause the flux to travel externally from one endcap to the other, which in turn can attract any magnetically susceptible object. The current can now be switched off and the external magnetic field will remain.

In order to return the electro-permanent magnetic into its "neutral-state". A current of the same strength, duration and opposite polarity would be passed through the coil in order to reverse the polarity of the Alnico magnet. The polarity of the Neodymium-Iron-Boron remains unchanged.

2.6.3 Applications

The electro-permanent magnet is one of the more recent publications in the field of magnetism. Current industrial use can be found in the injection moulding industry. The injection tool is held against the walls of the injection moulding machine [100] with an electro-permanent magnetic clamping system.

2.6.4 Magnetic Summary

The permanent magnet field has its advantages with regards to usage flexibility in relation to this research. The desired magnets either permanent or electro-magnet would be applied to a GRP tooling technique. The positive side to permanent magnets is the versatility with regards to providing constant and consistent force. However, a setback to permanent magnets is the lack of ability to turn "on or off" like the electro-magnets. Keeping in line with the aim of this research, the most appropriate magnet would now be investigated. Based on availability and strength the most commonly available magnet (Ferrite) as well as the strongest commercially available magnet (Neodymium) was selected. The Neodymium-Iron-Boron (Nd_2 Fe_{14} B) magnets are rare earth ferromagnetic magnets that are manufactured via the sintering process. These magnets have Antiferromagnetic [56] properties which have a Tetragonal crystalline micro-structure. Neodymium-Iron-Boron magnets have a larger flux density [**B**] and field intensity [**H**] when compared to the Ferrite magnets. These magnets are also considered to be hard magnets. According to J. M. D. Coey [73] a Ferrite magnet has one-tenth the energy density (**BH**) then an identical Neodymium-Iron-Boron magnet. The Ferrite magnets, also known as ceramic magnets are anisotropic with Ferrite properties. They are also manufactured using either a wet or dry pressed sintering technique. Various methods of magnetic implementation with the VARTM GRP tools would be assessed during the research experimentation.

2.7 Literature Review Summary

Due to the complexities and nature of the electromagnetics such as:

- Excess Heat
- Limited amperage required due to wire gauge.
- Constant risk of equipment failure (fuse failure) due to excess amperage.
- Electrical safety and security.
- Physical application methods with multiple wires running to and from the tooling.
- Manufacturing limitations, in which electromagnets can only be used were power is available.

- Being physically limited to certain designs that potentially may not adhere to the GRP tooling with complex geometry.

A fiber reinforced composite manufacturer would be inclined towards another conventional composite manufacturing technique and based on this, the research will peruse an experimental investigation in the field of permanent magnets. Focusing specifically on the force-distance relationship related to permanent magnets. This is keeping in line with the aim of this research, which is to investigate the use of magnetic forces to compress a fiber reinforced composite lay-up during manufacturing in order to achieve a more desirable volume fraction.

As mentioned in the magnetic summary (section 2.6.4) the most appropriate magnet would be investigated. Based on availability, strength the most commonly available magnet (Ferrite) as well as the strongest commercially available magnet (Neodymium) were selected. This research will investigate the magnetic forces, behavior and nature obtained by the selected magnets.

The magnetic forces would be measured via the means of a testing mechanism, with the aid of an Arduino microcontroller [101]. The information gained through the experimental procedure would provide a clear understanding of the forces generated at incremental distances. The findings would lead to the selection of the most appropriate magnet or a combination of magnets that would be used in the proposed experimentation. The desired magnetic compaction pressure [102] would be explored and compared to a Low pressure (GRP) composite manufacturing technique.

Current processes which utilize GRP tooling have inconsistent fiber volume fraction [31], this is undesirable if the item is a structural component. With the aid of magnetic compaction, an increased and consistent fiber volume fraction would be the desired outcome from this research.

The VARTM technique was selected to be the preferred manufacturing [103] technique which would be utilized in manufacturing the experimental laminates. This technique has the best degree of accuracy and consistency (related to GRP Tooling) for analyzing the comparative data generated from the experiments.

A direct comparison would be analyzed between a magnetic assisted VARTM technique and a standard VARTM technique. The isolation of all the parameters related to the VARTM technique will allow only the additional forces from the magnets to be the differentiating factor in the compaction between the laminates.

If there is a difference in the laminate thickness, this proves that the magnets do assist with regards to compaction and in turn provides a more consolidated panel. This will lead to a better volume fraction [24] which leads to better mechanical performances.

A recent study has been conducted by Amirkhosravi, Mehrad, Pishvar, Maya Altan and M Cengiz which examined the use of magnets in composite manufacturing in [104, 105]. These studies have shown that magnetic assistance can produce a product with improved mechanical properties. However, taken the research above into consideration, this research would be conducted in order to introduce a manufacturing process which has design flexibility, scalability and practicality, in order to produce a product that potentially has improved mechanical properties.

3. Experimentation and Equipment

3.1 Magnetic Experimentation and Equipment

A comprehensive experimental regime was undertaken in order to fully understand the force-distance nature of permanent magnets at incremental distances. The experimentation would comprise of two sections, the first of which would be related to various magnetic materials, dimensions as well as layouts and the second would be related to the comparative VARTM experimentation. The raw data provided by the magnetic experimentation would be interpreted and processed providing a clear indication on the type of magnet as well as the layout that would be utilized and integrated into a comparative VARTM experiment. The VARTM technique would be used in order to conduct a comparative experiment to investigate the use of magnets in composite manufacturing. The experiment would be conducted in such a manner that all parameters and conditions are fixed. The constraining of parameters would emphasize the one and only additional variable which is the additional magnetic units. The intended result would be aimed at obtaining a panel which is more consolidated than that of a regular VARTM technique. This would provide a positive outcome to the investigative research.

A jig was required in order to observe the force of the permanent magnets at incremental distances. The jig which was used; was an old tensile testing machine that was refurbished in order to use the motor as well the other moving components. The advantage of using a tensile testing machine is that it was designed to withstand high forces in a linear direction. The firm structure of the tensile machine is beneficial as it prevented any captured data from being inaccurate.

All the additional fittings both on the movable upper cross head and the fixed base platform were machined from aluminium. These precautionary measures were implemented in order to eliminate any possible magnetic interference from external materials. Further details related to the comparative VARTM experiment will be discussed in Chapter 5.

3.1.1 Magnetic Experimental Equipment Components and Instrumentation

The components and equipment which were utilized in conducting the experiments are numbered and listed below.

1. Testing jig (tensile testing machine) Figure 3.1 A
2. Lower aluminium rod, Figure 3.1 A.

   This aluminium rod was fixed to the base of the tensile machine. The lower magnets would be secured to this apparatus during experimentation.
3. Motor directional controller Figure 3.1 A.

   The controller was used to select the direction of the movable crosshead (item 7 below) in one of two ways, either up or down.
4. Arduino microcontroller display, Figure 3.2 A and B.

   The Arduino microcontroller was programmed (coded) to display the forces recorded by the load cell strain gauge (item 9 below)
5. Mitutoyo dial gauge, Figure 3.2 B.

   This dial gauge was used to accurately measure the distance between the magnets during experimentation.
6. Motor speed controller (Variac), Figure 3.2 C.

   This was used to control the speed and position (point-point) of the movable crosshead.
7. Movable crosshead, Figure 3.1 B and C.

   The upper aluminium rod (item 8) and strain gauge were fastened to the crosshead.
8. Upper aluminium rod, Figure 3.1 B and C.

   The opposite experimental components (magnets and plates) were secured to this apparatus during the experimentation.
9. Load cell strain gauge (5Kg & 20 Kg), Figure 3.1 B and C.

   The load cell would be used to measure the force of the magnets during the experimentation.
10. Mild steel (2mm) and aluminium (5mm) mounting plates. (No image).

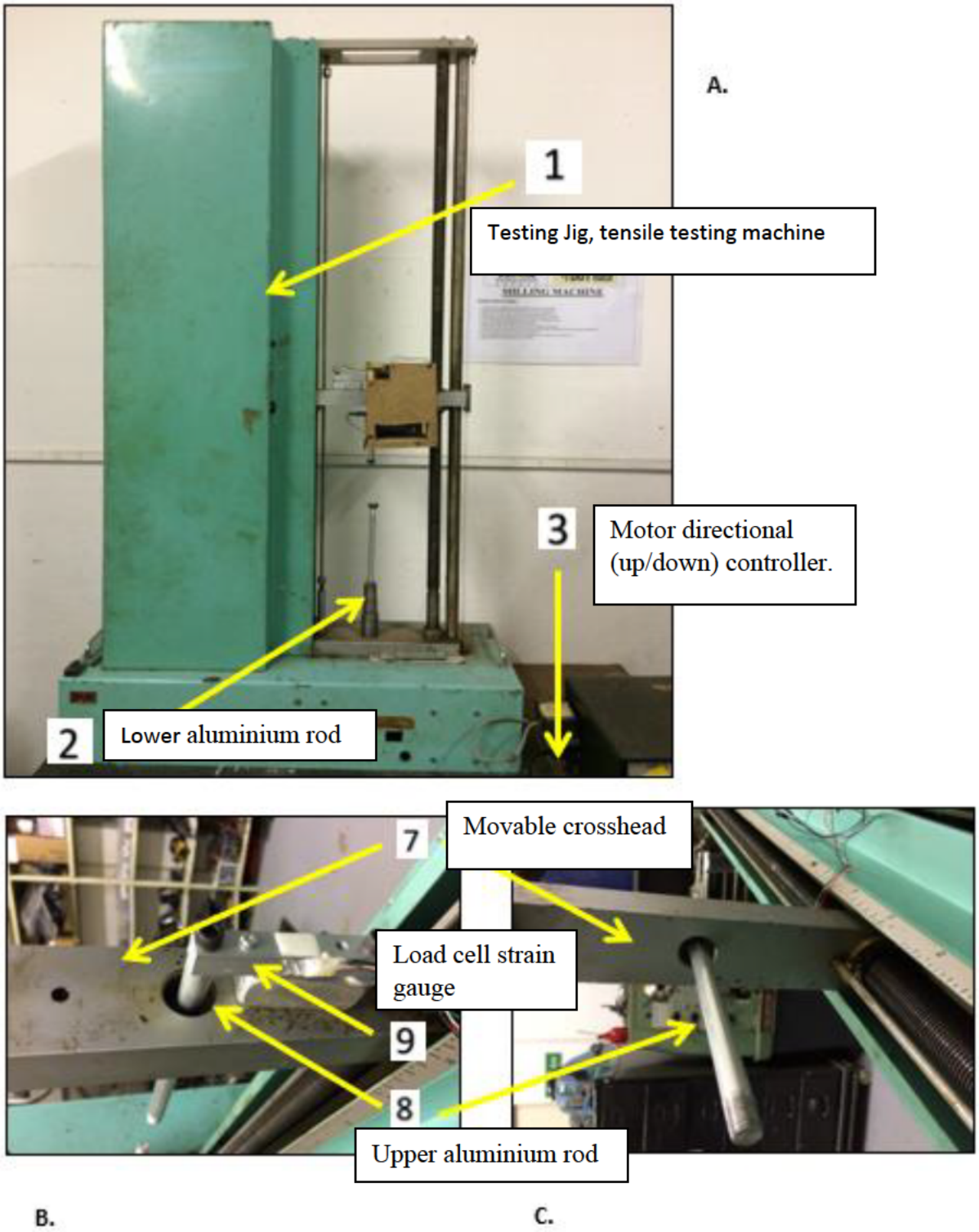

Figure 3.1 Experimental equipment, tensile testing machine with cross-head and load cell.

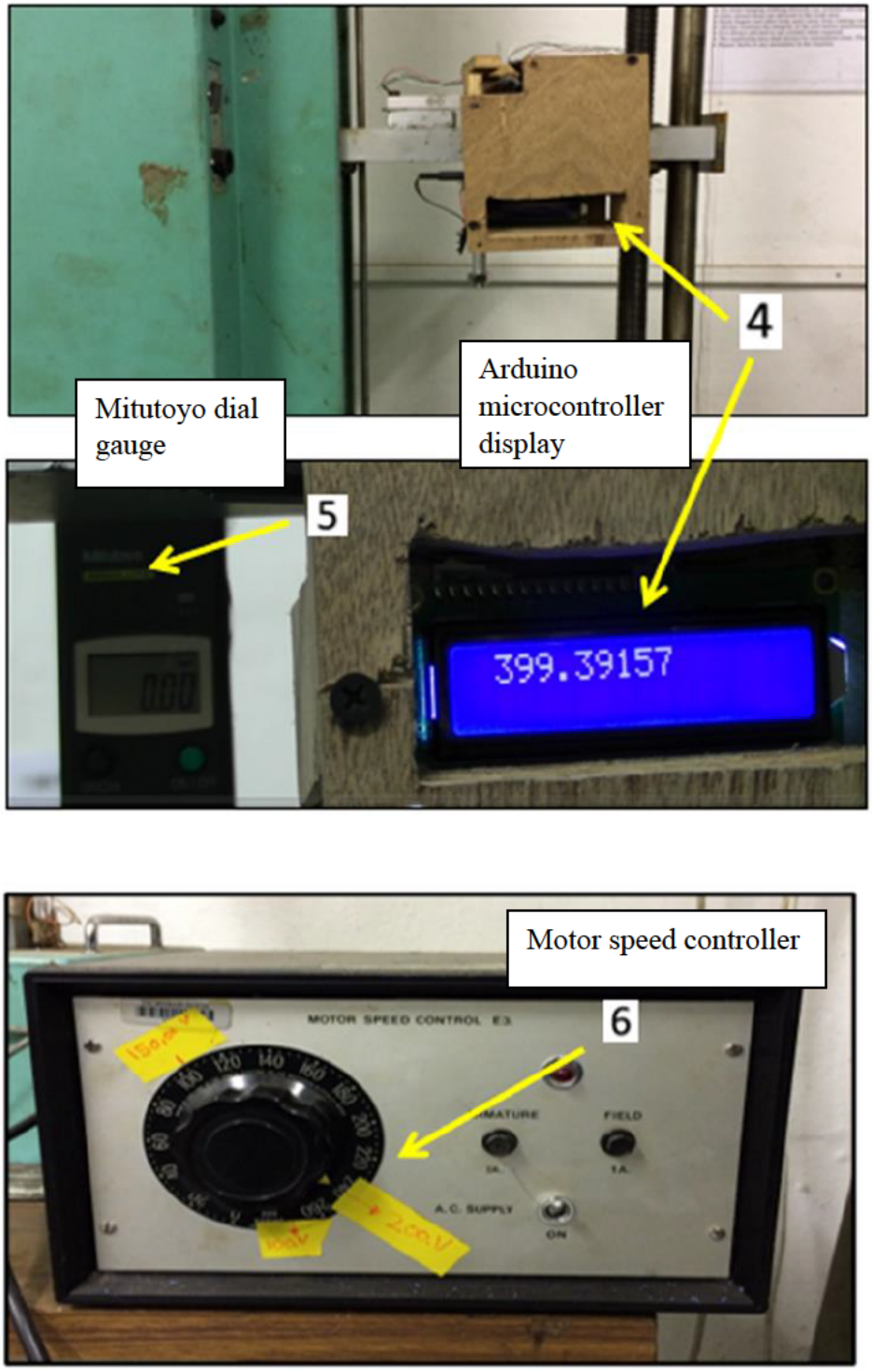

Figure 3.2 Experimental equipment, Scale reading, dial gauge and variac controller.

3.2 Experimental Procedure

After theoretical research and analyses was conducted regarding the field of magnetism, the most suitable field for this application would be the use of permanent magnets.

In order to measure the forces that the magnets obtain; an experimental procedure and plan was developed, to find out what force a magnet possesses at the desired distance. Therefore, a force-distance experiment was conducted to analyze the forces at incremental distances.

A magnet would be secured to the lower non-magnetic 5mm aluminum plate and a 2mm mild steel plate was secured to the upper moving crosshead. As the plate moves closer or further away from the magnet the forces would increase or decrease accordingly. This data would then be captured and analyzed to further understand the force-distance relationship of the magnets. These experiments would also guide the research into using the most ideal magnet for the comparative analyses.

There were two types of experiments conducted. The first number of experiments conducted were the preliminary experiments. These experiments were conducted in order to select the most appropriate magnetic material as well as combination of magnets to achieve sufficient force required for compaction.

3.2.1 Magnetic Experimental Procedure

The magnetic experiments were conducted in the following manner:

- To prevent any damage to the Mitutoyo dial gauge, ensure sufficient space between the upper and lower plates before removing them.
- Prepare the two 5mm aluminium plates by bonding (hot glue) the required experimental apparatus, such as the required magnets and the 2mm mild steel plate.
- Secure the upper and lower plates to the jig (items 2 and 8).
- Ensure the Mitutoyo dial gauge is in the fully compressed position; attach spacers to the lower plate if required to.
- Ensure the data capturing apparatus is setup and ready for recording.

- Select the desired direction on the Variac, turn on the Variac and lower the cross head at a desired speed.
- Return the Variac dial to the zero position once the desired distance (0.34mm) between the two plates has been attained.
- Turn the Variac off and reverse the direction into the upward position.
- Zero out the dial gauge.
- Record the time, date and initial scale reading.
- Begin the data capturing process with the desired data capturing apparatus.

- Record the force at 0.5mm intervals ranging from 0.34mm-20mm.
- Due to the nature of the VARTM experiment being static (fixed distance), a pause for 30 seconds at every 0.5mm interval allowing the scale to provide concrete data.
- Begin the experiment and observe the stop / start process.
- Turn off the Variac once the distance of 20mm is visible on the dial gauge.
- The directional switch is then placed into the neutral position.
- Stop the recording.
- Transfer, save, analyse, capture and process (graphs and tabulate) the data.
- The abovementioned procedures would be repeated for all the magnetic experimentation.

3.3 Magnetic Experimental Scheme

All the magnetic experiments were conducted to research the force-distance relationship of permanent magnets. Initial experimentation would be aimed at finding out which permanent magnet (material) possessed the highest force at the furthest distance. Based on the experimental data obtained, the most ideal permanent magnet requirements could be distinguished and selected for the desired purpose. Further experimentation would be guided by the magnets dimensions as well as strategic placements. Finally, the desired magnets in the most optimal design would be integrated into a comparative VARTM experiment to investigate the possibilities of improving laminate compaction in composite manufacturing.

Each of the experiments mentioned in Table 3.1 below will follow the Magnetic Experimental Procedure as mentioned in section 3.2.1 above.

Table of Magnetic Experimentation		
Number	Title Description	Reason
Experimental Set 1	The attractive force-distance relationship of various magnetic materials of identical size and quantities on an aluminium bottom plate.	Magnetic Material selection
Experimental Set 2	Magnetic placement and bottom plate material change	Magnet Placement & orientation
Experimental Set 3	Magnetic orientation and stacking of two - four neodymium magnets	
Experimental Set 4	Magnetic dimension change as well as the implementation of stacking	Magnet Dimension

Table 3.1 Table of magnetic experimentation

An accompanying flow chart (Figure 3.3) is presented below. The flow chart visually illustrates the magnetic experimental regime that would be undertaken.

Figure 3.3 below is linked to Table 3.1 above. Together with the experimentation progression it was designed to assist in understanding how the magnets were positioned, stacked, placed and orientated.

There are two sets of arrows within the flowchart, they are horizontal and vertical arrows. The horizontal arrows represent the inter-experimental progression and the vertical arrows represent a few points. The first being, the external-experimental progression between the experiments (1,2,3 and 4); the second being the utilizing of data gained and the last point being a point of comparison between the experiments. These vertical arrows were inserted to illustrate the pivotal points related to the magnetic experimentation.

3.4 Magnetic Experimentation Flow Chart

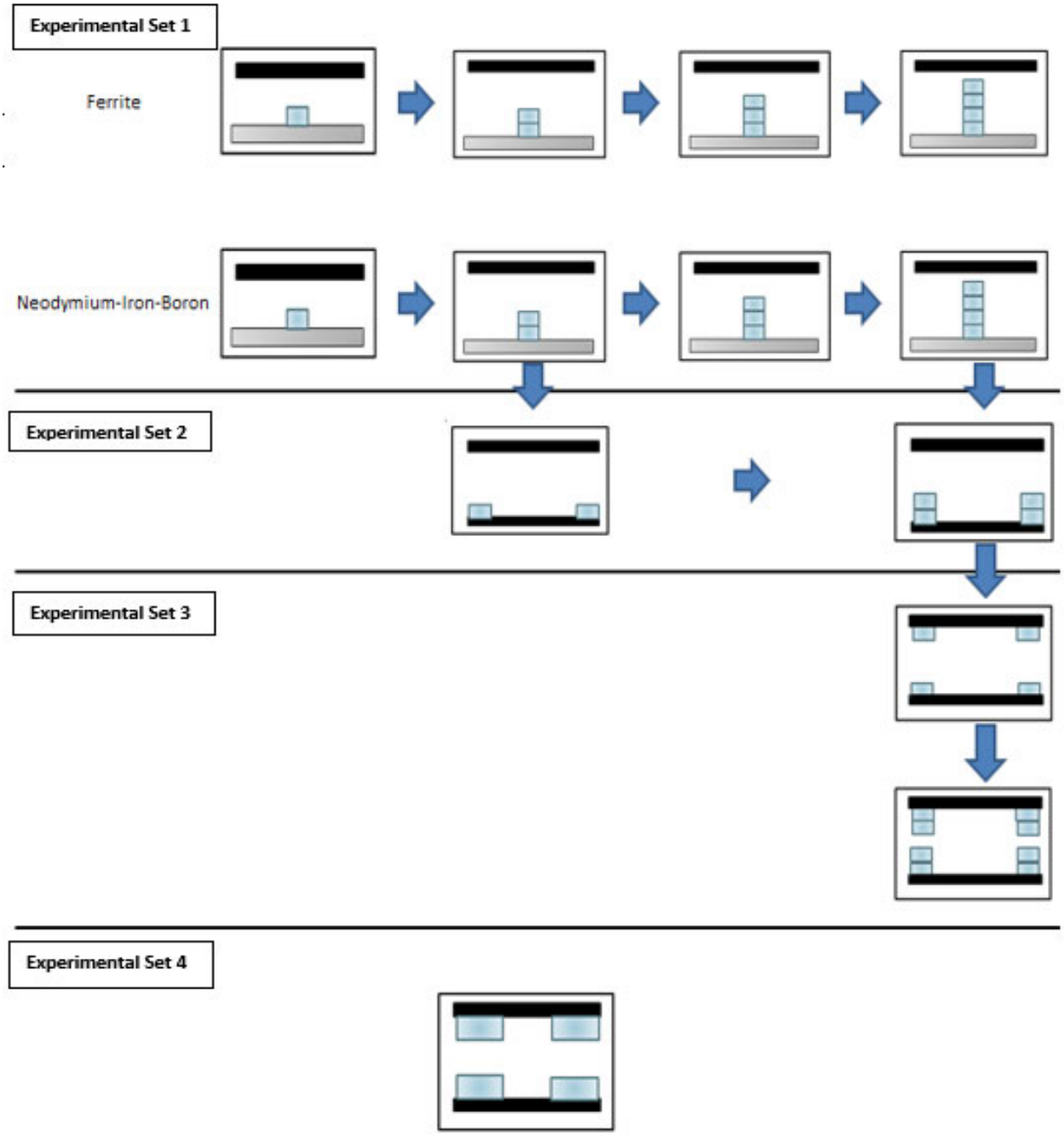

Figure 3.3 Magnetic experimentation flow chart

Experimental Set 1				
TITLE	The attractive force-distance relationship of various magnetic materials of identical size and quantities on an aluminium bottom plate.			
Material	FERRITE			
	Experiment ID	Quantity of Magnets	Diameter	Thickness
	1.1.1	1	10mm	5mm
	1.1.2	2	10mm	5mm
	1.1.3	3	10mm	5mm
	1.1.4	4	10mm	5mm
Material	NEODYMIUM			
	1.2.1	1	10mm	5mm
	1.2.2	2	10mm	5mm
	1.2.3	3	10mm	5mm
	1.2.4	4	10mm	5mm

Table 3.2 Experimental set 1

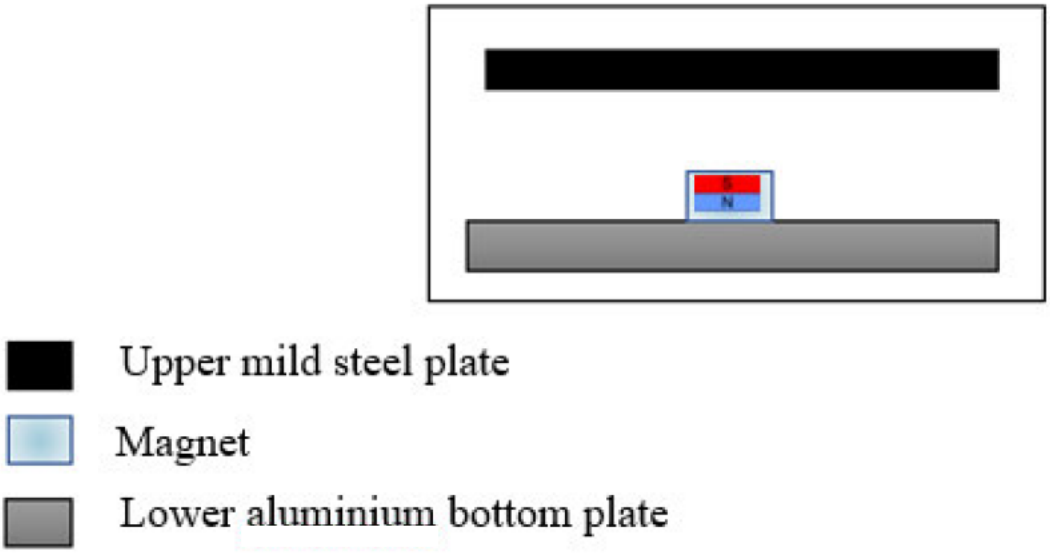

Figure 3.4 Experimental set 1 illustration

3.4.1 Experimental Set 1 Description

The aim of this experiment was to investigate the attractive force-distance relationship of various magnetic materials of identical size as well as quantities. This experiment was split into two parts; both of which would be run concurrently. The first part would be between the different magnetic materials and the second would be the investigation of magnetic stacking.

Based on the knowledge gained in section 2.4.5 (Literature review) related to the energy density of permanent magnets, the two types of magnets being investigated (in-terms of force-distance) in this experiment is a Neodymium-Iron-Boron as well as a Ferrite magnet. Both the magnets have identical dimensions, being 10mm in diameter and 5 mm thick.

The magnets would be secured with hot glue to a non-magnetic bottom plate (aluminum) which would then be fastened to the jig's base platform. The aluminium bottom plate was used to ensure there is no magnetic interference. Careful consideration was taken in order to eliminate any other factors that may interfere with the raw data and readings. The 2mm mild steel plate was secured to the upper crosshead.

Based on the knowledge gained in the Literature review relating to the stacking of permanent magnets, the second part to this experiment was aimed at investigating the effects magnetic stacking. The stacking was conducted in order to assess the difference (Force-Distance relationship) between a single magnet and several magnets stacked.

Table 3.2 illustrates that this experimentation would be conducted twice; the first being Ferrite magnets and the latter being the Neodymium-Iron-Boron magnets.

The results of this experimentation lead to the better understanding of the following:

- Which magnetic material would be the preferred material for the remainder of this research.
- Gaining knowledge related to the difference in magnetic stacking.
- In terms of stacking, the quantity of magnets that would be practical

Experimental Set 2				
TITLE	Magnetic placement and bottom plate material change			
Material	FERRITE			
	Experiment ID	Quantity of Magnets	Diameter	Thickness
	2.1.1	2	12mm	5mm
Material	NEODYMIUM			
	2.2.1	2	10mm	5mm
	2.2.2	4	10mm	5mm

Table 3.3 Experimental set 2

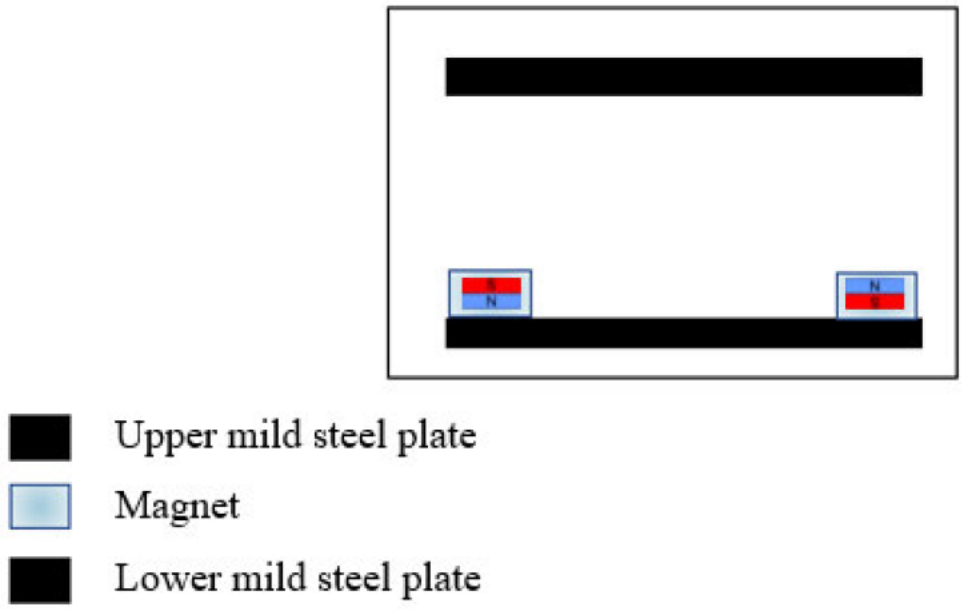

Figure 3.5 Experimental set 2 illustration.

3.4.2 Experimental Set 2 Description

This experiment investigated a new magnetic placement in comparison to experiment 1 and stacking as well as introducing a mild steel lower plate.

This experiment utilized the results gained from experiment 1. For the remainder of this investigation, these results assisted in identifying the most suitable permanent magnet material as

well as the desired quantity required for stacking. Hence experiment 2 only used the Neodymium-Iron-Boron permanent magnets as well as a maximum of 2 magnets per stack.

Like experiment 1 above this experiment was split into two parts; both of which would be run concurrently. The first part would assess what the effects a different magnetic placement would have in relation to the Force-Distance relationship. The second part to this experiment is the use of magnetically permeability materials coupled with core layouts.

With reference to section 2.4.5.1 Figure 2.11 there were multiple other permanent magnet core designs investigated. Due to several complexities these core designs were not perused. This led to the current placement being examined. This design has a few advantages over some of the other designs that were examined; these advantages are physical flexibility, scalability and practicality.

With the knowledge gained in section 2.4.5.1 related to the magnetic flux line interaction with magnetic and non-magnetic materials; this experiment substituted the non-magnetic bottom plate (aluminum) from experiment 1 to an iron bottom plate. This was done to enhance the magnetic flux over a further distance which is intended to a produce a higher force.

The magnets were placed (as illustrated in Figure 3.6) in a side-by-side pattern. The magnets themselves were however placed with their respective magnetic poles in the opposite orientation. For example, if the magnet on the left would be placed with the north pole facing up and the magnet on the right would be placed with the south pole facing up; the iron bottom plate would assist the magnetic flux travelling from the north pole of the right magnet to the south pole of the left magnet.

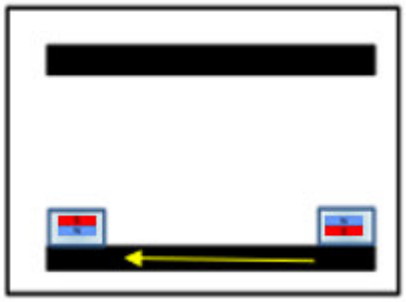

Figure 3.6 Desired flux flow due to new placement illustration.

By having the opposite upper plate in close proximity, this then allows the magnetic flux to follow the same pattern as the bottom mild steel plate. This interaction causes the opposite upper plate to be attracted to the lower magnets which creates a clamping force.

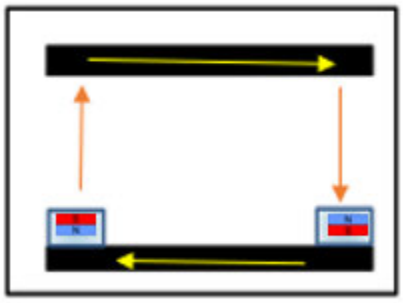

Figure 3.7 Desired flux flow through upper plate due to the new placement.

The magnets were secured to the lower bottom mild steel plate in the new configuration which was then fastened to the jig's base platform.

The result from this experiment would lead to a better understanding of the most appropriate magnetic placement; the ideal quantity of magnets in terms of stacking and the effects of using an iron bottom plate. Similarly to experiment 1 the results of this experiment 2 would be utilized for experiment 3 and would assist for the remainder of this research.

Experimental Set 3				
TITLE	Magnetic orientation and stacking of two and four neodymium magnets			
Material	NEODYMIUM			
	Experiment ID	Quantity of Magnets	Diameter	Thickness
	3.2.1	4	10mm	5mm
	3.2.2	8	10mm	5mm

Table 3.4 Experimental set 3

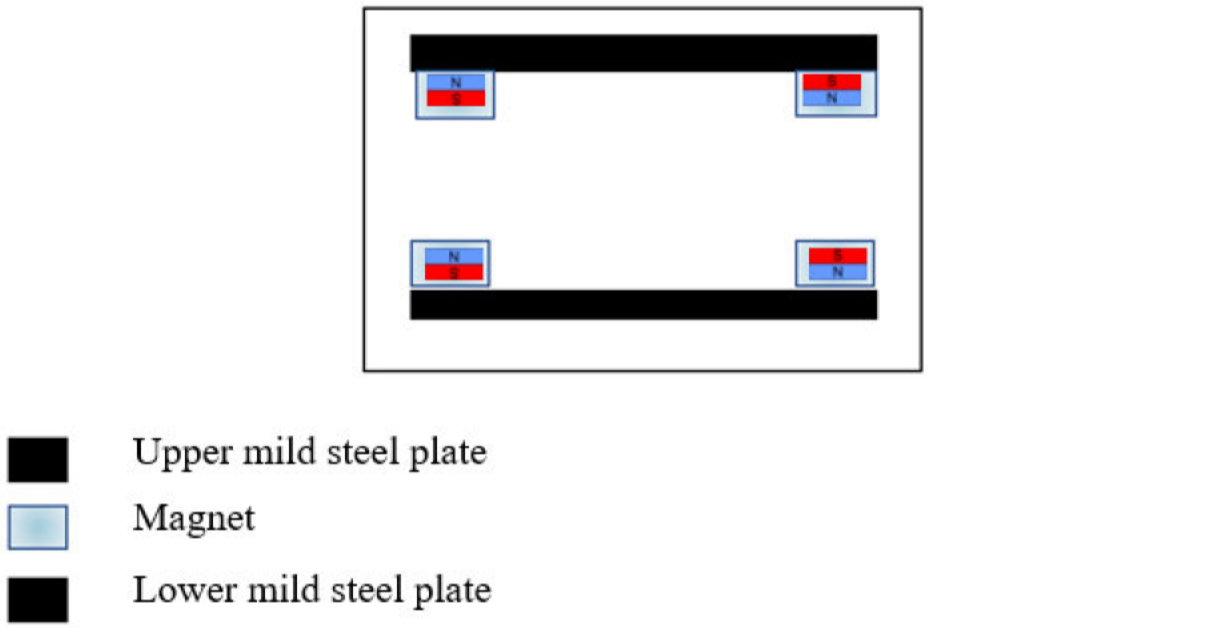

Figure 3.8 Experimental set 3 illustration

3.4.3 Experimental Set 3 Description

The aim of experiment 3 is to analyze and investigate a new mirrored orientation in comparison to experiment 2. The upper mild steel plate from experiment 2 was replaced with an identical magnetic arrangement as the lower magnetic plate. The effects of the new mirrored orientation were explored and compared to experiment 2.

The identical lower magnetic arrangement was used in the upper arrangement in reverse so that the opposite poles would attract to one another.

This experiment utilized the results gained from experiment 2, as these results assisted in identifying the most suitable magnet placement as well as the desired quantity required for stacking. In-terms of size and material, experiment 3 utilized the identical Neodymium-Iron-Boron magnets from experiment 2. Similar to experiment 2 this experiment only used a maximum of 2 magnets per stack. The only addition was the quantity required which was due the stacking of both the upper and lower arrangements. No analysis was conducted in order to assess if the magnets had similar strengths. Such analysis would be conducted in experiment 4.

By having the upper arrangement in close proximity; in identical fashion to experiment 2; this then allows the magnetic flux to flow from the North pole of the lower arrangement to the South pole of the upper arrangement and vice versa for the adjacent magnets, as the natural flow of magnetic flux is from the North pole to the South pole.

The result from this experiment would assist this research in obtaining the ideal magnetic orientation as well as analyzing the effects of stacking.

Experimental Set 4				
TITLE	Magnetic dimension change as well as the implementation of stacking			
Material	NEODYMIUM			
	Experiment ID	Quantity of Magnets	Diameter	Thickness
	4.2.1	4	20mm	3mm
	4.2.2	4	20mm	5mm
	4.2.3	8	20mm	5mm
	4.2.4	4	22mm	10mm

Table 3.5 Experimental set 4

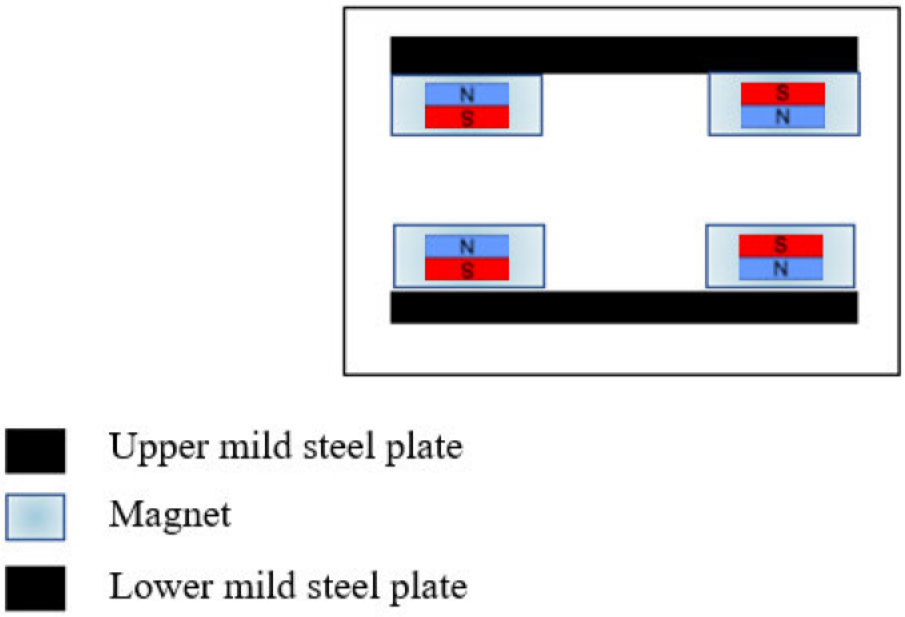

Figure 3.9 Experimental set 4 illustration.

3.4.4 Experimental Set 4 Description

The aim of this experiment is to obtain the ideal magnet dimensions. The larger the magnets used the larger the magnetic force generated. There are limitations to utilizing the largest available magnet as it may become impractical as well as unsafe during use.

This experiment is a continuation from experiment 3 with regards to the permanent magnetic material as well as design layout (placement and orientation). The only differentiating factor is the physical dimensions of the magnets.

There are certain factors related to the size of the magnets. Factors such as the availability of the magnets; physical difficulties and dangers related to the handling of large magnets. Another hazard related to the strong Neodymium-Iron-Boron magnets are collisions due to proximity. If two magnets are left unattended in close proximity; the magnets may collide and shatter. Therefore, additional personal safety gear such as gloves and face shields are required. Lastly, if the magnets are too large, then the physical requirements of being able to be applied on a composite mold may not practical.

In relation to this experiment, it would be run in identical fashion to experiment 3. The only difference was to ensure that the magnetic centers from the adjacent magnets on the same plate are further away than the opposite magnates on the upper plate. Reason being, if the magnetic centers are too close then the magnetic flux lines would rather travel to the closer adjacent magnets then to travel across to the upper arrangement. This would be undesirable as this could possibly reduce any attraction forces that may be present.

The result from this experiment could possibly conclude the magnetic aspects relating to this research; once the desired dimensions are obtained as well as the desired force at the required distances. The investigation would proceed to implementing these magnetic clamping units onto a comparative VARTM panel. This experiment was conducted several times is order to assess repeatability.

3.5 Magnet Experimentation Summary

Based on the above-mentioned experiments the possibility of utilizing a proposed magnetic configuration in a composite manufacturing process would be analyzed. The magnetic configuration will be implemented in a VARTM manufacturing process in order to investigate what effects the additional compaction pressure has on a laminate. The implementation process will be analyzed and would assess a safe apply and release procedure for the magnets. The ideal scenario would be the production of a panel which is thinner, as this would yield better mechanical properties. The results of the magnetic experiments are presented in Chapter 4.

4 Magnet Experimental Results

4.1 Experimental Results

A comprehensive experimental regime was conducted to fully understand the force-distance relationship of permanent magnets at incremental distances. The experiments as mentioned in Chapter 3 above comprised of two sections, the first of which would be related to the magnetism and the second would be related to the comparative VARTM experimentation.

Initial experimentation was aimed at finding out which permanent magnet (material) possessed the highest force at the furthest distance. Further experimentation would be guided by the magnets dimensions as well as strategic placements. Based on the experimental data obtained, the most ideal permanent magnet requirements could be distinguished and selected for the desired purpose.

This chapter will focus on the results pertaining to the magnetic aspect of the experimentation (Experiments 1-4). The raw data provided by the magnetic experimentation would be presented in this chapter. The interpretation and processing of the data gained (illustrated below) provide a clear indication on the type of magnet material, placement, orientation and dimensions.

Finally, the desired magnets in the most optimal design would be integrated into a comparative VARTM experiment to investigate the possibilities of improving laminate compaction in composite manufacturing.

The results from Experiments 1-4 are expanded on below.

4.2 Experimental Set 1 Results

The aim of this experiment was to investigate the attractive force-distance relationship of various magnetic materials (Ferrite and Neodymium-Iron-Boron) of identical size and quantity. This experiment was split into two parts; both of which would be run in succession. The first part would be between the different magnetic materials and the second would be the investigation of magnetic stacking. The permanent magnets used in this experiment are Neodymium-Iron-Born and Ferrite. The desired distance between the magnets would be investigated in the experiments to follow. As mentioned in the introduction the desired distance takes into consideration the two 5mm thick PMMA tools and fiber preform up to 5mm, hence the desired distance is from 10mm-15mm.

The table below is identical to Table 3.2 found in chapter 3. The only difference is the addition of the formula column to the right. These formulae were obtained through the MATLAB Curve Fitting application. The Curve Fitting application plots the data provided on a X and Y axis; the application then interpolates the raw data (via a selected mathematical function) in the form of a best fit curve. A variety of mathematical functions are available in which the most optimum function which best fits the raw data provided would be selected.

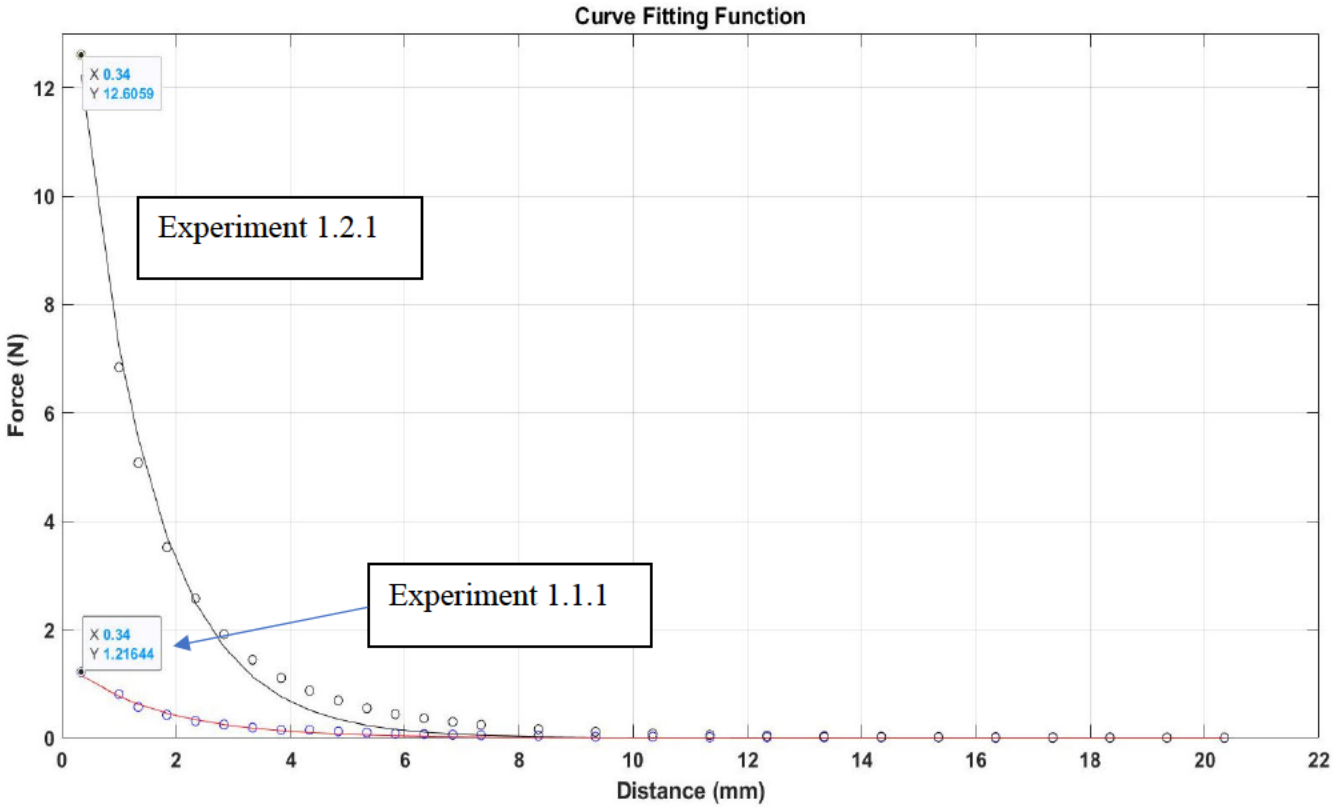

Figure 4.1 MATLAB curve fitting function, the smooth curve being generated by MATLAB curve fitting and the circular dots are the raw data point.

Figure 4.1 illustrates the curve fitting function in MATLAB. The circular points are the raw data points (Exp 1.1.1 and 1.2.1) and the smooth line curve is generated via the formula provided with an accuracy of 95% (according to MATLAB).

Upon processing the captured data in MATLAB. The mathematical function which was selected according to the MATLAB curve fitting application; which best fit the raw data inserted; was a natural logarithmic decay. These are the formula present in the formula column within the tables

below. The experiment ID's (e.g. Exp 1.1.1) as well as further details which are presented within the graphs, are tabulated in the tables related to each experiment.

The primary aim related to experiment 1 was to investigate the difference relating to the permanent magnetic materials.

The results from the experiment 1 relating to the Ferrite magnets are presented in the graph (Figure 4.2). After analyzing the information now present in the graphs below, there are immediately two highlighted aspects related to the plots above.

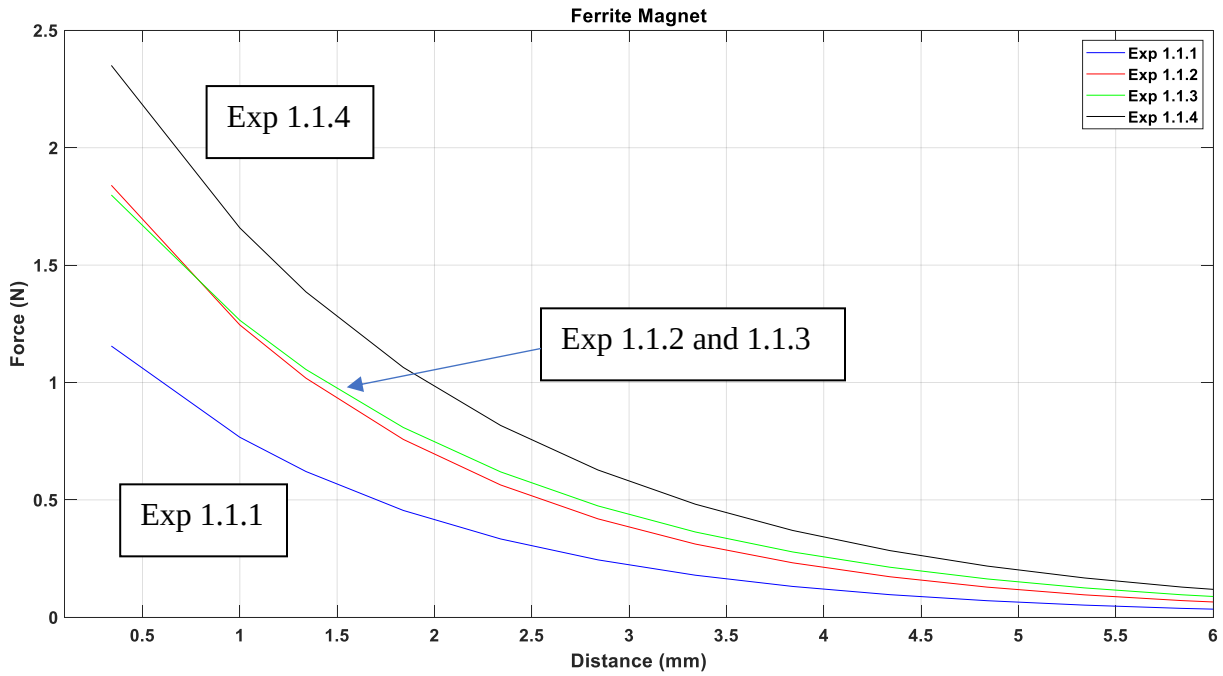

Figure 4.2 Experimental set 1: best fit ferrite plot

The first point illustrates that all the experiments tend to have identical characteristics. As the distances increase the force decreases in an identical manner. The second noticeable point is the effects of stacking. The forces do not double, triple or quadruple in relation to the number of magnets being stacked.

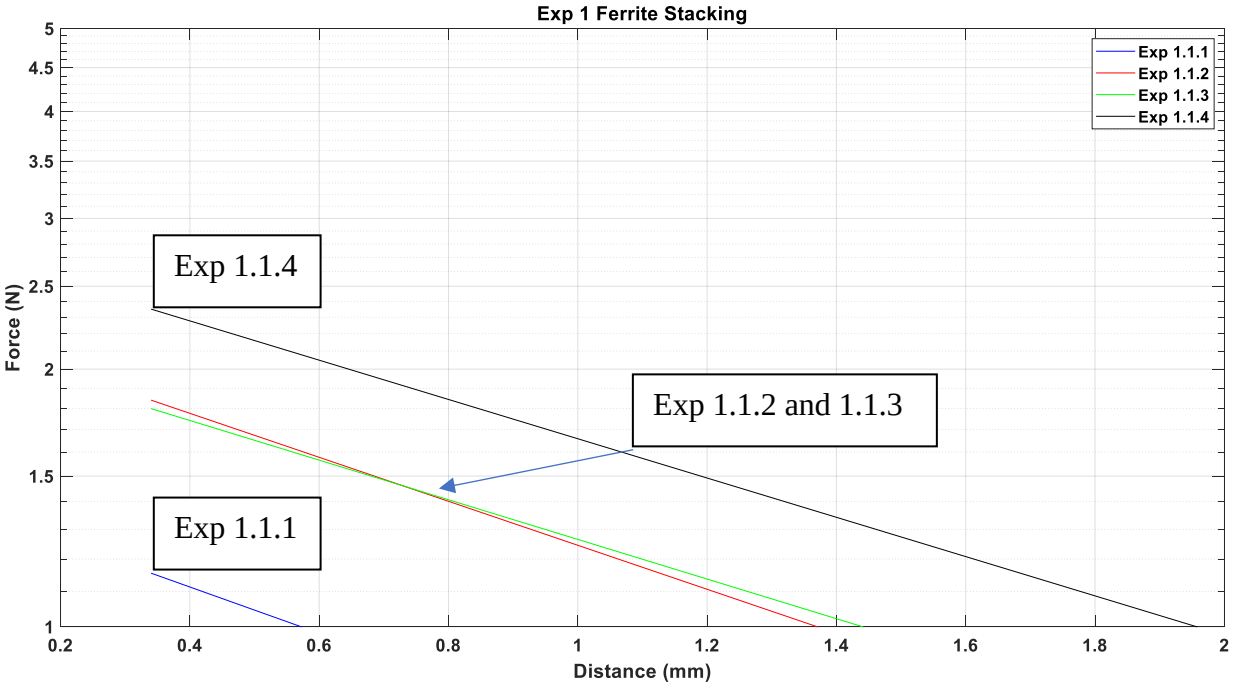

Figure 4.3 The logarithmic plot of Figure 4.2, illustrates the effects of magnetic stacking ferrite magnets.

The logarithmic graph presented above (Figure 4.3) graphically illustrates the effects of stacking. The force did increase; however it was incremental and not the product of the initial force (singular magnet) nor was it exponential.

The double stacking is approximately 70% times stronger, whereas the effects of triple and quadruple stacking are approximately 80% & 135% times stronger respectively.

As stipulated in Table 3.1 and Section 4.2, the primary objective related to experiment 1 was to investigate the difference in force-distance relationship between the two magnetic materials.

The experiments related to the Neodymium-Iron-Boron magnets are presented in the graph below.

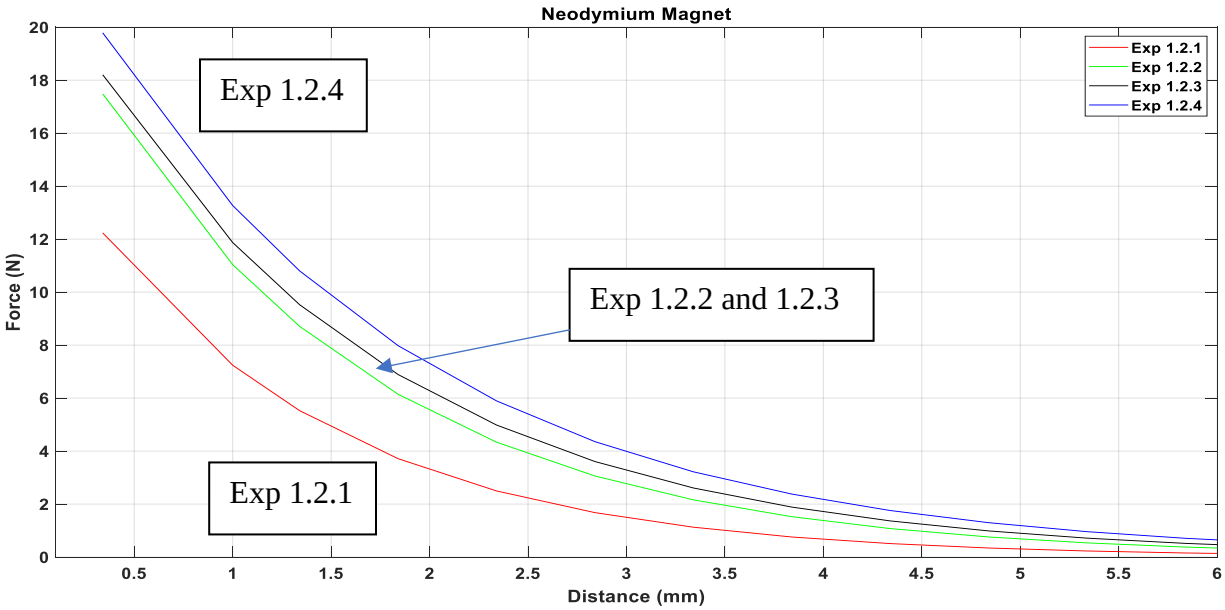

Figure 4.4 Experimental set 1: best fit neodymium plot

As mentioned above the forces at the desired distance (10mm-15mm) would be investigated in the following experiments. The nature of the results presented for the Neodymium-Iron-Boron graphs (Figure 4.4) have an identical, natural logarithmic decay encountered by the Ferrite magnets. The procedure for obtaining the formula for these graphs were conducted in the same manner as the Ferrite magnets. The effects of stacking also experienced the very similar pattern to the Ferrite.

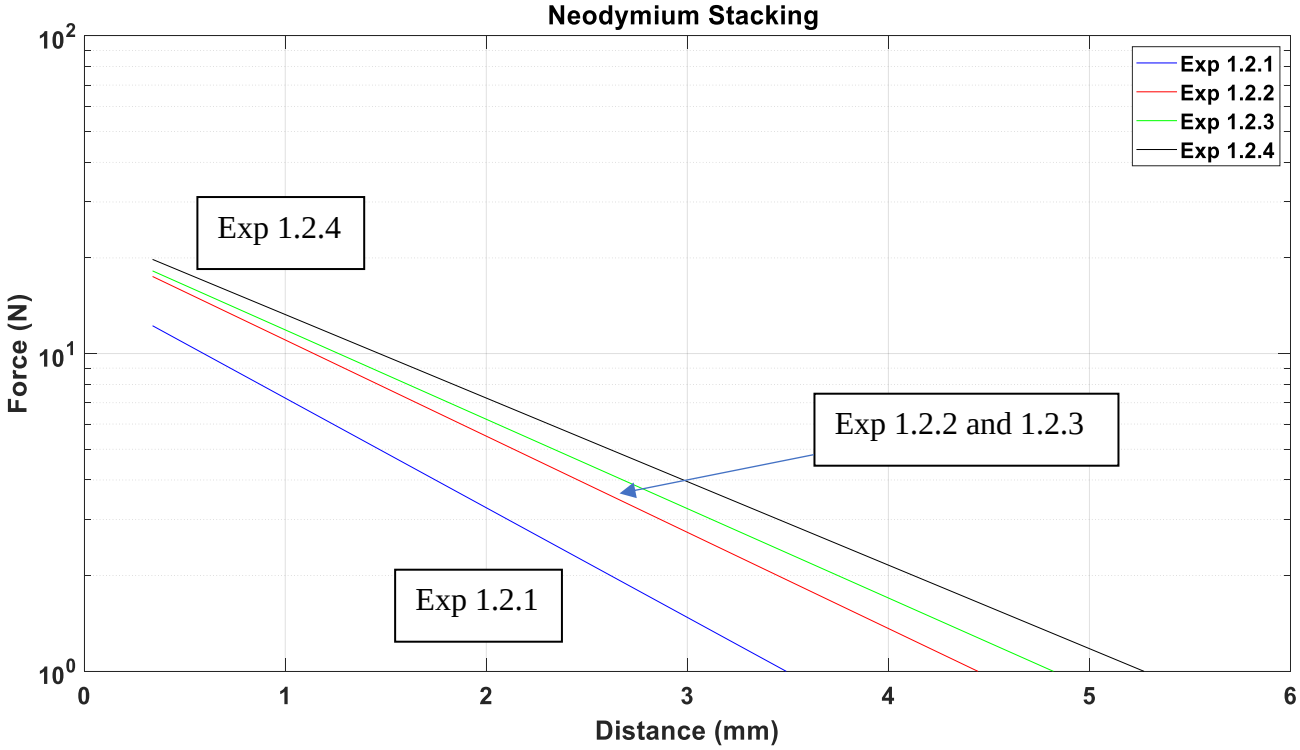

Figure 4.5 The logarithmic plot of Figure 4.4, Illustrates the effects of magnetic stacking Neodymium-Iron-Boron magnets.

The unique nature of stacking the Neodymium-Iron-Boron magnets can be viewed in the Logarithmic graph above. Similar to the Ferrite magnets the forces do not double, triple or quadruple in relation to the number of magnets being stacked.

The double stacking being approximately 50% - 60% times stronger when compared to that of triple or quadruple stacking which is approximately +/- 80% and 90% - 100% times stronger respectively.

Experimental Set 1 Results					
TITLE	The attractive force-distance relationship of various magnetic materials of identical size and quantity on an aluminium base plate.				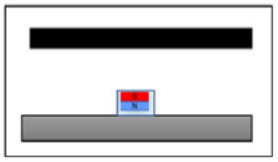
Material	FERRITE				Formula *
	Experiment ID	Quantity of Magnets	Diameter	Thickness	f(x) = a*e*exp(b*x)
					$f(x) = ae^{bx}$
	Exp 1.1.1	1	10mm	5mm	a = 1.427, b = -0.6211
	Exp 1.1.2	2	10mm	5mm	a = 2.25, b = -0.5916
	Exp 1.1.3	3	10mm	5mm	a = 2.156, b = -0.5331
	Exp 1.1.4	4	10mm	5mm	a = 2.813, b = -0.5283
Material	NEODYMIUM				
	Exp 1.2.1	1	10mm	5mm	a = 16.03, b = -0.7947
	Exp 1.2.2	2	10mm	5mm	a = 22.16, b = -0.6971
	Exp 1.2.3	3	10mm	5mm	a = 22.69, b = -0.6477
	Exp 1.2.4	4	10mm	5mm	a = 24.31, b = -0.6054

Table 4.1 Experimental set 1 results

The main and most obvious observation gained from this experiment was the ferrite magnets have one tenth the strength of the rare-earth neodymium-iron-boron magnets. This is in-line with the theoretical research found in section 2.4.5 according to J.M.D. Coey [73]. This can be seen from Figure 4.6.

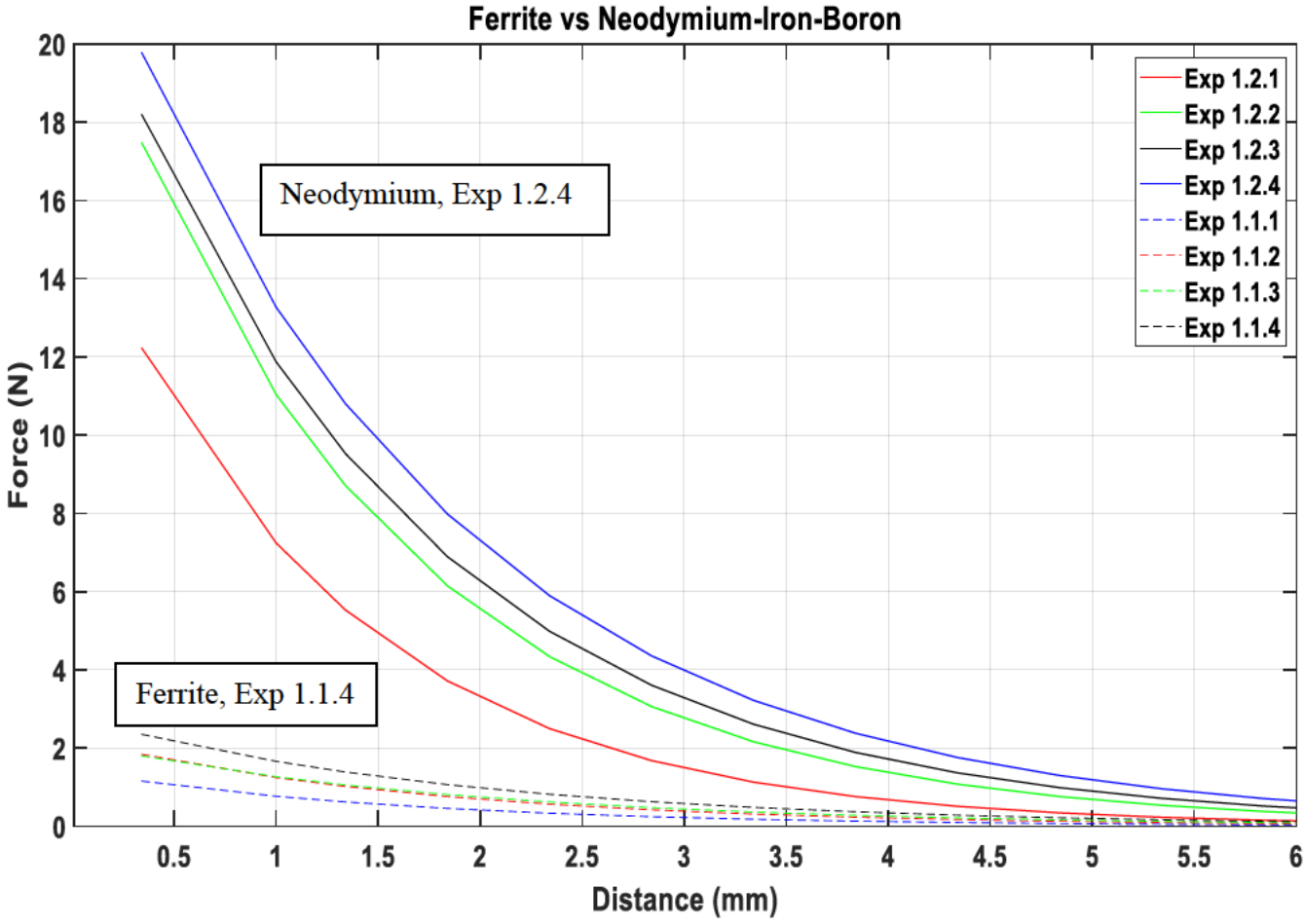

Figure 4.6 A direct force comparison between the Ferrite and Neodymium-Iron-Boron magnets.

The aim of this experiment which was to obtain the desired permanent magnet material and gain knowledge related to the nature of the force-distance relationship,

The results of this experimentation provided a better understanding of the force-distance relationship generated by the Neodymium-Iron-Boron and ferrite magnets. It is clear the attractive magnetic force-distance relationship experiences a natural logarithmic decay as the distance increases.

The preferred magnetic material (Neodymium-Iron-Boron) was selected as the desired material for the remainder of the experimentation and research.

Valuable knowledge related magnetic stacking and the differences in force generated was gained in terms of the most effective and practical quantity required. The knowledge gained was now implemented into Experiment 2 below. The aim of this experiment was successfully achieved.

4.3 Experimental Set 2 Results

With the results gained from the experiments conducted above, the aim of these experiments were to investigate a new magnetic placement for the Neodymium-Iron-Boron magnets in comparison to experiment 1. As well as introducing a magnetically soft material as the bottom plate.

Similar to experiment 1, this experiment was split into two parts; both of which would be run concurrently. The first part would assess what the effects a different magnetic placement would have in relation to the force-distance relationship. The second part to this experiment was the use of magnetically permeability material for the bottom plate.

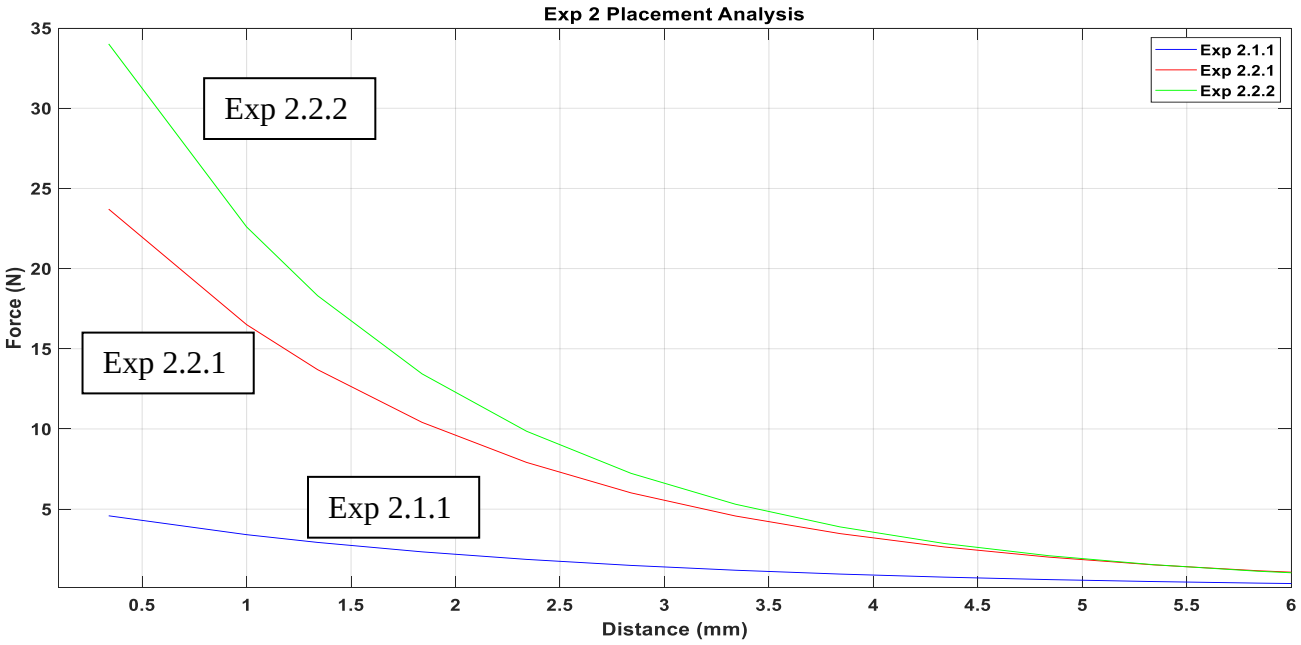

Figure 4.7 Experimental set 2, best fit placement plot.

Experimental Set 2 Results					
TITLE	Magnetic placement and base plate material change				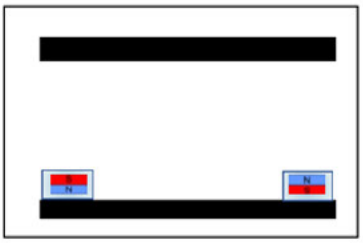
Material	FERRITE				Formula*
	Experiment ID	Quantity of Magnets	Diameter	Thickness	f(x) = a*e*exp(b*x)
					$f(x) = ae^{bx}$
	Exp 2.1.1	2	12mm	5mm	a = 5.342, b = -0.4493
Material	NEODYMIUM				
	Exp 2.2.1	2	10mm	5mm	a = 28.57, b = -0.5486
	Exp 2.2.2	4	10mm	5mm	a = 41.98, b = -0.6192

Table 4.2 Experimental set 2 results

Figure 4.7 reveals the results from experiment 2. There were three experiments conducted and differences between them are clearly visible. The lowest graph is a Ferrite magnet (Exp 2.1.1) and the upper two graphs are the Neodymium-Iron-Boron magnets from Exp 2.2.1 and Exp 2.2.2. The new layout with the new iron metal bottom plate produces more force than the aluminium bottom plate from experiment 1.

With this newly found knowledge related to placements and combined with the information related to magnetic stacking gained from experiment 1; the experiment began its second phase which was the implementation of magnetic stacking according to the new layout.

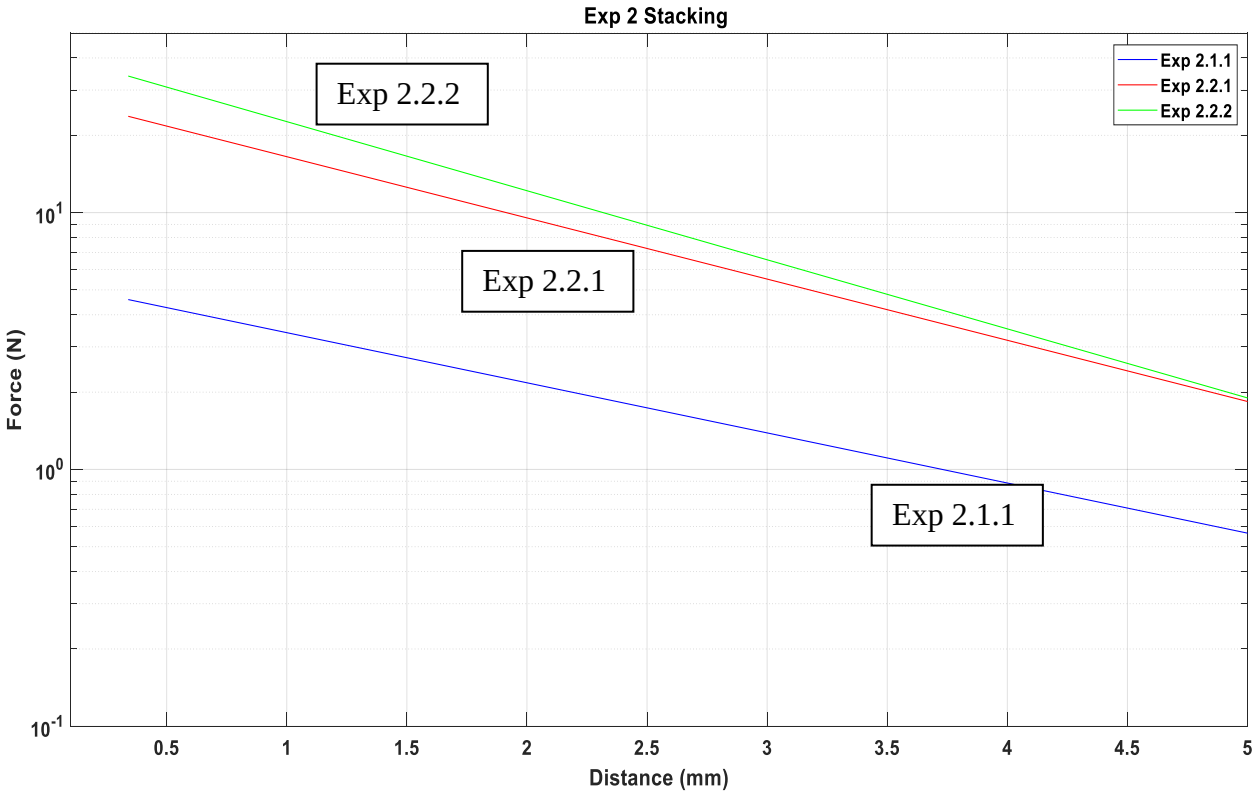

Figure 4.8 The logarithmic plot of Figure 4.7, illustrates the effects of magnetic stacking with the new placement.

As discussed, the new layout of Neodymium-Iron-Boron magnets were stacked one on top of another. This brought the total number of magnets for this particular experiment up to four. In the logarithmic plot (Figure 4.8) the difference in force is again distinct and well defined.

The upper graph (Exp 2.2.2) is approximately 40% stronger than the unstacked lower (Exp 2.2.1) graph. A unique trend related to double stacking seems to be forming. The effect of double stacking is approximately in the range of 40% - 60% times stronger than the single magnetic layout regardless of the material and placement.

The result from experiment 2 provided an improved understanding of a more appropriate magnet placement; an ideal quantity for magnetic stacking as well as the effects of utilizing a mild steel bottom plate. Similar to experiment 1 the results of this experiment 2 would be utilized for experiment 3 below as well as for the remainder of the research. The aim of experiment 2 was achieved with regards to investigating the effects of magnetic placements and stacking with a mild steel bottom plate.

4.4 Experimental Set 3 Results

With knowledge gained from experiments 1 and 2, a new orientation was explored. The aim of experiment 3 was to analyze and investigate the new mirrored orientation in comparison to experiment 2. This entailed the removal of the upper mild steel plate from experiment 2 and replacing it with the identical magnetic placement as the lower configuration creating a mirror image. The only difference was to ensure that desired magnetic poles face one another in order to generate an attractive force.

Experimental Set 3 Results					
TITLE	Magnetic orientation (mirroring) and stacking of two and four neodymium magnets				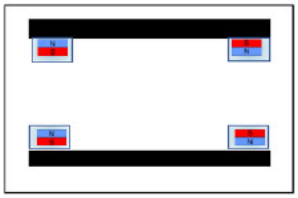
Material	NEODYMIUM				Formula*
	Experiment ID	Quantity of Magnets	Diameter	Thickness	f(x) = a*e*exp(b*x)
					$f(x) = ae^{bx}$
	Exp 3.2.1	4	10mm	5mm	a = 29.94, b = -0.2116
	Exp 3.2.2	8	10mm	5mm	a = 38.02, b = -0.1977

Table 4.3 Experimental set 3 results

Coupled with the new mirrored orientation the effects of stacking were implemented as well. The effects of the new mirrored orientation were explored and compared to experiment 2. Experiment 3 was conducted with the identical magnets that were utilized in experiments 1 and 2.

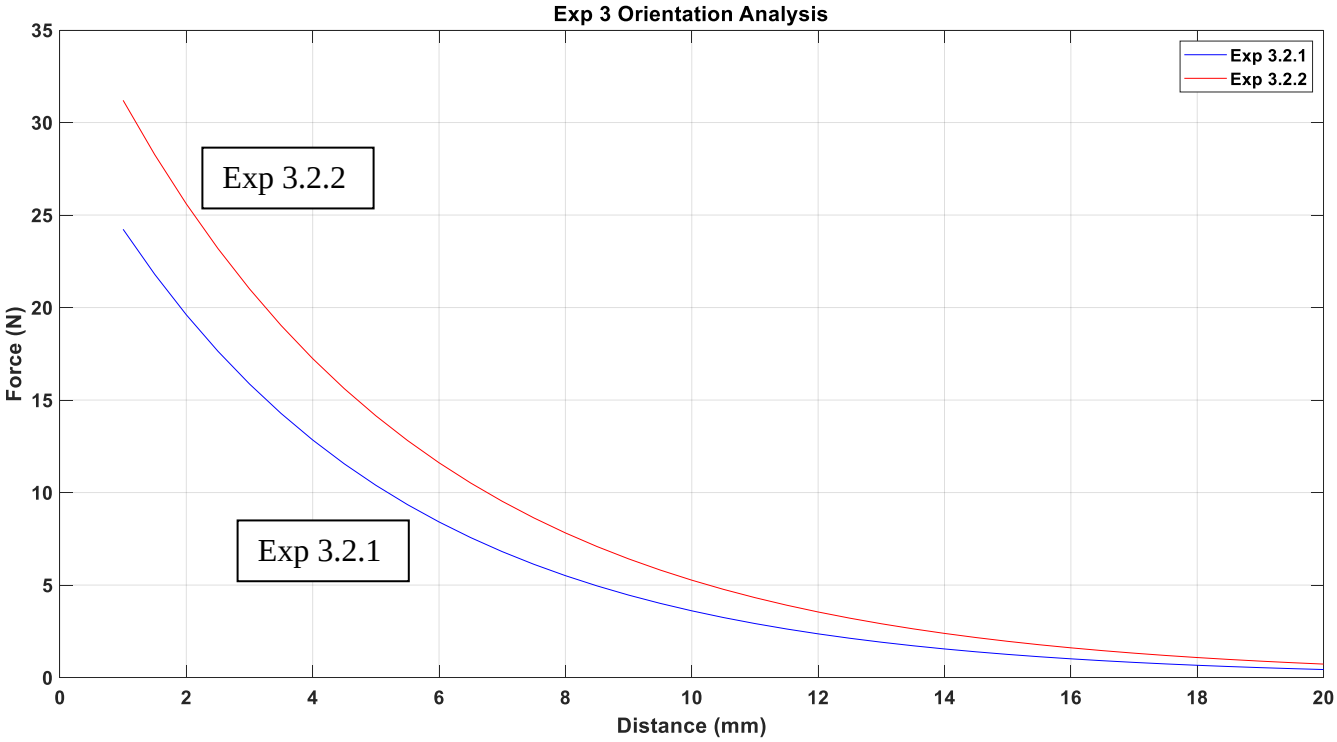

Figure 4.9 Experimental set 3, best fit mirrored orientation plot.

From Figure 4.9 there are two plots visible. The lower graph is experiment 3.2.1 and the upper graph explored the effects of the double stacking which was experiment 3.2.2. The force-distance relationship is very prevalent and similar. The nature of the data has shown the very same natural logarithmic decay as the initial experimentation. This highlights the uniformity and nature of the magnetic flux. The magnetic flux did not change in nature, but only in force when compared to the mild steel plates.

Due to the new mirrored orientation, the number of magnets per stack remained at two however the total number per the experimentation was 8. The effects of stacking are more clearly visible in the logarithmic plot Figure 4.10.

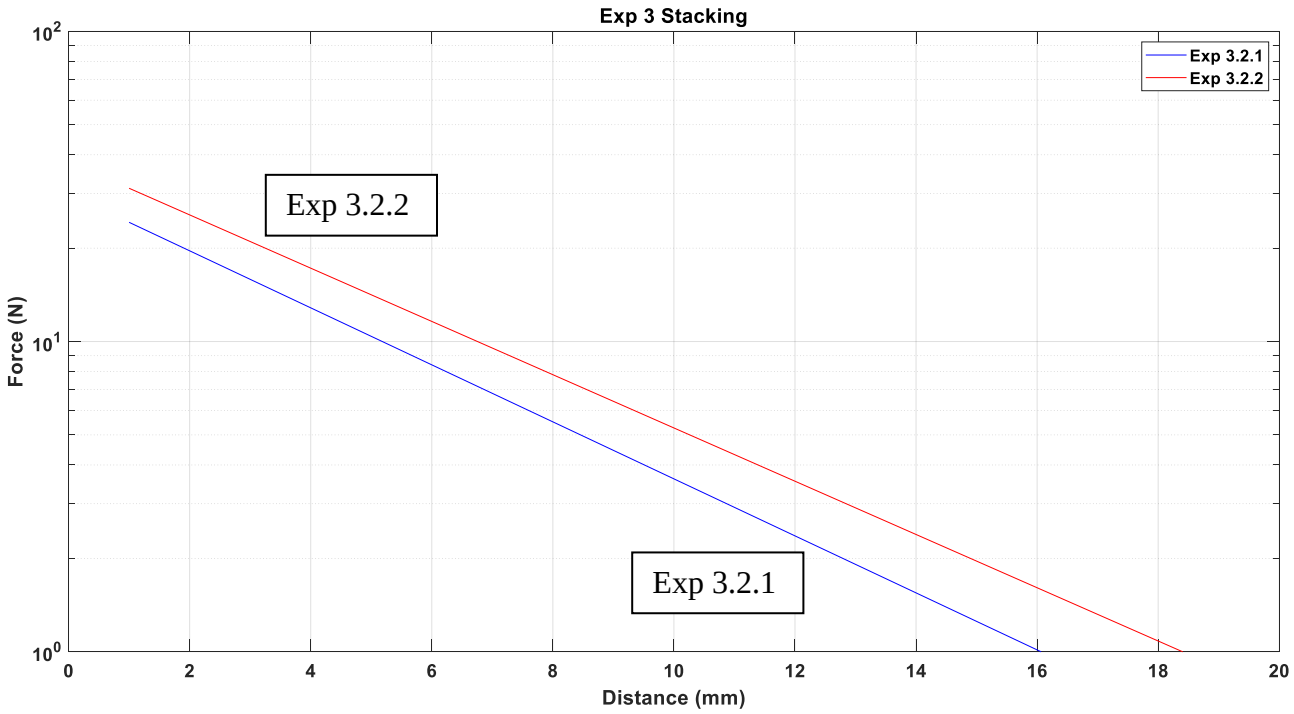

Figure 4.10 The logarithmic plot of Figure 4.9, illustrates the effects of the new mirrored orientation.

The results have shown that experiment 3.2.2 (double stacked) is on average approximately 1.33 times stronger than non-stacking (3.2.1). These results are favorable with regards to obtaining higher forces than previous experiments and assisting the research in pursuing further experimentation with this layout, orientation (mirror image) and material.

The data presented has confirmed the aim of experiment 3 in which a mirrored layout attracted to one another generates significantly more force, keeping in mind the identical magnets were utilized in this experiment. The details pertaining to the difference between the forces from experiments 2 and 3 will be discussed in the summary to follow. With the knowledge gained thus far from experiments 1,2 and 3; further experimentation related to the dimensions of the magnets would be explored in experiment 4.

4.5 Experimental Set 4 Results

Due to the positive results attained by the prior experiments, the aim of experiment 4 was to obtain the ideal magnet dimensions (volumetric) for the newly chosen mirrored layout from experiment 3 above. In theory the larger the magnets produce larger magnetic forces. There were three variations in terms of dimensions that were investigated. These are visible in the graphs below.

Experimental Set 4 Results					
TITLE	Magnetic dimension change as well as the implementation of stacking				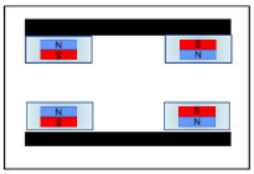
Material	NEODYMIUM				Formula*
	Experiment ID	Quantity of Magnets	Diameter	Thickness	f(x) = a*e*exp(b*x)
					$f(x) = ae^{bx}$
	Exp 4.2.1	4	20mm	3mm	a = 109.9, b = -0.1577
	Exp 4.2.2	4	20mm	5mm	a = 193.7, b = -0.1558
	Exp 4.2.3	8	20mm	5mm	a = 199.2, b = -0.1165
	Exp 4.2.4	4	22mm	10mm	a = 273.7, b = -0.121

Table 4.4 Experimental set 4 results

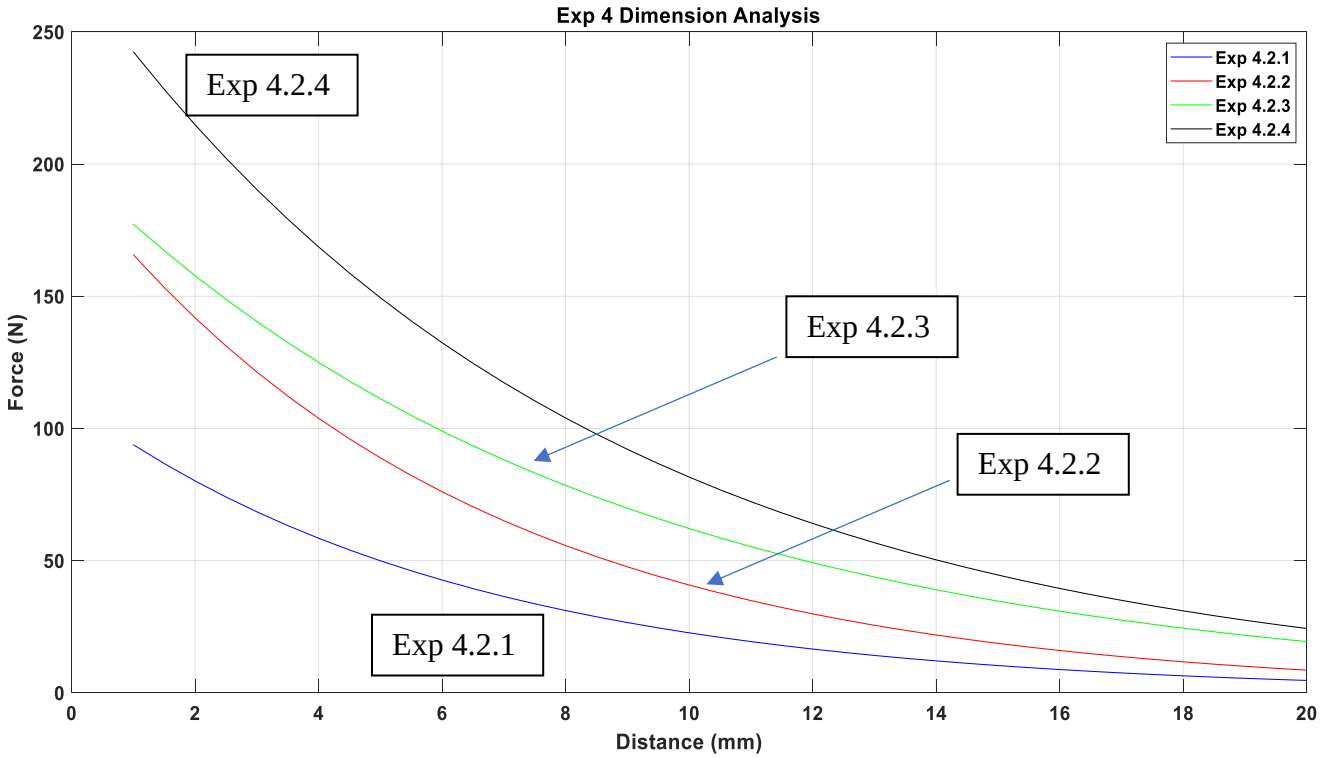

Figure 4.11 Experimental set 4, best fit dimension plot.

Figure 4.11 highlights the forces present between the three different dimensions. There were four experiments conducted, one of which was the implementation of magnetic stacking (Exp 4.2.3). The first and most common trait amongst all the experimentation conducted was the natural logarithmic decay experienced. The effects of increasing the magnets dimensions are clearly visible.

The steady climb in force between all the experiments from lowest to highest are from 4.2.1, 4.2.2, 4.2.3 and 4.2.4.

- Experiment 4.2.2 is approximately 1.78 times stronger than 4.2.1
- Experiment 4.2.3 is approximately 1.24 times stronger than 4.2.2
- Experiment 4.2.4 is approximately 1.34 times stronger than 4.2.3

It is known from the initial experimentation conducted (experiment 1) that effects of triple stacking the magnets do not triple the forces generated. Exp 4.2.4 is a single magnet. As mentioned in section 3.4.4; due to several factors from the magnet's availability to the physical difficulties and dangers related to the handling large magnets (in close proximity the magnets may collide and shatter) larger magnets were not utilized. In addition to the points mentioned; the physical

requirements of using excessively large magnets may be impractical for use in fiber reinforced composite manufacturing. Hence the final magnet used was in Exp 4.2.4.

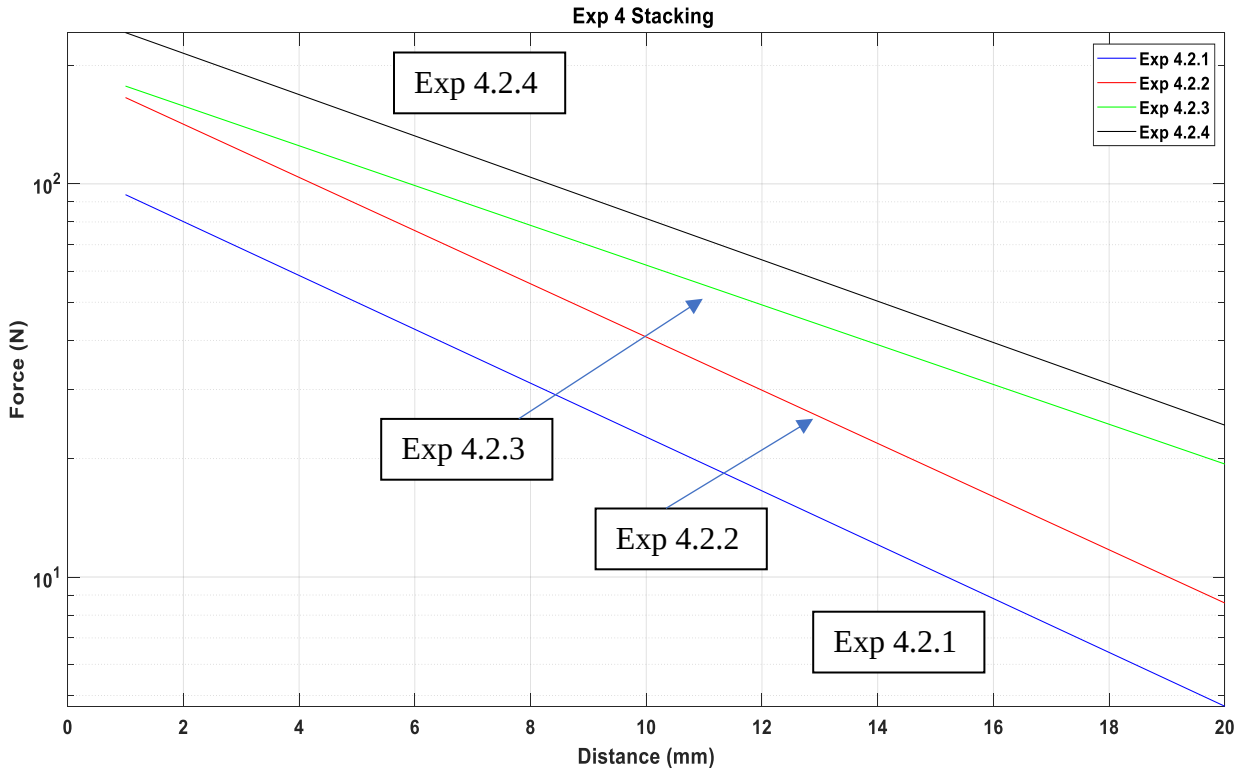

Figure 4.12 The logarithmic plot, illustrating the differences in forces between the different magnet dimensions.

From the logarithmic Figure 4.12, the force increments are more clearly defined and the desired dimensions for the permanent magnets have been identified in Exp 4.2.4. The standout feature from this experimentation is the pressure per cylindrical area of the magnet that is equal to 1 bar at 10mm. This is equal to the 1 bar of atmospheric pressure generated via the vacuum forming fiber reinforced composite manufacturing techniques.

The horizontal spacing was determined due to the following; the magnetic poles were placed further apart (over 15mm) from one another in order to prevent the magnetic flux from travelling across the surface, rather than to the opposite magnetic unit (within 10mm-15mm)

The aim of this experiment was to obtain the most suitable magnetic dimensions. The largest magnet that was available at the time of experimentation was utilized, which was the 22mm x 10mm Neodymium-Iron-Boron cylinder (4.2.4) was investigated. These dimensions provided the

highest force which results in the desired magnetic dimensions being selected. Experiment 4.2.4 was performed several times in order to assess the consistency of the magnetic units. The results of which can be viewed in Appendix B.

4.6 Summary

A common characteristic which was gained amongst all the experimentation was the nature of the graphs. Regardless of the quantity, position, material, placement, configuration (magnet vs plate / magnet vs magnet) and dimensions of the magnets the unique nature of the magnetic forces experienced a natural logarithmic decay at increasing distances. It can be assumed at this point that a natural logarithmic growth would be experienced if the experimental procedure was reversed. However, information related to the force-distance relationship of magnetic flux has yet to be fully explored. Current work makes mention of the force-distance relationship which is related to the L/R (thickness / radius) dimensions of the magnets at increasing distances.

The experimental work conducted was to obtain the most appropriate magnetic material, placement and lastly dimensions. There were four major experiments conducted and within each experiment a number of individual experiments. All of which led to the desired magnetic units being devised.

The initial experimentation began with the comparison between two different magnetic materials which were Ferrite and Neodymium-Iron-Boron. In conjunction with the above mention experiments, the effects of magnetic stacking were also investigated.

From the experimental data displayed (Figure 4.7), the Neodymium-Iron-Boron magnets were the stronger of the two materials. Figures 4.3 and 4.5 also illustrated the effects of stacking; in which double stacking was the most effective. A very unique finding related to the effects of stacking was, regardless of the material (Ferrite / Neodymium-Iron-Boron) the increase in force was in the region of approximately 50%.

With the desired knowledge gained in terms of magnetic material and stacking the second experiment proceeded. Experimental Sets 2 and 3 were both utilized to obtain the ideal magnetic placement as well as orientation. As mentioned in Chapter 3 there were other core material designs that were investigated, however the most effective design is presented in this research.

Experimental Set 2 was devised for selecting the most appropriate placement.

As mentioned in the above Chapter 3 section 3.1, an aluminium base plate was deliberately used to ensure that there were no magnetic flux interference (enhancements) and that the force readings were purely based on the interactive flux lines that are “permanently” present in a permanent magnet. Due to the magnets being fixed as well as the experiments being paused for 30 seconds at every 0.5mm interval (section 3.2.1); the aluminium plates would not have had any eddy currents within.

Here the aim was to investigate the most ideal magnetic placement as well as force enhancements in relation to the addition of the mild steel bottom plate. This required the experimentation to be spilt into two categories. Experimental Set 2 was related to the placements as well as materials and experimental set 3 was related to the magnetic orientations.

From the forces generated it is visible to see that the newly desired side-by-side horseshoe configuration has a higher force than the individually placed magnets from Experiment 1. From the formulae within Tables 4.1 and 4.2 experiment (2.2.2) has the initial force of 41.98N and experiment (1.2.3) has an initial force of 24.31N. This graph exhibits the difference between the two experiments (1 and 2) in which the same number and size of magnets were used; only the placement and backing plate were changed.

Experimental Set 3 was required for selecting the most appropriate orientation.

The desired orientation which was experimented on, will be referred to as a mirrored horseshoe layout. As discussed above:

- The top mild steel plate was replaced with the very same horseshoe layout as Experiment 2, only mirrored on the opposite side.
- The difference between experiments 2 and 3 is clearly visible from Figure 4.13. Which experiment 3 is progressively stronger than experiment 2.

The key noticeable aspect is how the force is maintained and gradually decreases as the distance increases, whereas the forces in Experiment 2 rapidly decrease.

The information obtained from experimental Set 3 was highly beneficial as the aim of obtaining the most suitable orientation was achieved. As magnetic forces were now reaching the target distance of 10mm-15mm.

With the aims of the first three experiments being achieved and the desired materials together with the ideal placements and orientations now known; the last aspect to the magnetic investigation was to obtain the desired magnetic dimensions. This was done in Experiment 4.

Experimental Set 4 was devised for selecting the most appropriate magnetic dimensions.

Experimental Set 4 utilized the same mirrored horseshoe layout as Experimental Set 3 only the dimensions were changed. The forces got progressively larger as the magnet's dimensions increased. There were three different sizes that were examined with the largest magnet being 22mm in diameter and 10mm thick. With reference to Figure 4.14, Experiment 4.2.4 on average produces 16 times more force than Experiment 3.2.2. Even though the entire experimentation examined and assessed magnetic stacking, the experiment (4.2.4) was not stacked. There were various reasons as to why this was the most suitable magnet. Some of these reasons are listed below.

The (22x10) magnet was the largest magnet available at the time of the experimentation. Construction of the mirrored horseshoe magnetic clamps became very hazardous. It required increased safety as well as focus. The magnets were so strong they could potentially shatter and seriously injure the user's limb / eye. Lastly the pressure per cylindrical area of the magnets generated 1 bar of clamping pressure.

A summary of all the experiments are presented in Figures 4.13 and 4.14. The logarithmic plot illustrates the force-distance progression made from the first to the fourth experiment. The plot clearly summarizes and illustrates the improvements made between the four experiments. On the plot the experiment ID is displayed as well as an accompanying flow chart (which was displayed in Chapter 3) with the selected graphic (circled) highlighting which material, placement, orientation and size is being displayed. The selected graphics were the best in their respective experiments.

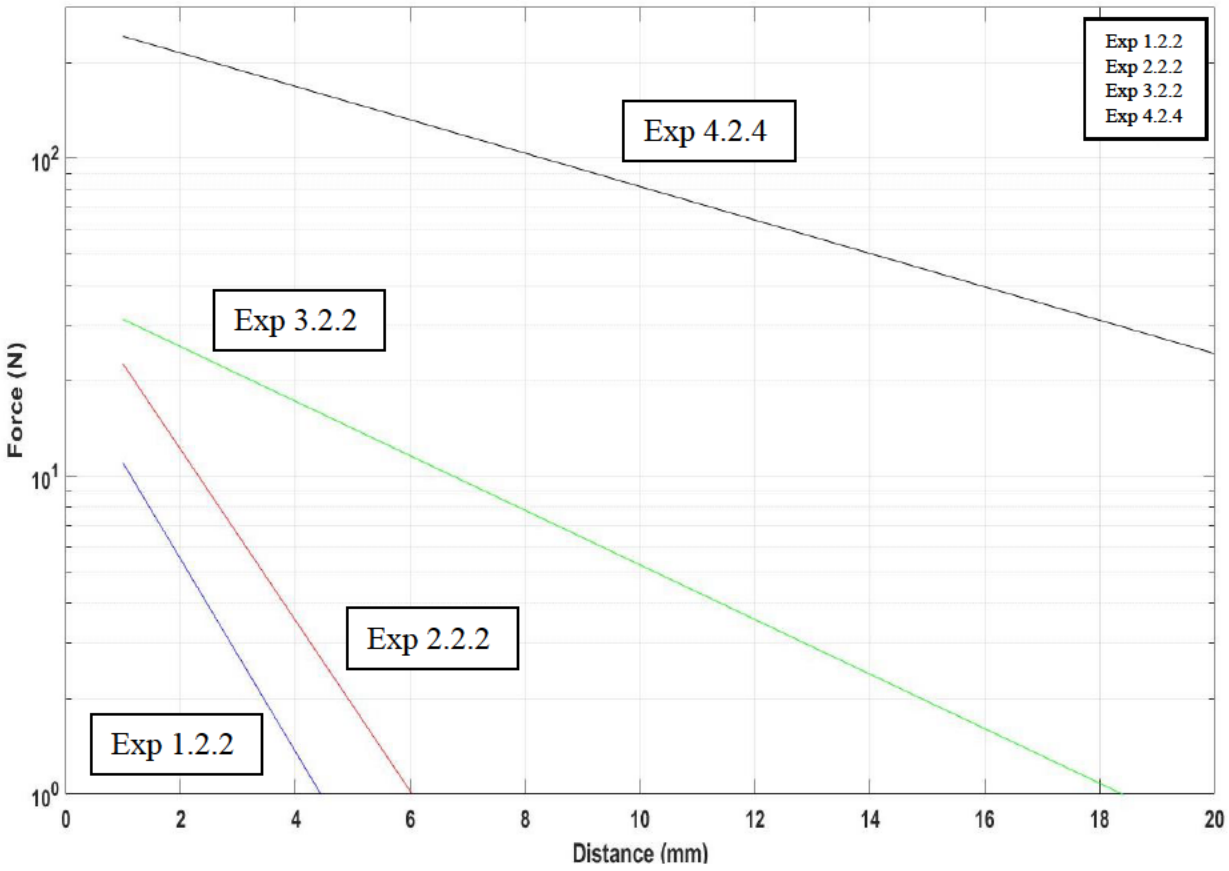

Figure 4.13 A logarithmic graph representing the progressive growth and comparison between all four experiments conducted, with selected data being displayed.

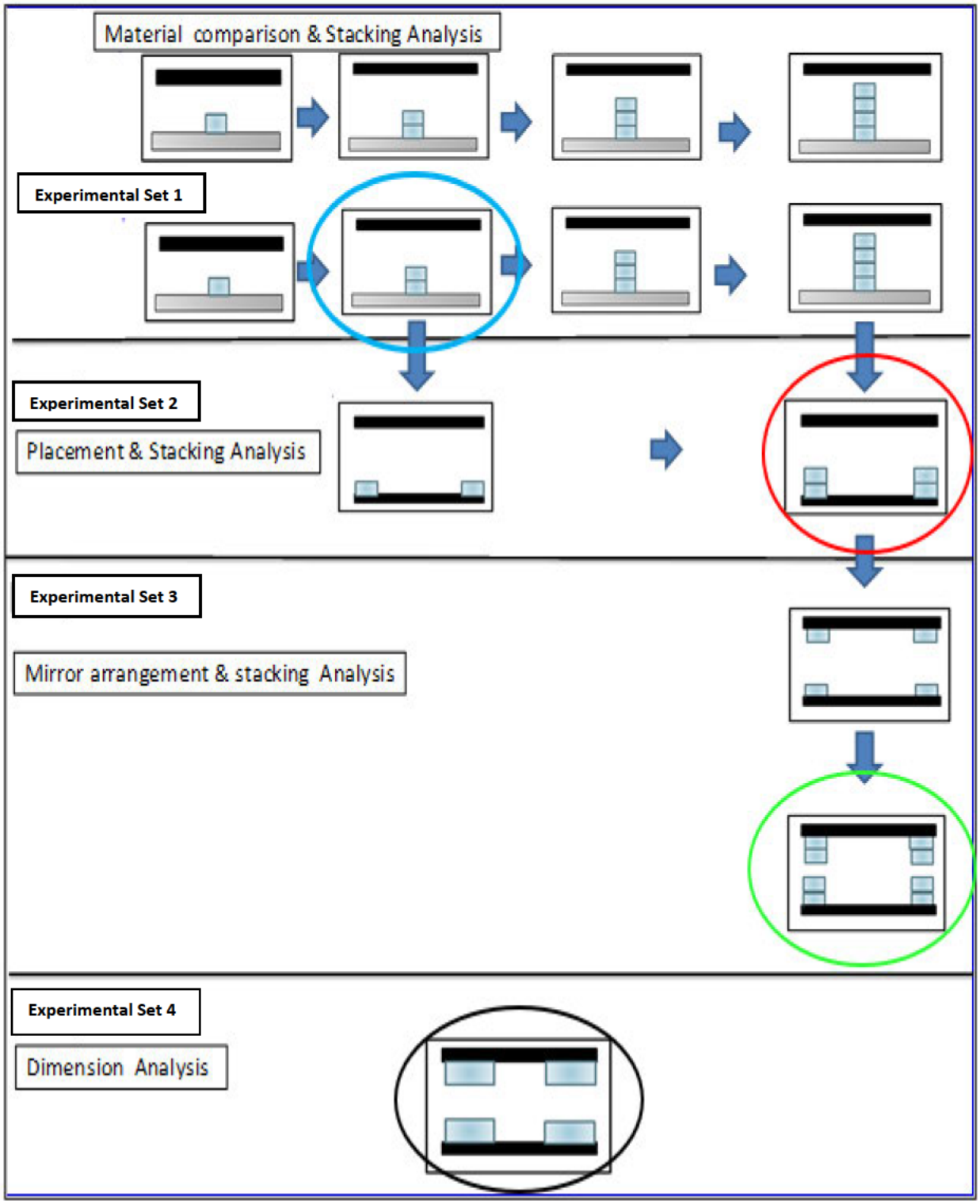

Figure 4.14 The selected experiments which are circled and colored are the ones displayed in the logarithmic graph (Figure 4.13).

With all the aims of the extensive magnetic experimentation being achieved a method of applying the magnetic clamping units to the tool were explored.

As touched upon in section 3.5 above, a very simple yet effective means of applying the magnetic clamps to the tooling was analyzed and devised. The technique utilized a stainless-steel nut and bolt (Stainless Steel Grade 316) that was bonded (tack weld) to the metal backing plate of the magnets. The means of which the magnetic units would be raised or lowered would done by rotating the nut in the clockwise and anticlockwise directions. The nut would then travel up and down the bolt which would gradually and gently bring the magnetic units into and out of position.

The magnetic clamping unit comprises of four 22mm diameter 10mm thick N35 Neodymium magnets (two on either side) placed on a 61mm x 25mm x 3mm iron backing plate with a center distance of 39mm between the magnet centers. There is a M12 stainless steel (grade 316) nut and bolt which is adhered to the mild steel plates for application purposes. The material of the nut and bolt has been specifically selected as stainless steel, so that the magnetic flux does not incur any interruption from one magnet to the other.

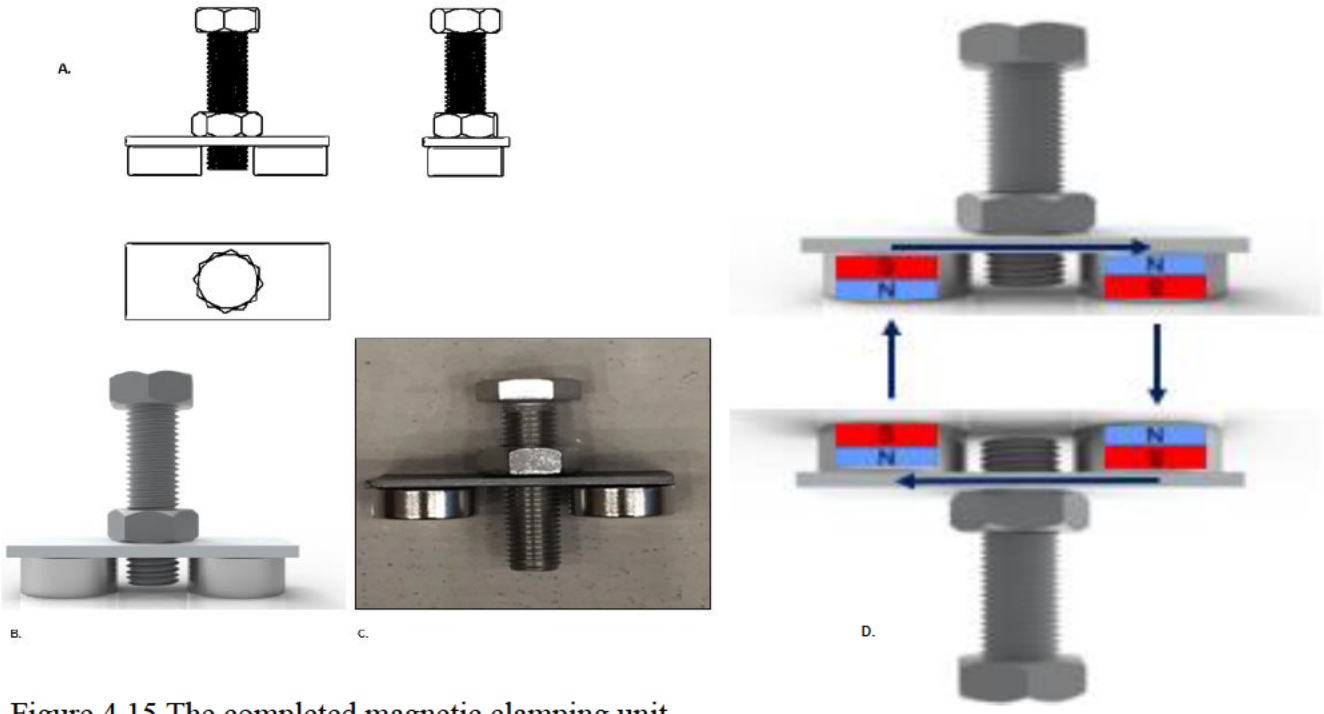

Figure 4.15 The completed magnetic clamping unit.

The magnetic clamping units (Figure 4.15) were implemented into the desired VARTM fiber reinforced composite manufacturing technique to investigate the possibilities of magnetic compaction in composite manufacturing.

5 Comparative VARTM Experiments

The comparative VARTM experiment was the second type of experiment conducted. This is the final set of experiment's related to this investigation. The aim of this experiment is to investigate the effects of magnetic compaction in fiber reinforced composite manufacturing. This experimentation would assess if the magnetic clamping units derived from the comprehensive magnetic experimentation can assist in compaction and to produce a more consolidated panel.

The VARTM technique was selected as the fiber reinforced composite manufacturing method to investigate the use of the magnetic clamping unit design. Three identical VARTM panels were setup. The experiment would make use of two Polymethyl Methacrylate (PMMA) sheets [39] which would represent two GRP (Glass Reinforced Plastic) tooling. One sheet would be placed at the bottom and the other would be placed above the dry fabric. The fabric preform consisted of 390gsm twill glass fiber, Prime 27 infusion resin. The same vacuum pump was used. All the experiments were conducted simultaneously at the same time and place. This was done to limit any variation between panels which in turn left the magnetic units as only difference between the three panels. The first panel had 5 magnetic units; the second panel had 3 magnetic units and the third panel was the conventional VARTM technique which had no magnetic units. Any potential effects such as fill times and flow paths, that the additional magnetic units have on the VARTM panels would be noted. The comparative experiment was run twice to ensure consistency.

5.1.1 The Comparative VARTM Equipment

The VARTM equipment and setup are as follows.

1. Resin Pot
2. Resin Line
3. VARTM Panel
4. Vacuum line
5. Vacuum gauge
6. Vacuum pump

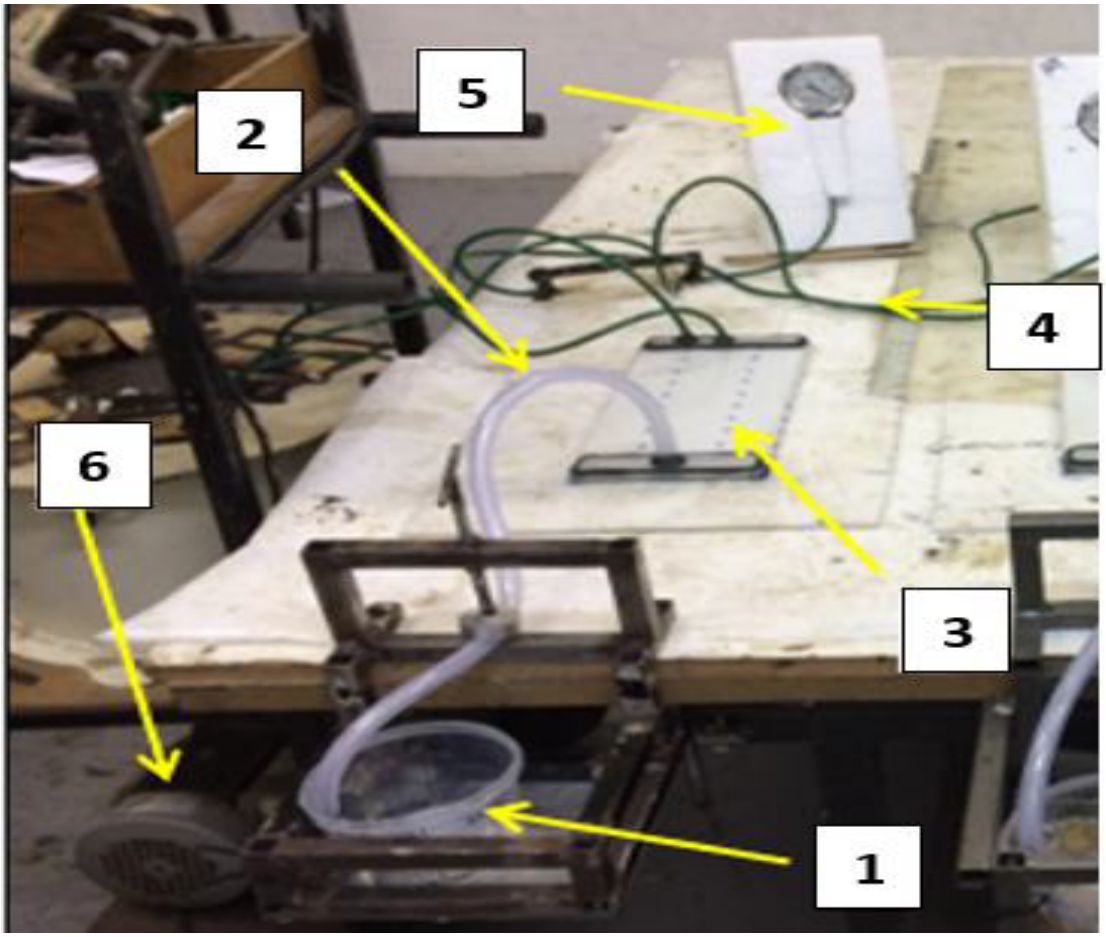

Figure 5.1 Comparative VARTM experimentation equipment

5.1.2 The Comparative VARTM Experimental Procedure

The comparative VARTM experimental procedure was conducted in two parts and in the the following manner. The first part was the setup and the second part was the actual experiment.

The setup was conducted as follows:

Part 1, Experimental Preparation

- Seven layers of 390 GSM glass twill fabric were cut.
- Two Perspex pieces were used to simulate the GRP tooling thickness of 5mm each.
- The bottom Perspex plate was cut to 500mm x 330mm
- The top plate was cut to 150mm x 309mm.

- Both plates were prepared with release agent wax
- The 7 Glass Fiber layers were laid the 0° / 90° orientation.
- A final cut was done to the Glass Fiber fabric.
- The vacuum and resin lines were installed into the top plate
- Clamp-off the resin line to prevent any air intake.
- Turn on the vacuum pump while applying silicone to the outer edge of the upper plates to ensure an air-tight seal with the lower plate. A silicone sealant was used as it is created a flexible airtight seal, in which the preform thickness would not be affected by any way.
- Ensure an equal vacuum pressure is obtained amongst all three panels.
- Once the silicone dried and equal pressure is obtained, clamp-off the vacuum lines.
- Turn the vacuum pump off.
- Assess if there are any leakage and amend if necessary.

Part 2, Comparative VARTM Procedure

- Record the date, time, temperature and humidity.
- Place the required magnetic units onto the desired panels,
  5 magnetic units onto the first panel and 3 magnetic units onto the second panel.
- Turn on the vacuum pump.
- Open the vacuum line, removing the G-clamps.
- Secure the resin pots
- Mix the desired amount of resin.
- Decant an equal amount of resin into the three separate resin pots.
- Begin the comparative VARTM procedure by opening the resin lines.
- Record the date, time, temperature and humidity once the infusion is complete.
- Close the inlet resin line.
- Close the vacuum line.
- Turn off the Vacuum pump.
- Label the panels according to the number of magnets [0,3,5]
- Allow for the resin curing time to complete (depends on the type of resin utilized)
- Demould
- Measure the thickness variations and compare the three panels.

Table 5.1 identifies the three experimental panels with their respective quantities of magnetic clamps. The comparative experimental process will follow the standard VARTM procedure.

Comparative VARTM Experiment	
TITLE	Comparative VARTM Experiment
NEODYMIUM	
Experiment ID	Quantity of Magnetic units
Panel 1	5
Panel 2	3
Panel 3	0

Table 5.1 Comparative VARTM experiment

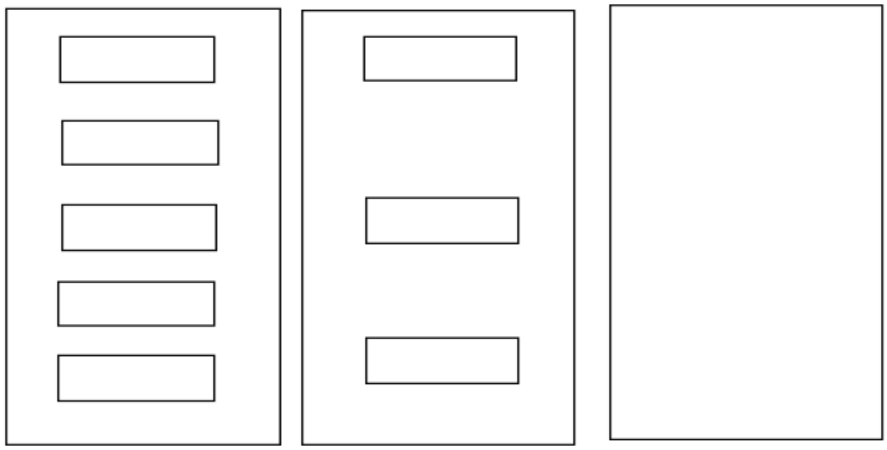

Figure 5.2 Top view of magnetic configuration on VARTM panels

Comparative VARTM Experiment Description

The comparative experiment would be aimed at improving the compaction pressure currently present in the VARTM technique; in order to produce a more consolidated panel.

This experiment would comprise of three separate VARTM panels infused concurrently. The first panel would have 5 magnetic clamping units, the second would have 3 magnetic clamping units

and the third panel would have zero magnetic clamping units. Panel 3 would be the regular VARTM panel.

All variable parameters were fixed in order to prevent any variation amongst the panels. This will allow the magnetic clamping units to be the only additional compaction pressure that is present. A high degree of consistency was implemented in order to ensure the panels remained equal in every variable condition. The variables which required being limited are:

- The resin
- Composite Fiber
- Inlet pipe material and length
- Outlet pipe material and length
- Resin pots
- Vacuum pump
- Same time and place
- Vacuum sealant

By limiting the above-mentioned variables, the results from the comparative VARTM experiment would provide a clear indication on the effects of the magnetic units.

The results are related to comparing the panel thicknesses between all three panels. The thickness would illuminate the effects of the additional magnetic clamping units. If there is a difference present, which is in favor of the magnetic panels. This would lead to an understanding the magnetic panel has a better fiber volume fraction and potentially possess improved mechanical properties. Both destructive (burn-off) and non-destructive (physical measurement) volume fraction tests were run in order to measure the laminates fiber volume fraction. A tensile test was also conducted to assess the infused panels mechanical performance.

The Comparative VARTM Experimental Sets 1 and 2 in Progress

Figures 5.3 and 5.4 are the final experiment setup prior to resin infusion. Once the desired vacuum pressure was attained, the magnetic clamps were added (Figures 5.7 ang 5.7) to the desired panels. Once the magnetic clamps were added, the resin impregnation was initiated via the opening of the resin inlet valves. Figures 5.3 and 5.4 below are both the comparative VARTM experiment being run concurrently.

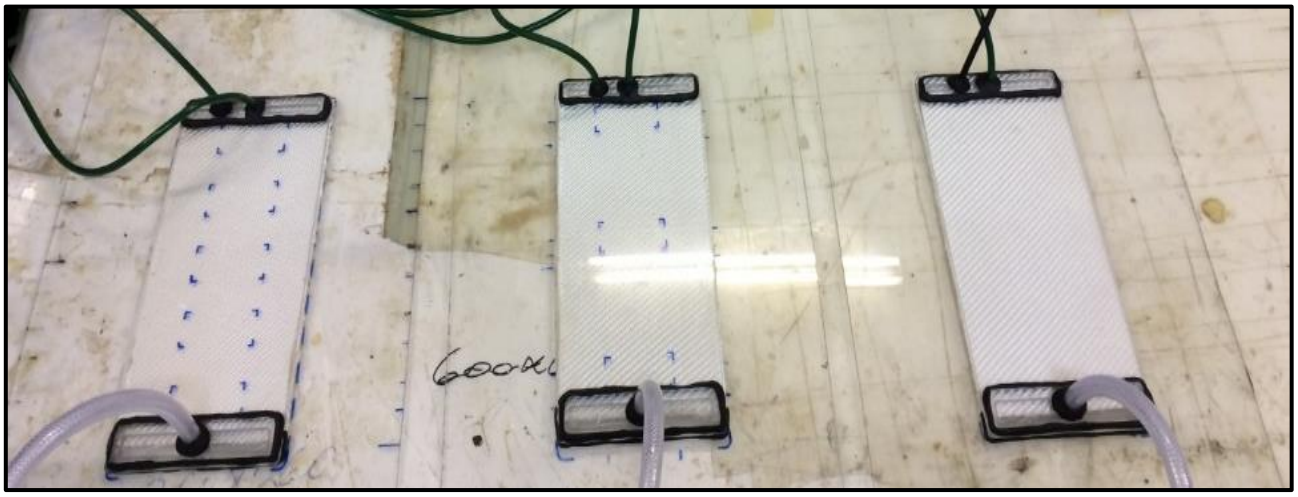

Figure 5.3 The three comparative panels from experimental set 1. The far left being panel 1 the center being panel 2 and the far right being panel 3 (regular VARTM).

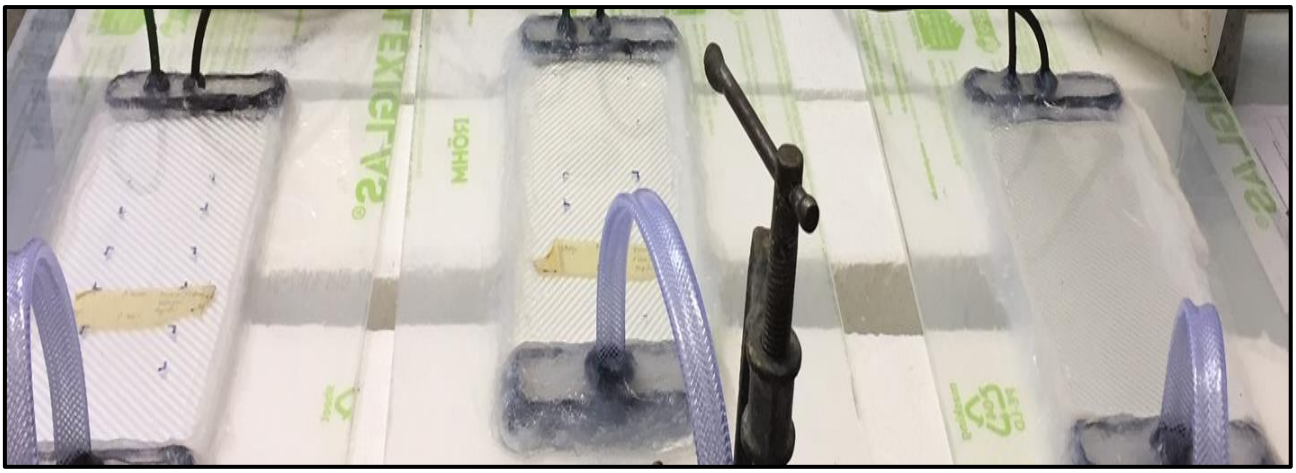

Figure 5.4 The three comparative panels from experimental set 2.

Figure 5.5 Pressure gauge test prior to running the VARTM process.

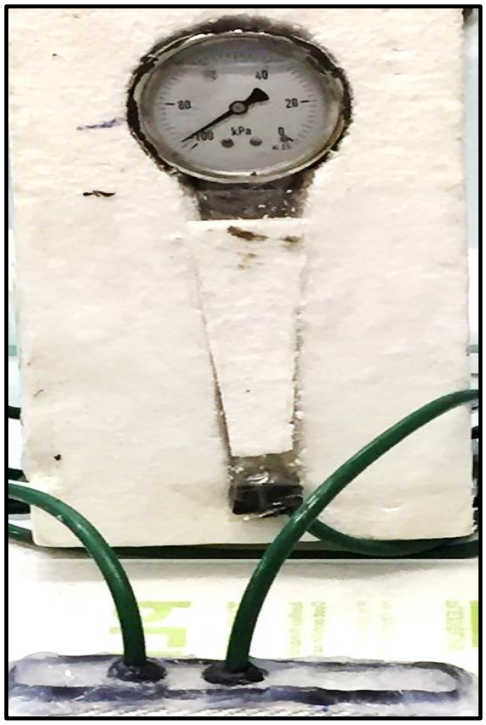

Figure 5.6 Pressure gauge reading during VARTM process.

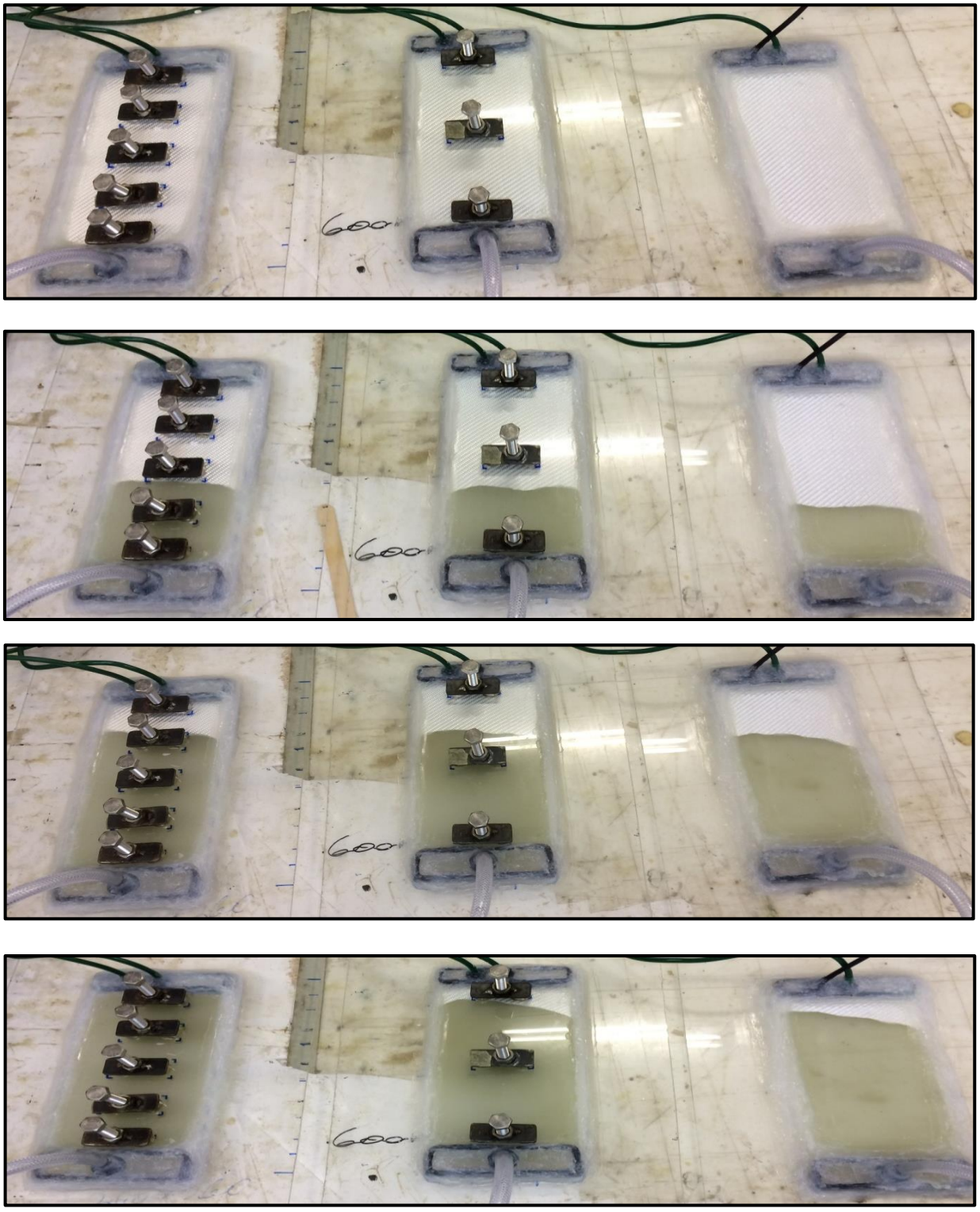

Figure 5.7 The first comparative experimental set being conducted concurrently.

The three panels are visible with the magnetic units attached to panels 1 and 2. The resin flow front is also visible through the duration of the experiment.

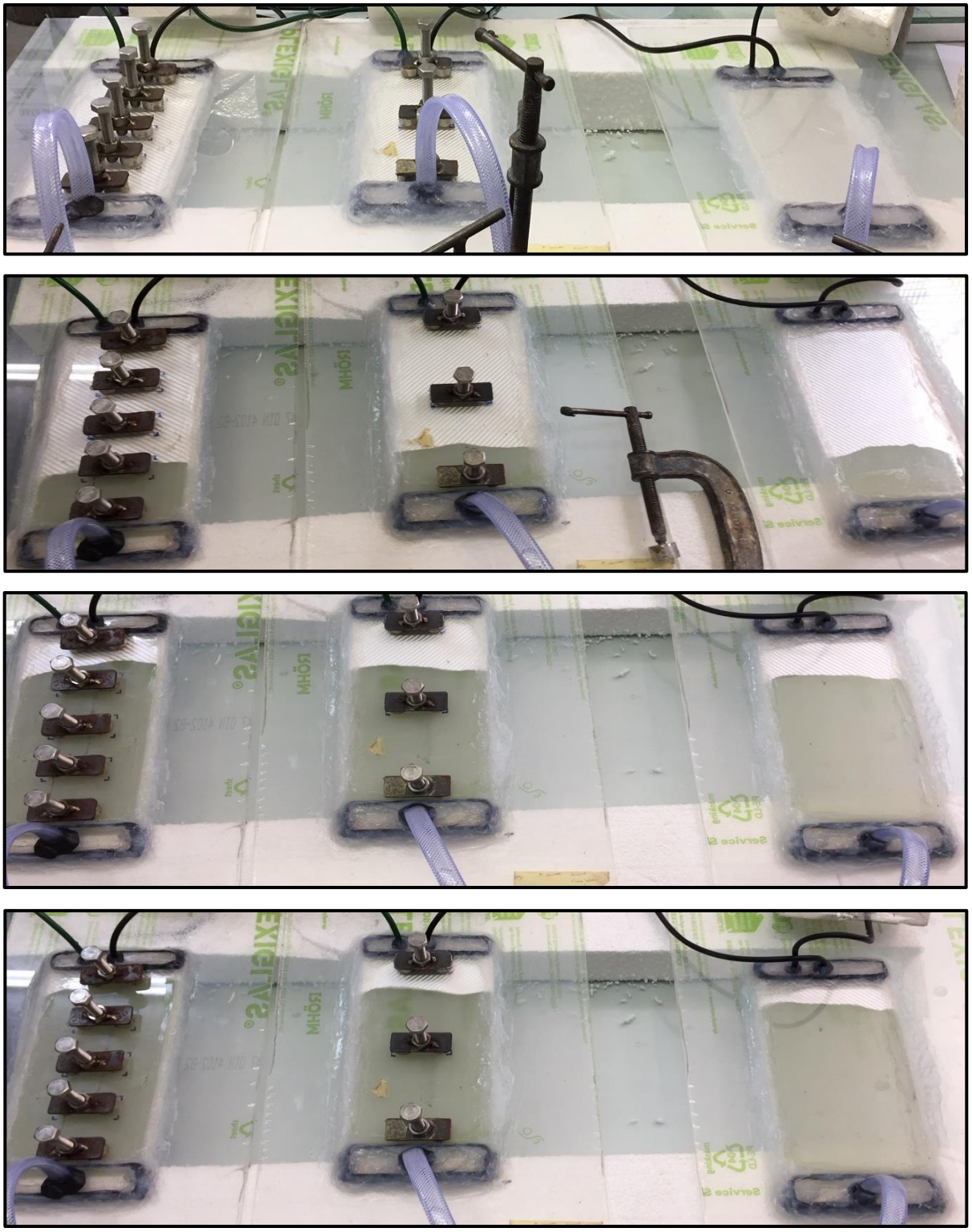

Figure 5.8 The second comparative experimental set being conducted concurrently.

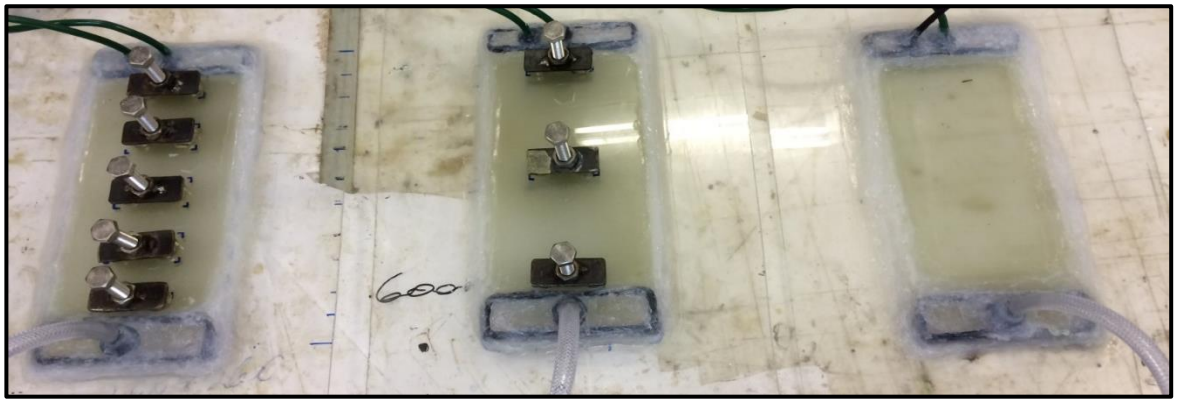

Figure 5.9 All three panels from the first comparative experimental set fully infused.

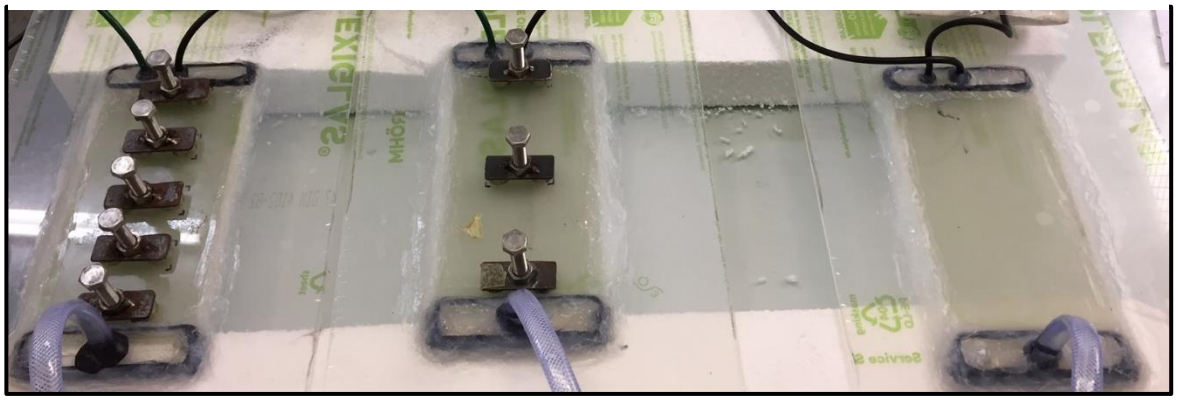

Figure 5.10 All three panels from the second comparative experimental set fully infused.

5.2 Comparative VARTM Experiment Summary

Once the comparative VARTM experiment is complete, a further and final analysis would be conducted. This analysis would be related to the physical measurement (panel thicknesses) of the three panels. The measurements would be required as the results would decipher if the additional magnetic clamping units are beneficial to the low compaction pressure GRP tooling composite manufacturing techniques. The results to the VARTM experiments are presented in Chapter 5.

6 Comparative VARTM Experimental Results

Based on the magnetic experimental results, the magnetic clamping units were utilized in a VARTM manufacturing process to investigate what effects the additional compaction pressure had on a laminate. The aim of this comparative VARTM experiment is to analyse if a magnetic assisted technique can consolidate a fiber reinforced laminate more than a regular VARTM technique, as a more consolidated panel would yield improved mechanical properties. Both destructive and non-destructive volume fraction tests were run in order to measure the laminates fiber volume fraction. A tensile test was also conducted in order to assess the infused panels mechanical performance.

The comparative VARTM experiment was generated to compare the differences (if any). It comprised of three separate VARTM panels infused concurrently. A high degree of consistency was implemented to insure the comparative experimental panels remained equal in every variable condition. This allowed the magnetic clamping units to be the only additional compaction pressure applied to the panels. Running the comparative VARTM experiments twice would allow for investigating the repeatability of any observations made in the first set.

Comparative VARTM Results				
TITLE	Comparative VARTM Experiment			
Material	Neodymium Magnetic clamping units			
	Panel ID	Quantity of Magnetic units	Additional Force	Additional pressure *
7 layers of 390 / gsm Twill Glass Fiber	Panel 1	5	317.16N	107.33 KPA
7 layers of 390 / gsm Twill Glass Fiber	Panel 2	3	190.29N	104.39 KPA
7 layers of 390 / gsm Twill Glass Fiber	Panel 3 (Regular VARTM Process)	0	0N	100.00 KPA
* The additional pressure illustrated is based on these experiments. The pressure is not limited to the above as the positioning and quantity of the magnetic units will either increase or decrease the pressure due to manufacturing parameters such as design size and geometric limitations.				

Table 6.1 Comparative VARTM experiment results.

The Comparative VARTM Experiment

VARTM Experimental Set 1 Details				
Time	Date	Temperature	Humidity	Atmospheric Pressure
11:00	25/03/2020	22.6 C	57%	1015 hPa
	Fill time			Duration
Panel 1	11:10am	12:05pm		55mins
Panel 2	11:10am	01:00pm		1Hr, 50mins
Panel 3	11:10am	01:00pm		1Hr, 50mins

Table 6.2 VARTM experimental set 1 details.

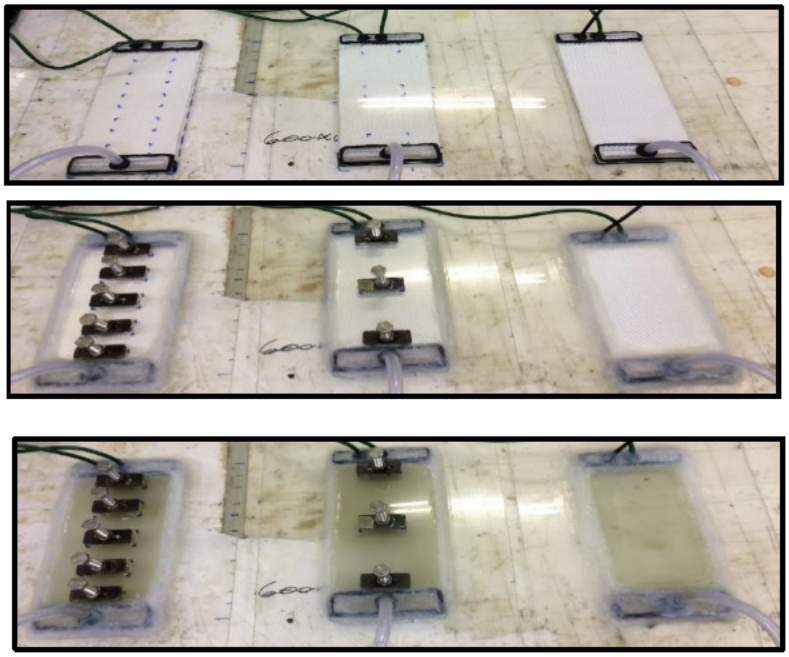

Figure 6.1 First comparative VARTM experiment.

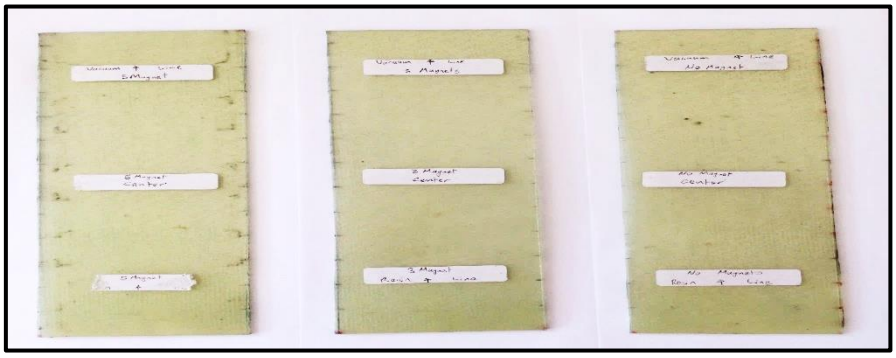

Figure 6.2 Three comparative VARTM panels, demoulded from experimental set 1.

VARTM Experimental Set 2 Details				
Time	Date	Temperature	Humidity	Pressure
10:00	26/01/2022	24.0 C	60%	1017 hPa
	Fill time			Duration
Panel 1	10:20am	12:05pm		1Hr, 45mins
Panel 2	10:20am	01:11pm		2Hrs; 51mins
Panel 3	10:20am	12:30pm		2Hrs, 10mins

Table 6.3 VARTM experimental set 2 details.

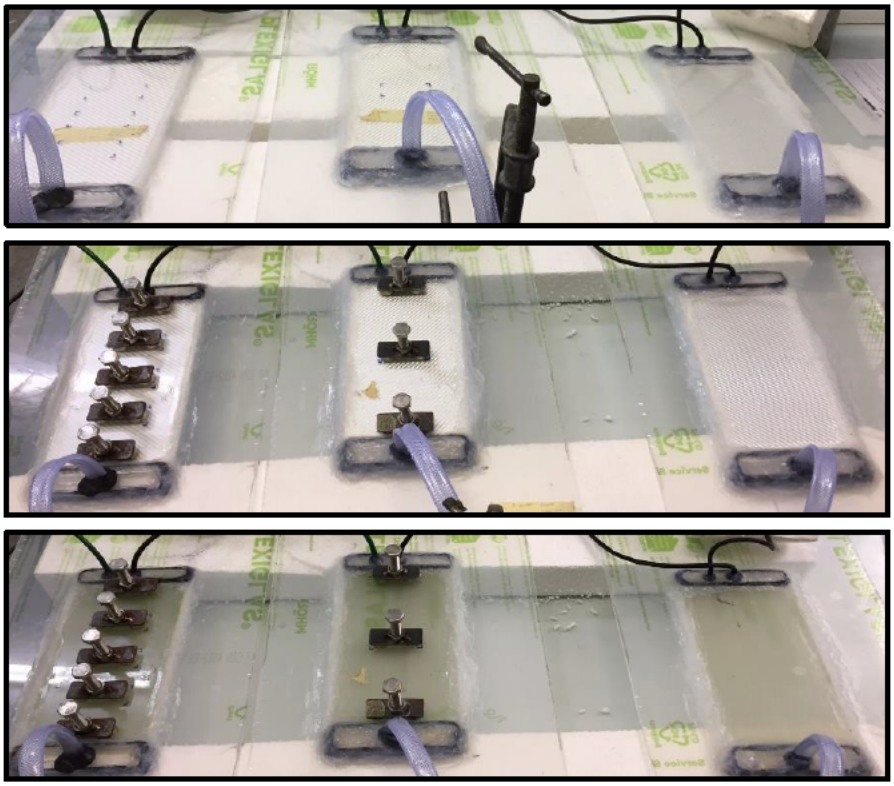

A.

B.

C.

Figure 6.3 Second comparative VARTM experiment.

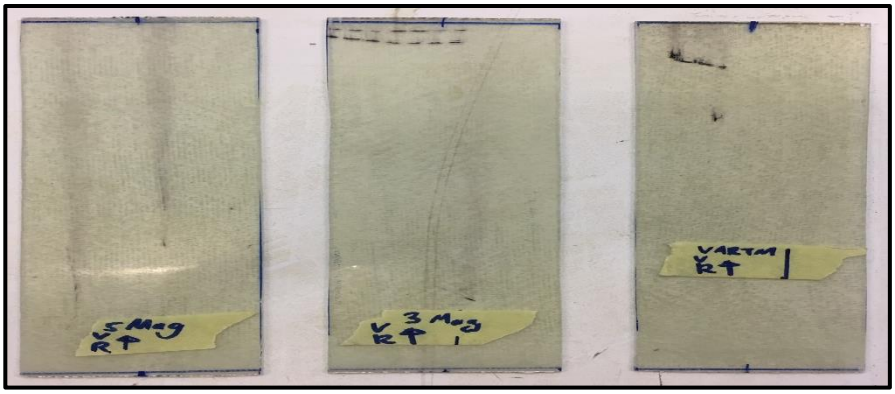

Figure 6.4 Three comparative VARTM panels, demoulded from experimental set 2.

The variation in duration fill times between the first and second experiments could have been affected by the increased temperature, humidity and pressure. As these factors influence the resin viscosity which would then result in the difference in infusion times, as researched by C. Polowick [106], the **p**ermeability as a function of volume fraction, which is related to the capillary pressure from soil mechanics. However, the 5-magnet panel 1 infused faster than the regular VARTM panel 3 on both occasions. This is a possible study for future research

6.1 Comparative Results

6.1.1 Thickness Variation

The panels were measured from the left-hand side which was the resin inlet line to the right-hand side being the vacuum outlet line. The measurements were taken at 12 points at 20mm increments along the length of the laminate and at 4 points along the width of the panel. The distance between the outer and inner points were 26mm. An illustration of the points taken for measurement can be viewed in Figure 6.5 These points were measured with a Mititoyo micrometer.

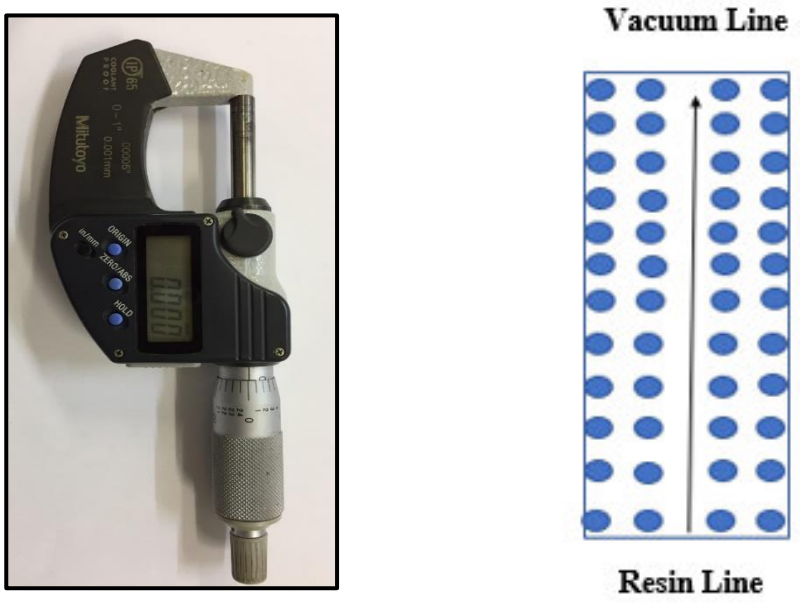

Figure 6.5 Mititoyo micrometer and the VARTM panels 12 x 4 points of measure.

The 4 measured points were then averaged and plotted on a graph. The data presented (Figure 5.6) highlights the variations within the panel. There are two points drawn from these measurements (both VARTM experiments). The first being the wedge shape profile (Figure 2.2), as well as the middle of the panels (lengthwise) is thinner than the outer sides of the panels. This is in-line with research found by C. N. A. C. Mateus [107] where the middle of the infused panel are thinner than the outer edge.

The graphs below are a graphical representation related to the thickness variations between the three VARTM panels. The green line represents the regular VARTM panel 3; the red line

represents panel 2 which had three magnetic clamping units and lastly the blue line represents panel 1 which had five magnetic clamping units.

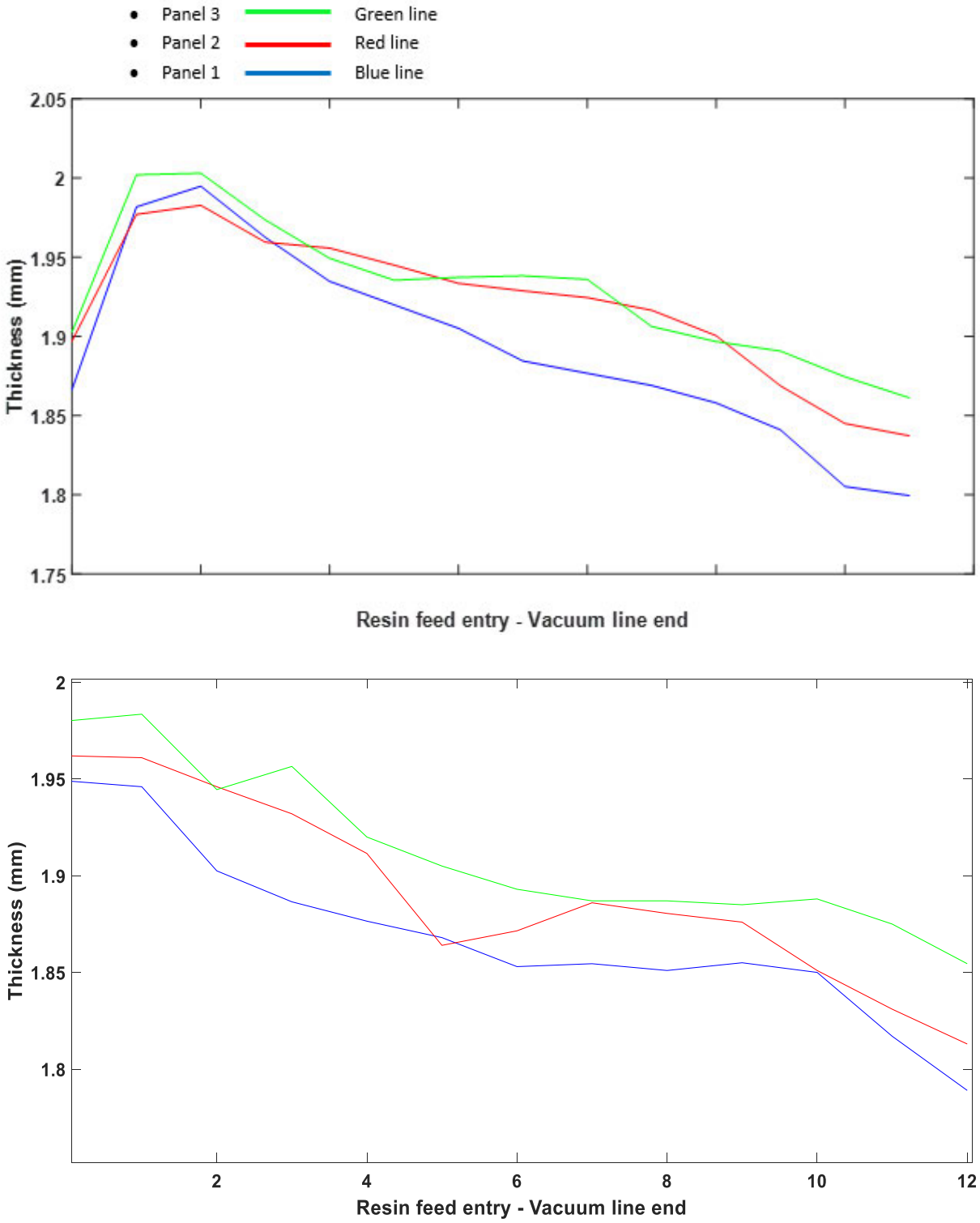

Figure 6.6 Thickness variation graphs from both experimental sets.

The VARTM experimental set 1 had an increase in thickness across all the panels near the resin line. A possible reason for the initial increase in thickness (located approximately 20-40mm within all three panels) is due to the resin curing process. The resin utilized in the comparative experiment was infused according to the manufacturing specifications (stipulated data sheet) provided by the resin manufacturer. Resin within the laminates cure at a different rate than the resin which is within the resin pot which is open to atmospheric temperatures, humidity and pressure. The resin may not have been 100% cured and ever so slightly viscous which caused a minor amount to continue to flow towards the lower pressure gradient vacuum line end. This created the minor "bump" in the readings. The thickness variation is common across all three panels and the variation is approximately 0.1mm. This variation could possibly be resolved by simply adding approximately 20mm-40mm of extra flanges (which is present in most GRP tool) to the tooling or analyzing the tooling for any defects (this case flatness).

The VARTM experimental set 2, also had the inherent wedge shape profile. However, from Figure 6.6, the most noticeable factor being the magnetically assisted panels which consolidates the composite laminate panels (Panel 1 & 2) more than the regular VARTM technique Panel 3 in both experiments.

An average thickness was taken between all three panels. As Figures 5.7 and 5.8 show; panel 1 is the thinnest followed by panel 2 and panel 3. The bar graph is the average difference in thickness between all three panels over the entire length of the laminate.

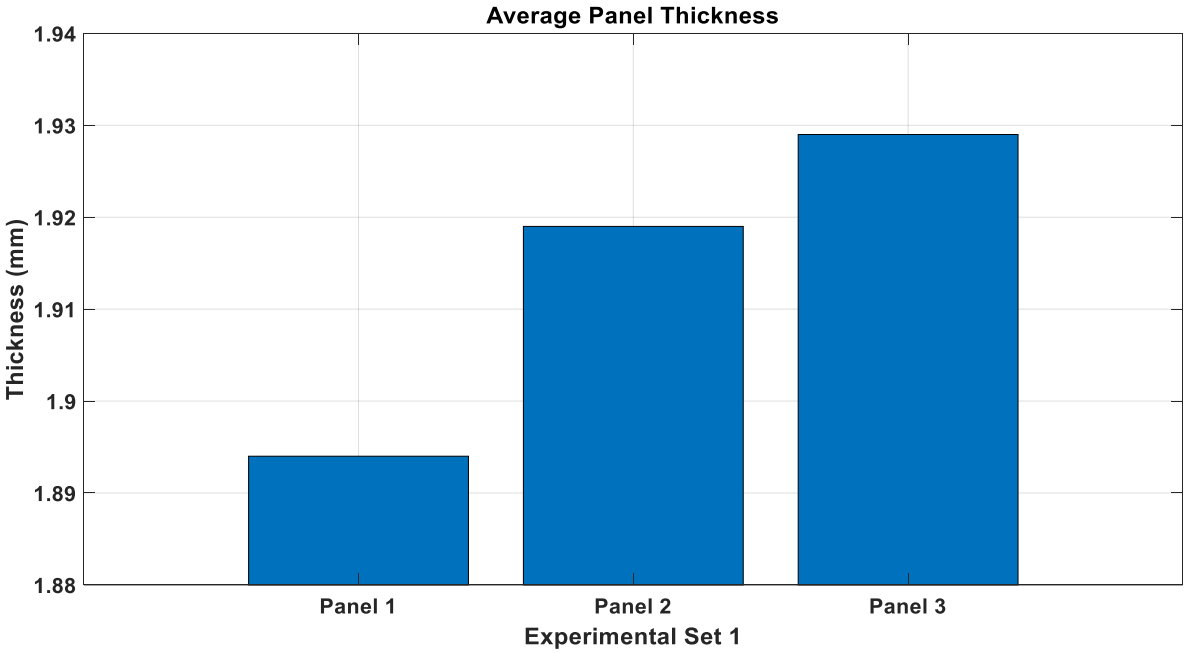

Figure 6.7 Average thickness variation bar graphs from experimental set 1.

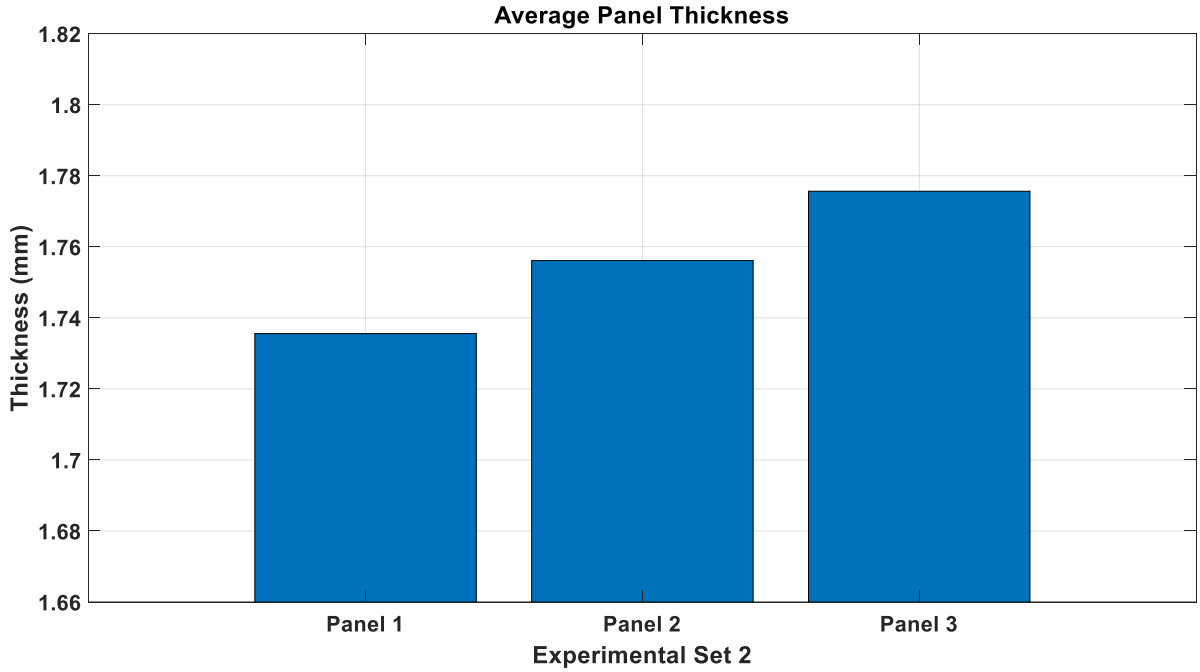

Figure 6.8 Average thickness variation bar graphs from experimental set 2.

The details pertaining to the second aspect to the comparative experimentation which is volume fraction will be elaborated on in the following section.

6.1.2 Volume Fraction Results

With reference to section 2.1.7 in the literature review; one of the most critical aspects that require attention in fiber reinforced composite manufacturing is known as the fiber volume fraction.

As mentioned under section 2.1.7 the most ideal and consistent fiber volume fraction is obtained with the use of prepreg materials in which the ideal amount of fiber volume ratio is approximately 60%. Due to certain manufacturing parameters linked to the other techniques, the fiber volume fraction is usually in the range of 50% to 65%. The volume fraction can be obtained via two methods. These are:

- Destructive: Ignition loss
- Non-destructive: Physical measurement

Both destructive and non-destructive volume fractions across all three panels from both experimental sets (ES1 and ES2) are presented in the form of bar graphs (Figures 6.10). For the non-destructive volume fraction results, the identical 12 points measured at 20mm increments that were used for the thickness variation analysis were utilized for this calculation. For the destructive testing, the results from the ignition loss (burn-off) are presented.

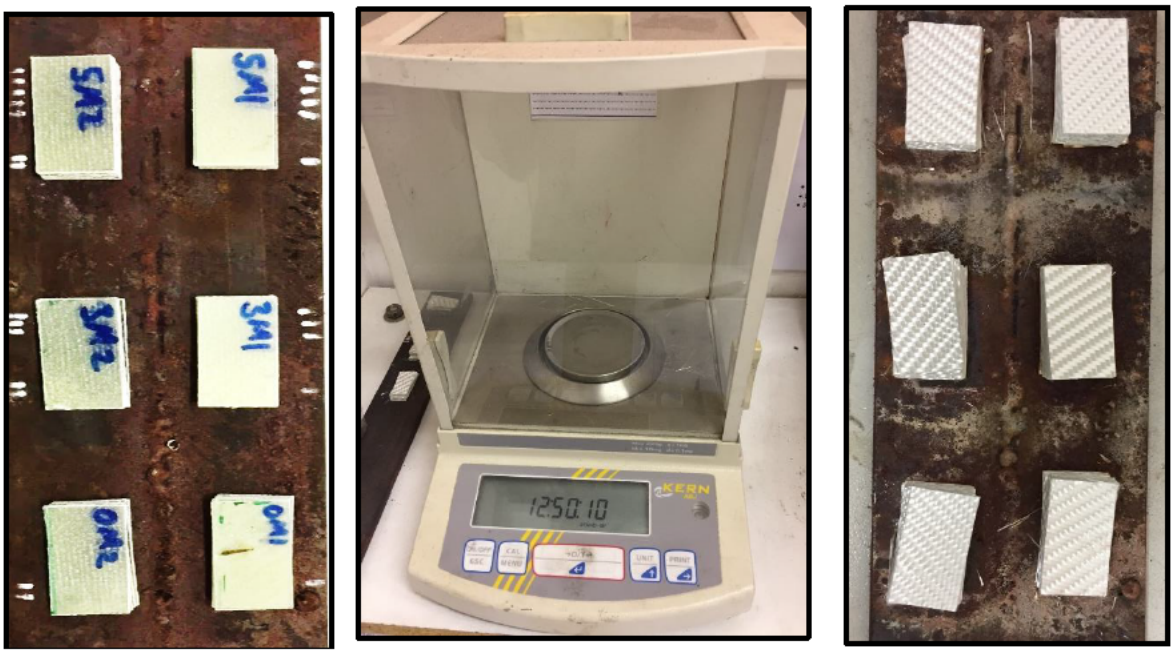

Figure 6.9 Panels before and after the ignition loss test. The measuring scale (center).

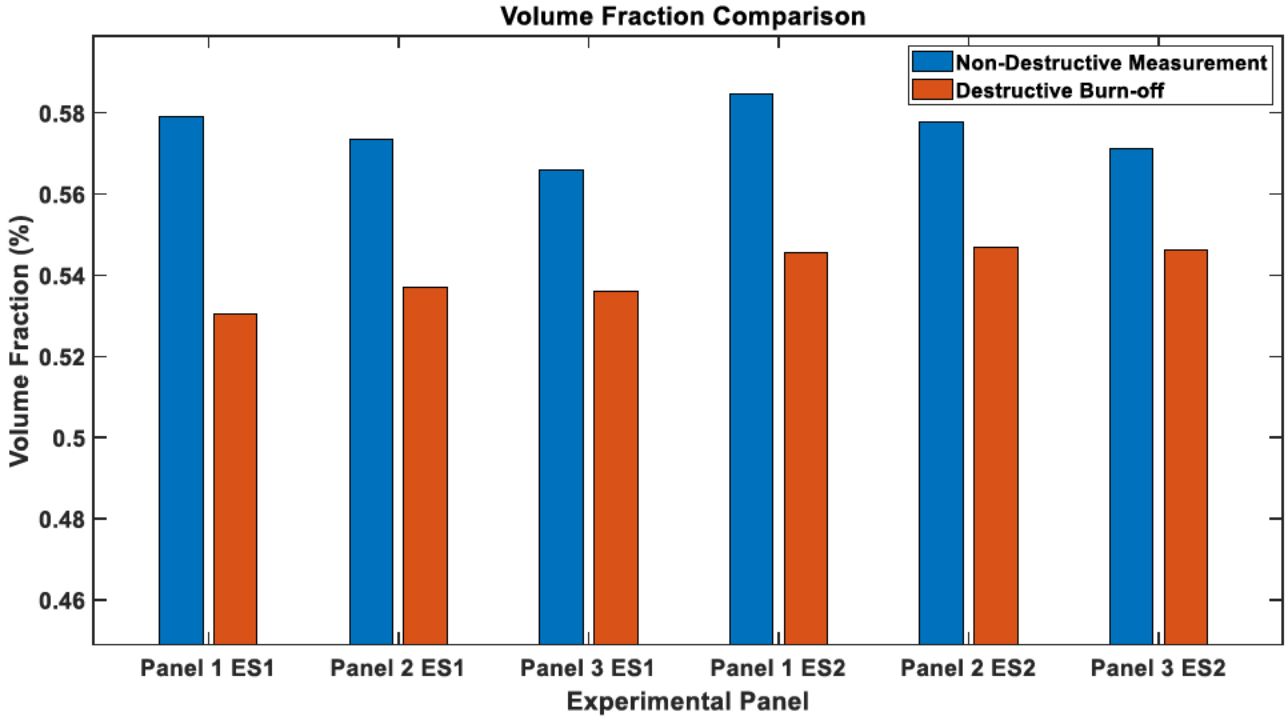

Figure 6.10 Volume fraction comparison, between both testing methods and experimental sets.

Although the magnetic assisted panels are more consolidated the results from the burn-off tests have shown that the volume fractions have not improved.

Due to there being no definitive result between the two types of volume fraction tests, the mass fraction's from both the experimental sets were investigated. As mentioned in section 2.1.7, the mass fraction is obtained via the burn-off test.

6.1.3 Mechanical Property Analysis

In relation to the mechanical properties, the VARTM panels from both experiments were subjected to tensile tests. These were conducted to investigate if the additional 107KPa had any effect with regards to improving the mechanical performance. According to the research conducted the improved volume fraction should improve the mechanical performance.

Average tensile strength			
VARTM experiment	Panel 1	Panel 2	Panel 3
First VARTM	434.08 MPa	452.12 MPa	471.589 MPa
Second VARTM	454.86 MPa	459.28 MPa	460.79 MPa
Average	444.47 MPa	455.7 MPa	466.19 MPa

Table 6. 4 Average tensile strength.

Contrary to the research expectation, the magnetic panels did not possess improved mechanical properties. A reason for this could be due to the lack of difference in the volume fraction based on the ignition loss volume fraction tests.

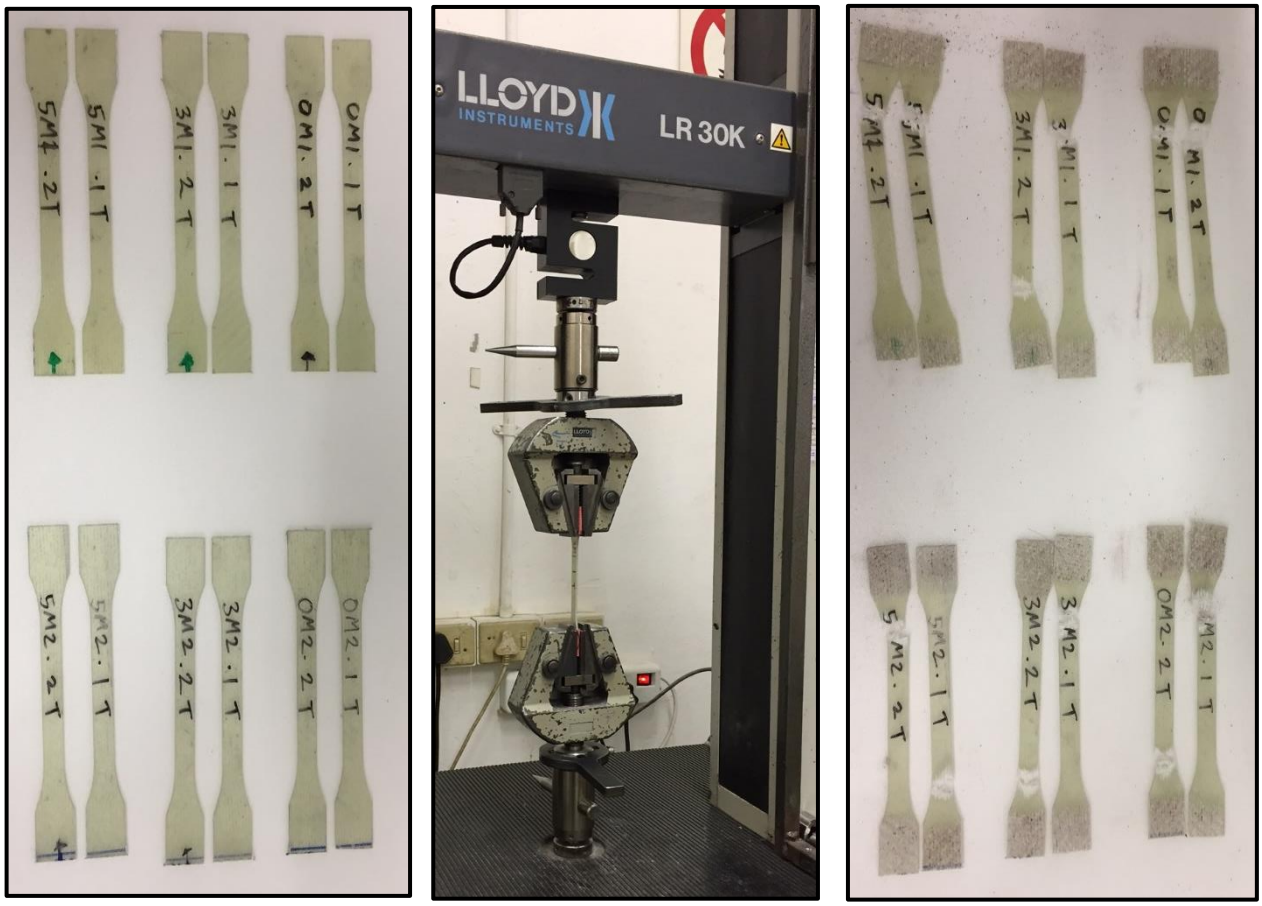

Figure 6.11 Tensile test panels before and after the test. Tensile test being conducted (center).

6.1.4 Mass Fraction Results

As mentioned in section 2.1.7, during the manufacturing process, resin is incorporated and infused into the fibers in which air voids may get trapped within the material. The mass fraction assists in estimating the void content within the composite laminate. The mass fraction formula is a direct ratio between the mass of the laminate (w_c) before and the mass of the fiber (w_f) after the ignition loss test (w_f / w_c). The difference in weight (w_c - w_f) is the amount of resin that was burnt-off during the ignition loss test. The results related to the mass fraction tests are displayed below.

Experimental set 1 (Burn-off test)				
	Total sample mass (g)	Mass of fiber (g)	Mass of resin (g)	Mass fraction (%)
Panel 1	19.5238	14.1231	5.4007	72.34%
Panel 2	19.4561	14.1758	5.2803	72.86%
Panel 3	19.6042	14.2703	5.3339	72.79%

Table 6. 5 Experimental set 1 (burn-off test)

Experimental set 2 (Burn-off test)				
	Total sample mass (g)	Mass of fiber (g)	Mass of resin (g)	Mass fraction (%)
Panel 1	19.2366	14.1463	5.0903	73.54%
Panel 2	19.2702	14.1892	5.0815	73.63%
Panel 3	18.7758	13.8747	4.9611	73.58%

Table 6. 6 Experimental set 2 (burn-off test)

The mass fractions are very similar, however both the 5 magnetic panel 1's are the thinnest and both have the highest amount of resin. Figure 6.12 is a graphical representation of the mass fraction and laminate thickness.

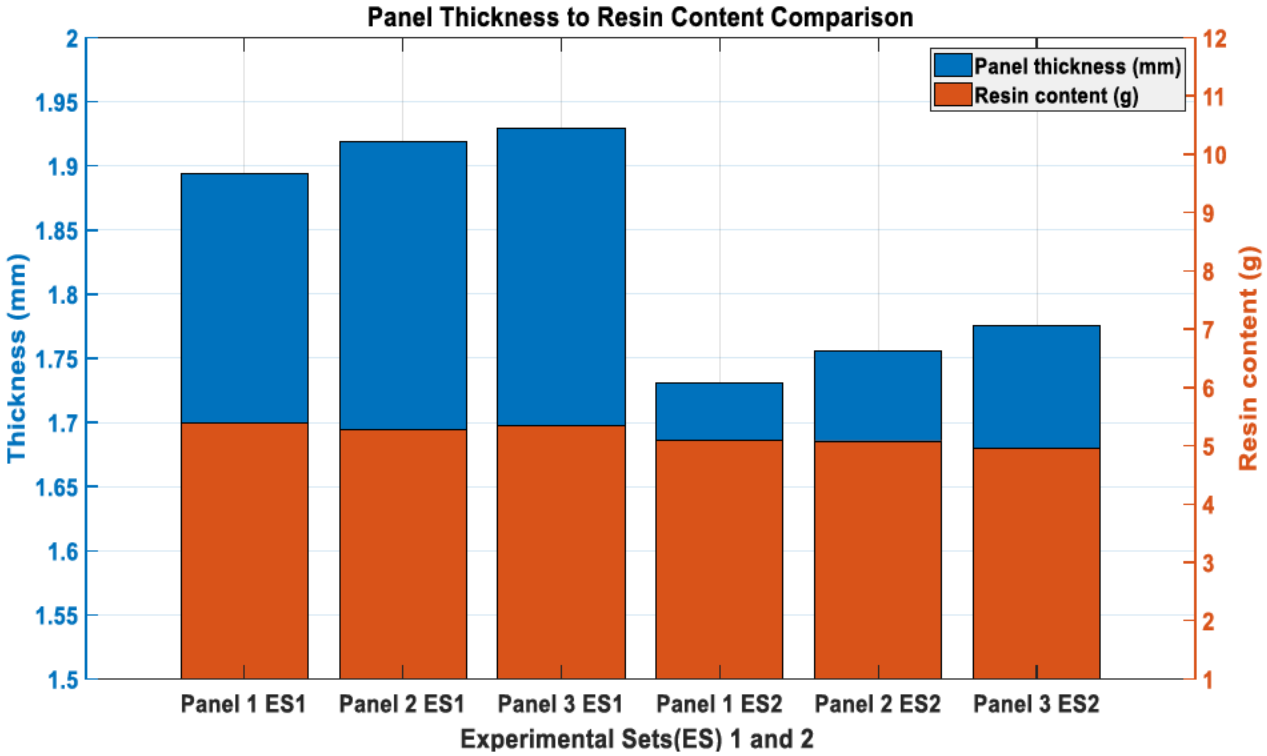

Figure 6.12 Panel thickness to resin content comparison between both experimental sets..

The magnetic panels from both experimental sets were thinner than the benchmark VARTM panels. The 5 magnet panels from both experimental sets 1 and 2 obtained the same outcome of being thinner with more resin. This demonstrates that the additional magnetic forces produced composite panels with less voids.

6.1.5 Discussion

The comparative VARTM results indicate the positive effects of magnetically assisted VARTM manufacturing. The aim of the experimentation was to analyses the effects of magnetic assisted compaction on a fiber reinforced composite laminate produced through the VARTM process. The investigation followed a direct experimental comparison between the VARTM process performed with and without magnets.

Increased compaction was noted in the laminates produced in the magnetically clamped VARTM tests. This was apparent as a reduced thickness was proportional to the number of magnets applied. The thickness variations were initially believed to indicate an increase in fiber volume faction. The fiber volume fractions were determined using two methods, non-destructive and destructive techniques. The results of the tests demonstrated no distinctive change in the calculated values present in the comparative samples. This did not explain the differences in measured thicknesses.

As fiber volume fraction calculations do not accommodate for porosity; mass fractions were interrogated. As illustrated in Table 6.5 and 6.6, the measured masses and mass factions were approximately equal regardless of the measured thickness of the laminate. Therefore, the difference in thickness between samples is attributed to differences in porosity as voids occupy volume but have no associated mass. Magnetically clamped VARTM produced thinner panels with less porosity when directly compared to the benchmark VARTM test. Y. M Akif, S. E Murat and A. M Cengiz [45] noted similar behavior in compaction pressure reducing the presents of voids.

Further mechanical testing were conducted on all VARTM panel in order to identify any mechanical improvements. Increase fiber volume fraction is associated with higher tensile strength. However, no distinguishable differences in strength were noted within the samples (Table 6.4). This further supported the finding that the thinner panels possessed less porosity rather than an increase in volume fraction.

In summary, the magnetically clamped VARTM tests produced thinner, more compact laminates when compared to standard VARTM. The thickness of the laminate is directly influenced by the amount of magnets applied during manufacture and is associated with reduce porosity.

7 Conclusion

The aim of this research was to investigate the effects of magnetic forces used in the VARTM process to increase laminate compaction. The highlighted factor related this research was, the compaction pressure. The additional pressure compacted the fibers allowing the manufactured part to become thinner.

The compaction pressure can differ according to the manufacturing technique. The techniques which utilized wet fiber, required large equipment to generate high positive compaction pressure and the dry fiber techniques utilize negative compaction pressure. The high-pressure techniques have elevated economic requirements when compared to the more economically viable, lower negative pressure methods.

A major drawback of the negative compaction pressure techniques was that they are limited to negative 1 atmospheric pressure. The added complexities related to the negative compaction pressure techniques, contributes to items that are produced inconsistently. These items have a variation in thickness which was due to the pressure gradient that was experienced during the manufacturing process. The inconsistent thickness variation led to an item which possesses inconsistent mechanical properties. This was undesirable as the desired design specifications may not be achieved.

In order to investigate the laminate thickness based on pressure alone; an experimentation was conducted that limited all variable parameters. The comparison was conducted between three panels produced using the same fiber reinforced composite technique. The VARTM technique was selected for the comparative experimentation for this research.

In addressing the research aims, the novel contribution of this research was to illustrate the direct effects of magnetic assisted compaction in composite manufacturing. The aim was to generate a scalable solution which would be implemented onto the VARTM technique without significantly increasing tooling cost or requiring major tooling modifications. A comparison between 3 identical VARTM panels, one of which being a regular VARTM panel and the remaining two panels utilizing magnetic assistance was analyzed. The fiber reinforcement used for the comparative experiment would be seven layers of 390g, twill glass fiber. All the parameters were identical and fixed, allowing the magnetic forces to be the only differentiating factor. By limiting all the

variables, the comparison between the two processes (magnetic assisted VARTM vs VARTM) isolated the thickness variation.

A comprehensive experimental investigation was undertaken in order to fully understand the force-distance nature of permanent magnets at incremental distances. The experimentation comprised of two sections, the first was related to the magnetic materials, dimensions as well as layouts and the second would be related to, two sets of comparative VARTM experimentation. The raw data provided by the magnetic experimentation was interpreted and processed providing a clear indication on the type of magnet as well as the layout that would be utilized and integrated into a comparative VARTM experiment. The VARTM experimentation was conducted such that all parameters and conditions were fixed. The constraining of parameters emphasized the only additional variable which was the additional magnetic units. The intended result was aimed at obtaining a panel which is more consolidated than that of a regular VARTM technique. Further volume fraction and mechanical testing was conducted to interrogate the VARTM panels once manufactured. The volume fraction tests were both, destructive and non-destructive in the forms of an ignition loss test and physical measurement. The mechanical tests analyzed the panels tensile properties.

The observations that were made during the experiments provided a clearer understanding of the nature of the magnetic forces. The magnetic forces experienced an exponential decay as the distance between the magnets increased and the nature of the decaying forces followed a natural logarithmic curve. The nature and pattern of the natural logarithmic decay remained consistent, but it changed in ratio of strength with regards to the magnet's material, size and dimensions. Based on the initial experiments it was found that the ferrite magnets were one-tenth the strength than the neodymium-iron-boron magnets. The neodymium-iron-boron magnets was chosen as the preferred permanent magnetic material. The effects magnetic stacking was noted to be most effective with one magnet on top of another. The magnetic strength does increase in a non-linear pattern with further stacking. However, it was decided to stack only two magnets.

The magnetic placement as well as orientation was obtained through experimentation. With regards to placements, having the magnets orientated in opposite directions rather than the same direction generated a greater force. Further findings which were related to the increase of force were made when the aluminium backing plate was switched to a mild steel backing plate. With regards to the orientation, by having the magnets placed such that the magnetic poles were opposite

and not alike, proved to be more beneficial than the upper mild steel plate. The initial knowledge gained form magnetic stacking was then implemented into the horseshoe layout.

Following initial magnetic tests, consisting of different magnet types, configurations and orientations, a magnetic clamping unit setup was proposed. The magnetic unit layout replicated a mirrored horseshoe design, as there are two halves with four magnets. The magnetic clamping unit comprised of four 22mm diameter 10mm thick N35 Neodymium magnets (two on either side) placed on a 61mm x 25mm x 3mm iron backing plate with a center distance of 39mm between the magnet centers. An M12 stainless steel nut and bolt is adhered (hot glue) to the mild steel plates for application purposes.

The VARTM experimentation was then performed with the magnetic units. The effect of the magnets was isolated due the experimental setup and testing procedure for all panels being identical. As mentioned above, both VARTM experimental sets consisted of 3 panels. One panel with no magnets and was used as the benchmark VARTM panel while the other two panels had 3 and 5 magnet units applied. The setup allowed for both the magnetic assisted and regular processes to be compared an analyzed**.**

Although not an integral part of this research, a visual observation that was made whilst the comparative experiment was being conducted, was the magnetic panels had the quickest infusion time. As mentioned in section 2.2 the additional pressure from the magnetic compaction limited the resin pressure from reaching complete atmospheric pressure and thus maintained a higher compaction pressure (in relation to the 5 magnet and 3 magnet panels) during the infusion. It would then be assumed that a larger delta pressure was present within the magnetic panels resulting in a faster filling time. This is in line with the research conducted by Dr. M. Gilpin [31].

It was noted that thickness variations occurred for all 3 panels. The average comparative thickness for each panel was proportional to the number of magnetic units applied. Both the magnet unit tests had reduced thickness compared to the benchmark VARTM panel in both experimental sets.

Initially this indicated an increase in fiber volume fraction. However, some porosity was noted within each panel. The comparative VARTM experimental set was conducted twice to investigate repeatability, validate, and verify the findings observed. Burn off tests and mechanical tests were then performed to investigate whether the fiber volume fraction had increased. According to the burn off tests, the mass fraction for the 3 panels in the VARTM experimental set were

approximately equal to each other. As the thickness of the panels were different, the variation was attributed to voids and therefore porosity. In this case, this had indicated that the increased compaction reduced porosity but did not increase volume fraction.

As a further verification of this observation, the mechanical tests were performed on all 3 panels from both experimental sets. All the panels showed similar tensile strength and did not vary as would have been expected if the volume fraction had increase. The testing further supported the observation that reduced porosity rather than increase volume fraction was responsible for the thickness variations.

The repeated set results showed good correlation with the original set. The mass fractions and tensile strength results were approximately equal in magnitude to the initial experiment set.

Based on the results from the comparative VARTM experiment, this research shows that magnetic assistance can be utilized to produce a more consolidated composite panel. The process can be implemented on regular GRP tooling without increasing the tooling costs or requiring any modifications.

In the experiments the mild steel backing plates were flat. However, the mild steel backing plates can be conformed to meet a particular tools design in order to make use of the magnetic clamping units on curved geometry.

There are possible limitations related to the magnetic clamping units. The magnetic clamping units may not be able to produce an item with a tubular design which is hollow and they cannot be used in manufacturing procedures which have an inflatable bladder. Producing composite parts that are tubular in design would need additional research and investigation. Process optimization could be further researched in which the 3-magnet panel could be negated and more magnetic units added onto a panel with a reduced surface area. All of which, will contribute to a further increase in compaction pressure. It was observed in the experimentation that the magnetic panels infused before the regular VARTM panels. This finding could be a point of future investigation into resin flow behavior during infusion.

The aim of this research was to investigate the use of magnetic forces to increase the compaction pressure in a fiber reinforced polymer composite lay-up during manufacturing. This research demonstrates that magnetic assistance can be utilized to produce a more consolidated composite

panel. The process of utilizing the magnetic clamping units can be implemented on regular GRP tooling without increasing the tooling costs or requiring any modifications.

References

[1] R. j. Parker, Advances in permanent Magnetism. Canada: john Wiley and Sons Inc, 1990.

[2] A. N. Knaian, "Electropermanent magnetic connectors and actuators: devices and their application in programmable matter," Massachusetts Institute of Technology, 2010.

[3] J. William D. Callister, Materials science and engineering : an introduction, 7th ed. John Wiley & Sons, Inc. (in english), 2007.

[4] F. M. Systeme. Magnetic Gripping and Holding. [Online]. Available: https://www.flaig-te.de/en/lifting-magnets/selection-guide-for-lifting-magnets-and-air-gap-tables/permanent-raw-magnets-installation-instructions.html

[5] C. Polowick, "Optimizing Vacuum Assisted Resin Transfer Moulding (VARTM) Processing Parameters to Improve Part Quality," Master of Applied Science, Aerospace Engineering, , Ottawa, Ontario, Canada, Carleton University, Library and Archives Canada, 978-0-494-94650-3, 2013.

[6] Knight, Magnetic Fields and Forces. Pearson, 2020.

[7] K. H. Fumihito Takeda, Yasuo Suga, Shigeru Nishiyama, Yasuhiro Komori, Nobuo Asahara, "Research in the Application of the VaRTM Technique to the Fabrication of Primary Aircraft Composite Structures," Mitsubishi Heavy Industries Ltd.Technical Review vol. Vol 42, no. No. 5, pp. 1-6, Dec 2005.

[8] V. S. Jagadale, "Effect of change in Volume Fraction on Mechanical Properties of Glass Fiber/Epoxy Resin Composites," July 2018 2018. [Online]. Available: https://www.researchgate.net/publication/326557948_Effect_of_change_in_Volume_Fraction_on_Mechanical_Properties_of_Glass_FiberEpoxy_Resin_Composites.

[9] Shrewsbury, Handbook of Composite Fabrication. GBR: Smithers Rapra Technology, 2001.

[10] L. Tong, A. P. Mouritz, and M. Bannister, 3D fibre reinforced polymer composites. Elsevier, 2002.

[11] L. B. BD. Agarwal, K. Chandrashekhara, Analysis and performance of fiber composites. India: Wiley, 2006.

[12] G. Gardiner. "The making of glass fiber." Composite world. https://www.compositesworld.com/articles/the-making-of-glass-fiber (accessed 6/12/2020, 2020).

[13] M. I. Kiron. "Glass Fiber: Types, Properties, Manufacturing Process and Uses." Textile Learners https://textilelearner.net/glass-fiber-types-properties/ (accessed March 1.

[14] J. W. Hearle, High-performance fibres. Elsevier, 2001.

[15] P. Bhatt and A. Goe, "Carbon fibres: production, properties and potential use," Material Science Research India, vol. 14, no. 1, pp. 52-57, 2017.

[16] D. Dawson. "Sizing for carbon fiber." https://www.compositesworld.com/articles/sizing-for-carbon-fiber (accessed.

[17] V. Mcconnell. "The making of carbon fiber." Composite World. https://www.compositesworld.com/articles/the-making-of-carbon-fiber (accessed 3/31/2020, 2020).

[18] D. Cripps. "Aramid Fibre." Net composites https://netcomposites.com/guide/reinforcements/aramid-fibre/#:~:text=Aramid%20fibre%20is%20a%20man,giving%20very%20high%20specific%20strength. (accessed 24 /01/2019.

[19] H. S. Erik Tempelman, Bruno Ninaber van Eyben, "Manufacturing and Design Understanding the Principles of How Things Are Made," Elsevier, Manufacturing and Design, vol. 1, pp. 172-185, 2014.
[20] L. J. B. Bhagwan D. Agarwal, K. Chandrashekhara, Analysis and Performance of Fiber Composites. Wiley, 2015.

[21] P. K. Mallick, Fiber Reinforced Composites Material, Manufactruing and Design, Third Edition ed. USA: Taylor and Francis Group, LLC, 2007, p. 412.
[22] S. K. Mazumdar., Composite Manufacturing: Materials, Product and Process Engineering Taylor and Fancis Group, 2002.
[23] Reach for the sky Supporting the Aerospace Industry. [Online] Available: http://www.mitsubishicarbide.com/en/magazine/article/vol0-1/tec_vol05
[24] E. J.Barbero, Introduction to Composite Materials Design second ed. CRC Press, 2011.
[25] E. Composites, "Beginners' Guide to Out-of-Autoclave Prepreg Carbon Fibre ", ed.

[26] M. F. F. Edward Bernardon, "Resin transfer molding system," United States Patent Patent Appl. 271561, 1995.
[27] Manufacturing techniques for polymer matrix composites (PMCs). Woodhead Publishing Limited, 2012, p. 261.
[28] L. J. B. Bhagwan D. Agarwal, K. Chandrashekhara, Analysis and Performance of Fiber Composites, Third ed.: Wiley, 2015, p. 45. Accessed on: 05/20/2022.
[29] Manufacturing techniques for polymer matrix composites (PMCs). USA: Woodhead Publishing, 2012.

[30] R. A. Markets. "Global Composites Industry Overview 2018-2023 - Increasing Demand for Lightweight Materials in the Aerospace & Defense and Automotive Industry." PR Newswire. https://www.prnewswire.com/news-releases/global-composites-industry-overview-2018-2023---increasing-demand-for-lightweight-materials-in-the-aerospace--defense-and-automotive-industry-300673139.html (accessed.
[31] M. Gilpin, "Material characterisation for the modelling of the vacuum infusion process," 2015.
[32] E. Rodriguez, F. Giacomelli, and A. Vazquez, "Permeability-porosity relationship in RTM for different fiberglass and natural reinforcements," Journal of composite materials, vol. 38, no. 3, pp. 259-268, 2004.
[33] Manufacturing techniques for polymer matrix composites (PMCs). Woodhead Publishing Limited, 2012, p. 258.
[34] J. Li, Modeling, design and control of vacuum assisted resin transfer molding (VARTM) for thickness variation reduction. The Florida State University, 2006.
[35] M. Gilpin, "Material characterisation for the modelling of the vacuum infusion process," 2015.
[36] Manufacturing techniques for polymer matrix composites (PMCs). Woodhead Publishing Limited, 2012, p. 464.
[37] D. Modi, M. Johnson, A. Long, and C. Rudd, "Investigation of pressure profile and flow progression in vacuum infusion process," Plastics, rubber and composites, vol. 36, no. 3, pp. 101-110, 2007.
[38] C. Polowick, "Optimizing Vacuum Assisted Resin Transfer Moulding (VARTM) Processing Parameters to Improve Part Quality," Master of Applied Science, Aerospace

Engineering, , Ottawa, Ontario, Canada, Carleton University, Library and Archives Canada, 978-0-494-94650-3, 2013.

[39] D. Chen, K. Arakawa, and M. Uchino, "Effects of the addition of a cover mold on resin flow and the quality of the finished product in vacuum-assisted resin transfer molding," Polymer Composites, vol. 37, no. 5, pp. 1435-1442, 2016.

[40] J. A. Woods, A. E. Modin, R. D. Hawkins, and D. J. Hanks, "Controlled atmospheric pressure resin infusion process," ed: Google Patents, 2008.

[41] K. Abdurohman, T. Satrio, and N. Muzayadah, "A comparison process between hand lay-up, vacuum infusion and vacuum bagging method toward e-glass EW 185/lycal composites," in Journal of Physics: Conference Series, 2018, vol. 1130, no. 1: IOP Publishing, p. 012018.

[42] M. A. Yalcinkaya, E. M. Sozer, and M. C. Altan, "Dynamic pressure control in VARTM: Rapid fabrication of laminates with high fiber volume fraction and improved dimensional uniformity," Polymer Composites, vol. 40, no. 6, pp. 2482-2494, 2019.

[43] O. Maclaren, J. Gan, C. Hickey, S. Bickerton, and P. Kelly, "The RTM-light manufacturing process: experimentation and modelling," in The 17nth International Conference on Composite Materials (ICCM), Edinburgh, 2009, vol. 27: Citeseer.

[44] Manufacturing techniques for polymer matrix composites (PMCs). Woodhead Publishing Limited, 2012, p. 315.

[45] M. A. Yalcinkaya, E. M. Sozer, and M. C. Altan, "Effect of external pressure and resin flushing on reduction of process-induced voids and enhancement of laminate quality in heated-VARTM," Composites Part A: Applied Science and Manufacturing, vol. 121, pp. 353-364, 2019.

[46] Z. Lombard, "A composite manufacturing process for producing class A finished components," 2014.

[47] M. W. Hyer, Stress analysis of fiber-reinforced composite materials McGraw-Hill International, 1998.

[48] P.K.Mallick, Fiber Reinforced Composites, Materials, Manufacturing and Design Third ed.: CRC Press Taylor and Francis Group, 2007, p. 408.

[49] S. G. Advani and K.-T. Hsiao, "Manufacturing techniques for polymer matrix composites (PMCs)," p. 252, 2012.

[50] F. C. Campbell, Manufacturing Processes for Advanced Composites First ed. Elsevier Science 2003.

[51] T. Clyne and D. Hull, An introduction to composite materials. Cambridge university press, 2019.

[52] P. K. Mallick, Fiber Reinforced Composites Material, Manufactruing and Design, Third Edition ed. USA: Taylor and Francis Group, LLC, 2007, p. 120.

[53] L. P. N. M. Elkolali, P. O. Rønning and A. Alcocer, "Void Content Determination of Carbon Fiber Reinforced Polymers: A Comparison between Destructive and Non-Destructive Methods," Polmers, 2022.

[54] A. A. Abdulmajeed, T. O. Närhi, P. K. Vallittu, and L. V. Lassila, "The effect of high fiber fraction on some mechanical properties of unidirectional glass fiber-reinforced composite," Dental materials, vol. 27, no. 4, pp. 313-321, 2010, doi: 10.1016/j.dental.2010.11.007.

[55] A. Endruweit, F. Gommer, and A. Long, "Stochastic analysis of fibre volume fraction and permeability in fibre bundles with random filament arrangement," Composites Part A: Applied Science and Manufacturing, vol. 49, pp. 109-118, 2013.
[56] W. D. Callister, Material Science and Engineering, 7 ed. John Wiley and Sons, 2007.
[57] S. G. Advani and K.-T. Hsiao, "Manufacturing techniques for polymer matrix composites (PMCs)," p. 283, 2012.
[58] R. Arbter, Beraud, J. M., Binetruy, C., , "A benchmark exercise'," Composites: Part A: Applied Science and Manufacturing pp. 1157–1168, 2011.
[59] C. Polowick, "Optimizing Vacuum Assisted Resin Transfer Moulding (VARTM) Processing Parameters to Improve Part Quality," Master of Applied Science, Aerospace Engineering, , Ottawa, Ontario, Canada, Carleton University, Library and Archives Canada, 978-0-494-94650-3, 2013.
[60] X. Song, "Vacuum assisted resin transfer molding (VARTM): model development and verification," Virginia Polytechnic Institute and State University, 2003.
[61] F. Robitaille and R. Gauvin, "Compaction of textile reinforcements for composites manufacturing. I: Review of experimental results," Polymer composites, vol. 19, no. 2, pp. 198-216, 1998.
[62] B. W. Grimsley, "Characterization of the vacuum assisted resin transfer molding process for fabrication of aerospace composites," Virginia Tech, 2005.
[63] E. J. Rigas, T. J. Mulkern, S. M. Walsh, and S. P. Nguyen, "Effects of processing conditions on vacuum assisted resin transfer molding process (VARTM)," Army research lab aberdeen proving ground md weapons and materials research …, 2001.
[64] John.D.Kraus, Electromagnetics, 2nd ed. McGraw-Hill, 1973.
[65] T. R. Kuphaldt, "Lessons In Electric Circuits, Volume I–DC," Vol. Fifth Edition. Open Book Project, 2006.
[66] J. H. Edward Hughes, Keith Brown, ian McKenzie, Hughes Electrical and Electronic Technology, 10th ed. Edinburgh Gate, Harlow, Essex CM20 2JE, England: Pearson Prentice Hall, 2008, p. 1029. 1960.
[67] H. Materials. Noedymium iron boron magnets. (2011). TDK.
[68] M. N. O. Sadiku, Elements of Electromagnetics Fourth ed. Oxford University Press.Inc., 2007.
[69] G.A.G.Bennet, Electricity and modern physics Hodder education, 1970.
[70] V. S. Juan Manuel Camacho, "Alternative method to calculate the magnetic field," 2013.
[71] C. Physics. "Magnetic Fields and Magnetic Field Lines." http://cnx.org/contents/031da8d3-b525-429c-80cf-6c8ed997733a/College_Physics (accessed.
[72] W. D. Callister, "Materials science and engineering," in An introduction, J. Hayton Ed., 7th ed.: John Wiley & Sons, Inc., 2007, ch. 20, p. 78.
[73] J. M. D. Coey, Rare-earth iron permanent magnets (no. Book, Whole). Oxford: Clarendon, 1996.
[74] A. LLC. "Magnetic Guide and Tutorial." Alliance LLC. https://allianceorg.com/ (accessed 2018.
[75] R. J. Parker, Advances in Permanent Magnets USA: John Wiley and Sons, Inc (in english), 1990.
[76] W. D. Callister, "Materials science and engineering," in An introduction, J. Hayton Ed., 7th ed.: John Wiley & Sons, Inc., 2007, ch. 20, p. 79.

[77] X. Liu, Q. Lin, and W. Fu, "Optimal design of permanent magnet arrangement in synchronous motors," Energies, vol. 10, no. 11, p. 1700, 2017.
[78] J.M.D.Coey, "Rare-Earth Iron Permanent Magnets," ed. USA: Oxford University Press, 1996.
[79] A. F. Kip, Fundamentals of electricity and magnetism McGraw-Hill book company, 1985.
[80] S. Laurent et al., "Magnetic properties," in MRI Contrast Agents: Springer, 2017, pp. 5-11.
[81] E. Tutorials, "Magnetic alignment," ed: Aspencore Inc, 2020.
[82] J. Allemand, A. Letant, J. Moreau, J. Nozieres, and R. P. De La Bathie, "A new phase in Nd2Fe14B magnets. Crystal structure and magnetic properties of Nd6Fe13Si," Journal of the Less common Metals, vol. 166, no. 1, pp. 73-79, 1990.
[83] Manilo.G.Abele, Structure of permanent magnets (Generation of uniform fields). John WIley and Sons, 1993.
[84] S. F. Masato Sagawa, Hitoshi Yamamoto, Yutaka Matsuura, "Journal of Applied Physics," Permanent Magnet Materials Based on the Rare EarthIronBoron Tetragonal Compounds, vol. 20, no. 5, 1984.
[85] A. N. Knaian, "Electropermanent magnetic connectors and actuators: devices and their application in programmable matter," Massachusetts Institute of Technology, 2010.
[86] O. Gutfleisch, M. A. Willard, E. Brück, C. H. Chen, S. Sankar, and J. P. Liu, "Magnetic materials and devices for the 21st century: stronger, lighter, and more energy efficient," Advanced materials, vol. 23, no. 7, pp. 821-842, 2011.
[87] S. Dris. "Magnetic Hysteresis." Engineering LibreTexts. https://eng.libretexts.org/Bookshelves/Materials_Science/Supplemental_Modules_(Materials_Science)/Magnetic_Properties/Magnetic_Hysteresis (accessed 21/10/2020.
[88] W. D. Callister, "Materials science and engineering," in An introduction, J. Hayton Ed., 7th ed.: John Wiley & Sons, Inc., 2007, ch. 20, pp. 94-95.
[89] John G, "Wiley encyclopedia of electrical and electronic engineerng " vol. 22, Webster, Ed., 1 ed: Wiley-interscience, 1999, p. 369.
[90] M. H. N. M. K. Brussel, Electricity and magnetism John Wiley and sons, 1985.
[91] A. A. I. Kostov, "Modelling of Magnetic Fields Generated by Cone-Shaped Coils for Welding with Electromagnetic Mixing," Journal of the University of Chemical Technology and Metallurgy, 40, 3, 2005, 261-264, pp. 261-264, 20 June 2005 2005.
[92] S. Babic and C. Akyel, "Mutual inductance and magnetic force calculations between thick bitter circular coil of rectangular cross section with inverse radial current and filamentary circular coil with constant azimuthal current," IET Electric Power Applications, vol. 11, no. 9, pp. 1596-1600, 2017, doi: 10.1049/iet-epa.2017.0244.
[93] H. Edward, Hughes electrical and electronic technology, 10th ed. Longman imprint: Pearson Education Limited, 1960.
[94] A. Helmenstine. "Table of Electrical Resistivity and Conductivity." https://sciencenotes.org/table-of-electrical-resistivity-and-conductivity/ (accessed January 16 2019.
[95] P. A. Rinck. "Magnetic Resonance " The Basic Textbook of the European Magnetic Resonance Forum. https://magnetic-resonance.org/print-version.html (accessed.
[96] F. Charles, "Design and Construction of a one meter electromagnetic railgun," 1996.

[97] C. WHYTE. "How Maglev Works." Brookhaven National Laboratory, . https://www.energy.gov/articles/how-maglev-works#:~:text=In%20Maglev%2C%20superconducting%20magnets%20suspend,matching%20poles%20face%20each%20other.&text=Here%2C%20both%20magnetic%20attraction%20and,train%20car%20along%20the%20guideway. (accessed 14 June 2016.
[98] L. J. Dunne, E. J. Brändas, and H. Cox, "High-temperature superconductivity in strongly correlated electronic systems," in Advances in Quantum Chemistry, vol. 74: Elsevier, 2017, pp. 183-208.
[99] P. K. B, M. S. K. , M. S. , and K. D. , "Design of Magnetic Actuator," vol. 4, 2015.
[100] The Worlds Thinnest (37mm) Magnet Clamp Japan, MEK002-04-GB, 2013. [Online]. Available: http://www.kosmek.co.jp/data/pdf/en/MEK002-04-GB.pdf.
[101] M. S. Scott Fitzgerald, M. S. Scott Fitzgerald, Ed. Arduino projects book. Arduino LLC, 2012.
[102] Y. Y. Deepesh Upadrashta, Lihua Tang, "Journal of Intelligent Material Systems and Structures," Material strength consideration in the design optimization of nonlinear energy harvester, 2014.

[103] J. Li, C. Zhang, R. Liang, and B. Wang, "Statistical characterization and robust design of RTM processes," Composites Part A: applied science and manufacturing, vol. 36, no. 5, pp. 564-580, 2005.
[104] M. Amirkhosravi, M. Pishvar, and M. C. Altan, "Void reduction in VARTM composites by compaction of dry fiber preforms with stationary and moving magnets," Journal of Composite Materials, vol. 53, no. 6, pp. 769-782, 2019.
[105] M. Pishvar, M. Amirkhosravi, and M. C. Altan, "Magnet assisted composite manufacturing: A flexible new technique for achieving high consolidation pressure in vacuum bag/lay-up processes," JoVE (Journal of Visualized Experiments), no. 135, p. e57254, 2018.
[106] C. Polowick, "Optimizing Vacuum Assisted Resin Transfer Moulding (VARTM) Processing Parameters to Improve Part Quality," Master of Applied Science, Aerospace Engineering, , Ottawa, Ontario, Canada, Carleton University, Library and Archives Canada, 978-0-494-94650-3, 2013.

[107] N. A. C. M. Correia, "Analysis of the vacuum infusion moulding process," University of Nottingham, 2004.

Appendix A

Glass Reinforced Plastic (GRP)Tooling				
Manufacturing Procedure				
Step 1	Apply seal and release to the designed plug			
Step 2	Apply 3mm of Gel Coat to the plug, wait approximately 60 min			
Step 3	Touch up any deficiencies on the Gel Coat			
Step 4	Apply Gel Coat + Cabosil + Cotton Flocks + Millifibres			
Step 5	Apply the Quasi-iso layup below			
Step 6	Apply Peel ply			
Step 6	Apply Perforated film			
Step 7	Apply Bleeder			
Step 8	Apply a Vacuum bag and seal off the ends with Adhesive (Tacky) Tape.			
Step 9	Apply vacuum			
Step 5 above				
Layup Schedule:	**Material**	**Weave Type**	**Material Weight (g/sm)**	**Orientation**
Ply 1	Glass Fiber	2 x 2 Twill	163	90°
Ply 2	Glass Fiber	2 x 2 Twill	163	45°
Ply 3	Glass Fiber	2 x 2 Twill	290	90°
Ply 4	Glass Fiber	2 x 2 Twill	290	45°
Ply 5	Glass Fiber	2 x 2 Twill	390	90°
Ply 6	Glass Fiber	2 x 2 Twill	390	45°
Ply 7	Glass Fiber	2 x 2 Twill	390	45°
Ply 8	Glass Fiber	2 x 2 Twill	390	90°
Ply 9	Glass Fiber	2 x 2 Twill	290	45°
Ply 10	Glass Fiber	2 x 2 Twill	290	90°
Ply 11	Glass Fiber	2 x 2 Twill	163	45°
Ply 12	Glass Fiber	2 x 2 Twill	163	90°
Further Details				
Processing method	Hand Lay-up			
Ambient Temperature	26° C			
Post Cure Max Temp	120° C			
Duration	5 Hours at 120° C			
Ramp Rate	0.25° C per min			
Cooling time before use	24 Hrs			

Appendix B

Magnetic Clamping Unit Consistency Analysis

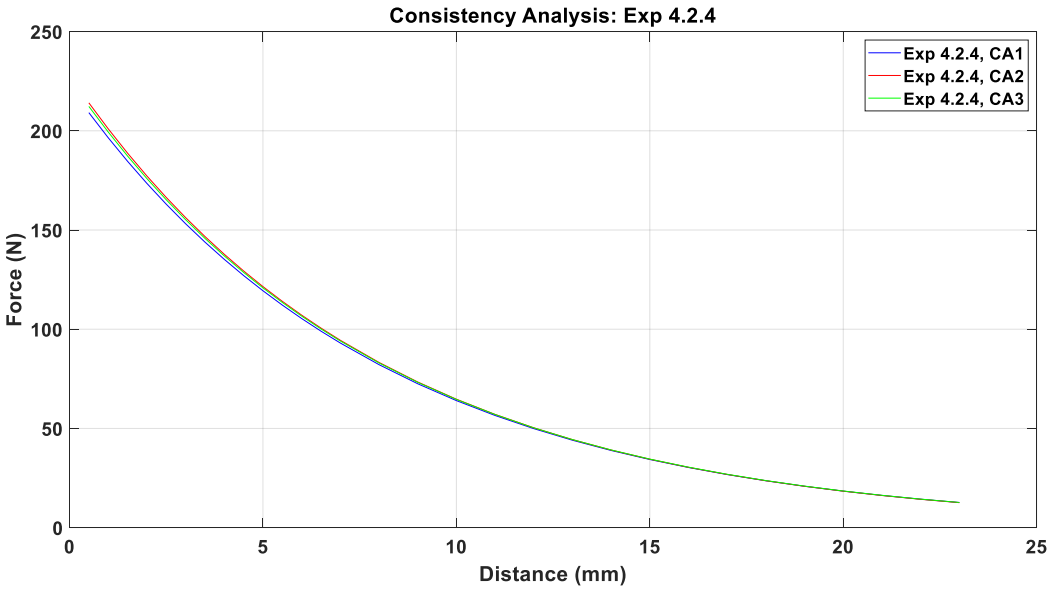

Consistency analysis of experiment 4.2.4.